



universität  
wien

# MASTERARBEIT / MASTER'S THESIS

Titel der Masterarbeit / Title of the Master's Thesis

„EcO83-OMV and their interaction with the host immune system“

verfasst von / submitted by

Daniela Kerekes, BSc

angestrebter akademischer Grad / in partial fulfilment of the requirements for the degree of

Master of Science (MSc)

Wien, 2021 / Vienna, 2021

Studienkennzahl lt. Studienblatt /  
degree programme code as it appears on  
the student record sheet:

UA 066 830

Studienrichtung lt. Studienblatt /  
degree programme as it appears on  
the student record sheet:

Masterstudium Molecular Microbiology, Microbial  
Ecology and Immunobiology

Betreut von / Supervisor:

Assoc. Prof. Univ. Doz. Dr. Irma Schabussova



## **Acknowledgement**

First of all, I want thank Uni. Prof. Dr. Ursula Wiedermann, who enabled me to do my Master's thesis at the ISPTM. Next, I want to honor and thank my supervisor Assoc. Prof. Dr. Irma Schabussova, who was always available in every situation during my time at the ISPTM and helped me a lot with her excellent expertise and her amazing hospitality.

Furthermore, I want to say thank you to all the members at the ISPTM institute. I am grateful for everyone of them for their care and willingness to always help me and I also enjoyed the exchange with them as good colleagues and also as friends.

I am also very thankful for my family and friends who played a great part in my time of studies, and I am very grateful for their love and support through all the years.

And at last, I want to say thank you to God who has been my hope, my anchor in every good and every stormy season of my life and I thank Jesus for his love and his promises, his plans, and purposes for my life that he finishes every good work in me that he started and brings it to completion.



## Table of contents

1	Abstract .....	8
2	Zusammenfassung auf Deutsch.....	9
3	List of abbreviations .....	11
4	Introduction.....	13
4.1	Allergy.....	13
4.2	Allergy treatment .....	15
4.3	Probiotic bacteria and allergy.....	15
4.4	<i>E. coli</i> O83 .....	16
4.5	Outer membrane vesicles.....	16
4.6	Outer membrane vesicles and their immunomodulatory effects.....	17
4.7	Lipopolysaccharide and Toll-like receptor 4.....	18
5	Aims .....	19
6	Material and Methods.....	20
6.1	Isolation of EcO83-OMV .....	20
6.2	Bicinchoninic acid assay .....	21
6.3	Limulus Amoebocyte Lysate assay .....	21
6.4	Sodium-dodecyl sulfate-polyacrylamide gel electrophoresis .....	22
6.5	Nanoparticle tracking analysis.....	22
6.6	Transmission electron microscopy .....	22
6.7	<i>In vivo</i> and <i>in vitro</i> studies.....	22
6.7.1	OVA-induced mouse models .....	22
6.7.2	Bronchoalveolar lavage .....	24
6.7.3	Lung cell isolation and single cell suspension.....	24
6.7.4	Spleen cells isolation and single cell suspension.....	25
6.7.5	Bronchial lymph nodes .....	25
6.7.6	Cytokine ELISA .....	25
6.7.7	Histology of lung tissue .....	26
6.7.8	Haematoxylin and Eosin staining.....	26
6.7.9	Periodic Acid-Schiff staining .....	26
6.7.10	Isolation, cultivation, and stimulation of bone marrow derived dendritic cells .....	26
6.7.11	Flow cytometry – Fluorescence activated cell sorting (FACS).....	27
6.7.12	Gating strategy .....	28
6.7.13	Rat basophil leukaemia cells assay.....	30
6.7.14	Antibody ELISA.....	30

6.7.15	Cultivation and stimulation of HEK 293 transfected with NOD1, NOD2, TLR2, TLR2/CD14 and TLR4/CD14/MD2.....	30
6.7.16	RNA isolation and reverse transcription.....	31
6.7.17	Reverse transcription and real time quantitative polymerase chain reaction.....	32
6.8	Statistic .....	33
6.9	Media and Solutions.....	33
7	Results .....	38
7.1	Characterisation of EcO83-OMV .....	38
7.1.1	Transmission electron microscopy .....	38
7.1.2	Nanoparticle tracking analysis.....	38
7.1.3	Measuring the endotoxin levels and protein content.....	39
7.2	Stimulation of mouse splenocytes derived from wild type and TLR4-deficient mice with EcO83-OMV .....	39
7.3	Stimulation of mouse bone marrow derived dendritic cells derived from wild type and TLR4-deficient mice with EcO83-OMV .....	41
7.4	The role of TLR4 in the recognition of EcO83-OMV in the mouse model of OVA-induced allergy 43	
7.4.1	Lung cell population analysis.....	45
7.4.2	<i>Ex vivo</i> stimulation of lung and spleen cells derived from sensitised and challenged TLR4 KO BALB/c mice.....	49
7.4.3	Production of OVA-specific antibodies.....	51
7.5	The suppression of allergy by the intranasal application of EcO83-OMV IL-1 $\beta$ independent 52	
7.5.1	Lung cell populations in IL-1 $\beta$ KO C57BL/6J mice with and without EcO83-OMV treatment .....	53
7.5.2	Production of cytokines in lung and spleen derived from EcO83-OMV-treated/non-treated OVA sensitised and challenged IL-1 $\beta$ KO C57BL/6J mice .....	54
7.5.3	Levels of IgA in BAL fluid of IL-1 $\beta$ KO mice treated with EcO83-OMV and sensitised and challenged with OVA .....	57
7.5.4	OVA-specific antibody production in sera from IL-1 $\beta$ KO C57BL/6J mice .....	57
7.6	Stimulation of mouse splenocytes derived from TLR9 KO C57BL/6J mice and WT C57BL/6J mice with EcO83-OMV .....	59
7.7	Stimulation of BMDCs derived from TLR9 KO C57BL/6J mice and WT C57BL/6J with EcO83-OMV 60	
7.8	The role of human TLR2, TLR2/CD14, TLR4/CD14/MD2, NOD1, and NOD2 for recognition of EcO83-OMV by using transfected HEK 293 cells .....	62
8	Discussion .....	65
9	Conclusion .....	69

10	References .....	70
11	List of tables.....	75
12	List of figures: .....	76

# 1 Abstract

*E. coli* A0 34/86 (*E. coli* O83; serotype O83:K24:H31) has already been used for a long period of time as a probiotic bacterium and is commercially available as Colinfant Newborn and is known to reduce the development of atopic diseases in infants. It has been shown that oral application of *E. coli* O83 to neonates reduces allergic sensitization later in life but had no beneficial effects on allergic lung disease. Different results showed that it reduces several allergic hallmarks when administered intranasally in ovalbumin (OVA)-induced allergic mouse models. Further studies concentrated on the outer membrane vesicles (OMV) of *E. coli* O83 and their beneficial effects that contributed to the reduction of allergic airway inflammation were observed. In this thesis we continued the studies emphasizing on the immunomodulatory effects of *E. coli* O83 derived OMV (EcO83-OMV) by isolating them from the parental *E. coli* O83 strain by ultracentrifugation, furthermore, analysing them by Limulus amoebocyte lysate (LAL) assay and Bicinchoninic acid (BCA) assay and characterising them via nanoparticle tracking analysis (NTA) and transmission electron microscopy (TEM). We wanted to know in more detail if EcO83-OMV interact with the host immune system via the toll-like receptor (TLR) 4 and TLR9. We have shown that TLR4-dependency in the interaction of EcO83-OMV with the immune system *in vivo* in a mouse model of OVA-induced allergy in TLR4 knockout (KO) BALB/c mice which were intranasally treated with EcO83-OMV. The TLR4 dependency was confirmed *in vitro* we could also observe a TLR4 dependency by stimulating splenocytes and bone marrow derived dendritic cells (BMDCs) from TLR4 KO BALB/c mice with EcO83-OMV. Several cytokines were downregulated in TLR4 KO mice including IL-6, TNF- $\alpha$ , IL-1 $\beta$ , IL-12/23p40 and IL-23 when compared to wild type (WT) controls. The *in vitro* stimulation of TLR9 KO C57BL/6J and C57BL/6J WT mice showed no TLR9-dependency in the immunomodulatory effects of EcO83-OMV.

In our preliminary studies, *E. coli* O83 bacteria, induced high levels of IL-1 $\beta$ . Here we tested whether EcO83-OMV reproduce the effect of the parent bacteria and whether IL-1 $\beta$  plays a role in the prevention of experimental OVA-induced allergic airway inflammation by EcO83-OMV. Therefore, IL-1 $\beta$  KO C57BL/6J mice were treated intranasally with EcO83-OMV followed by allergic sensitization and airway challenge. The results indicate that the immunomodulatory effects of EcO83-OMV were not IL-1 $\beta$  dependent. The beneficial effects of EcO83-OMV-treatment such as reduction of eosinophilic infiltration in bronchoalveolar lavage fluid and reduction of Th2 cytokines in the lungs accompanied by increase of regulatory/anti-inflammatory cytokines was observed in these mice.

To study further the mechanisms how EcO83-OMV interact with the host immune system through their pattern recognition receptors we performed several *in vitro* studies with human embryonic kidney 293 (HEK 293) cells transfected with human TLR4, TLR2, TLR2/CD14, nucleotide-binding oligomerization domain-containing protein (NOD) 1 and NOD2. We observed an IL-8 cytokine production induced by EcO83-OMV in TLR4, TLR2, TLR2/CD14, NOD1 and NOD2 transfected HEK 293 cells, which indicates that EcO83-OMV use these different receptors to interact with the host immune system.

EcO83-OMV are a promising tool for future studies in order to apply them as a treatment for prevention and/or treatment of allergic disease in humans.



## 2 Zusammenfassung auf Deutsch

*E. coli* A0 34/86 (*E. coli* O83; Serotyp O83:K24:H31) wurde bereits für einen längeren Zeitabschnitt als ein probiotisches Bakterium verwendet, welches kommerziell erhältlich ist als Colinfant Newborn und ist bekannt dafür, dass es die Entwicklung von atopischen Krankheiten in Kleinkindern reduziert. Es wurde gezeigt, dass die orale Anwendung von *E. coli* O83 in Neugeborenen allergische Sensibilisierung später im Leben reduziert, es hatte aber keine positiven Auswirkungen in allergischen Lungenerkrankungen.

Verschiedene Ergebnisse zeigten, dass es unterschiedliche allergische Symptome reduziert, bei der intranasalen Verabreichung in OVA-induzierten allergischen Mausmodellen. Weitere Studien konzentrierten sich auf die Außenmembranvesikel (OMV) von *E. coli* O83 und die positiven Auswirkungen, die zur Reduktion von allergischer Atemwegsentszündung beigetragen haben. In dieser Thesis konzentrierten wir uns weiter auf die Forschung von den immunomodulatorischen Auswirkungen durch OMV entstammend von *E. coli* O83 (EcO83-OMV), indem wir sie von dem Elternstamm, den *E. coli* O83, durch Ultrazentrifugation isolierten. Des Weiteren analysierten wir sie mit Hilfe des Limulus Amoebocyte Lysate Assay (LAL) Assays und Bicinchoninic Acid (BCA) Assays und die Charakterisierung der Vesikel erfolgte über die Nanopartikel Tracking Analyse (NTA) und Transmission Elektron Mikroskopie (TEM). Wir wollten im weiteren Detail wissen, ob EcO83-OMV mit den Wirtsimmunsystem über den Toll-like Rezeptors (TLR) 4 durch das Lipopolysaccharid (LPS) der Vesikel interagiert und ob Toll-like Rezeptor9 (TLR9) auch ein wichtiger Rezeptor für die Immunantwort ist. Betrachtet man die Rolle von TLR4 in der Erkennung von EcO83-OMV, war es uns möglich eine TLR4-Abhängigkeit in der Interaktion mit dem Immunsystem *in vivo* zu sehen, in dem wir OVA-induzierte allergische TLR4 Knock-out (KO) BALB/c Mäuse intranasal mit EcO83-OMV behandelt haben. *In vitro* war es uns ebenfalls möglich eine TLR4 Abhängigkeit zu beobachten, indem wir Milzzellen und Knochenmark entstammende dendritische Zellen (BMDCs) von TLR4 KO BALB/c Mäusen und BALB/c Wildtyp (WT) Mäusen mit EcO83-OMV stimulierten. Verschiedenste Zytokine wurden in TLR4 KO Mäusen hinunterreguliert wie IL-6, TNF- $\alpha$ , IL-1 $\beta$ , IL-12/23p40 und IL-23. Die *in vitro* stimulierten Milzzellen und BMDCs von TLR9 KO C57BL/6J und C57BL/6J WT Mäusen zeigten keine TLR9 abhängigen immunomodulatorischen Auswirkungen bei EcO83-OMV.

In unseren vorherigen Studien wurde ein hoher Level an IL-1 $\beta$  Zytokinproduktion, von *E. coli* O83 Bakterien induziert, beobachtet und wir wollten hier testen, ob ähnliche Auswirkungen mit EcO83-OMV reproduziert werden und ob IL-1 $\beta$  durch EcO83-OMV eine Rolle in der Vorbeugung von experimentellen OVA-induzierten allergischen Atemwegsentszündung spielt. Deswegen wurden IL-1 $\beta$  KO C57BL/6J Mäuse intranasal mit EcO83-OMV behandelt, gefolgt von einer allergischen Sensibilisierung und Atemwegs Challenge. Die Ergebnisse indizieren, dass die immunomodulatorischen Effekte der EcO83-OMV nicht IL-1 $\beta$  abhängig waren, wir konnten noch immer positive Auswirkungen wie die Reduktion von Zuwanderung an Eosinophilen in Bronchoalveolarlavage Flüssigkeit sehen, die Reduktion von Th2 Zytokinen und die Zunahme von regulatorischen/anti-inflammatorischen Zytokinen.

Um weitere Mechanismen von EcO83-OMV und der Interaktion mit ihrem Wirtsimmunsystem durch die Pattern Recognition Receptors (PRRs) zu studieren, führten wir mehrere *in vitro* Studien mit Human Embryonic Kidney Cells 293 (HEK 293), die mit TLR4, TLR2, TLR2/CD14 und Nucleotide-Binding Oligomerization Domain-Containing Protein 1 (NOD1) und NOD2 transfiziert waren. Wir beobachteten eine IL-8 Zytokinproduktion induziert von EcO83-OMV

bei TLR4, TLR2, TLR2/CD14, NOD1 und NOD2 transfizierte HEK 293 Zellen, was darauf hinweist, dass EcO83-OMV verschiedene Rezeptoren verwendet, um mit dem Wirtsimmunsystem zu interagieren.

EcO83-OMV sind ein versprechendes Werkzeug für zukünftige Forschungen, um sie für die Vorbeugung und/oder als Behandlung von allergischen Erkrankungen in Menschen einzusetzen.

### 3 List of abbreviations

AAI	Allergic airway inflammation
AIT	Allergen immunotherapy
Alum	Aluminium hydroxide
BAL	Bronchoalveolar lavage
BCA	Bicinchoninic acid Assay
BHI	Brain heart infusion
BHR	Bronchial hyperresponsiveness
BMDC	Bone marrow derived dendritic cell
BSA	Bovine serum albumin
CD	Cluster of differentiation
CFU	Colony forming unit
ConA	Concanavalin A
CpG	Cytosine-phosphate-guanosine
CXCL8	C-X-C Motif Chemokine Ligand 8
DC	Dendritic cell
dH <sub>2</sub> O	Distilled water
DMEM	Dulbecco's modified eagle medium
DNA	Deoxyribonucleic acid
<i>E. coli</i>	<i>Escherichia coli</i>
<i>E. coli</i> O83	<i>Escherichia coli</i> A0 34/86 serotype O83:K24:H31
EcO83-OMV	<i>E. coli</i> O83-derived outer membrane vesicles
EDTA	Ethylenediaminetetraacetic acid
ELISA	Enzyme-linked immunoassay
FACS	Fluorescence associated cell sorting
FCS	Fetal calf serum
GM-CSF	Granulocyte-monocyte colony stimulatory factor
HRP	Horseradish peroxidase
IFN	Interferon
Ig	Immunoglobulin
IL	Interleukin
i. n.	Intranasal
i. p.	Intraperitoneal
MAMPs	Microorganism-associated molecular patterns
MDP	Muramyl dipeptide
NaCl	Sodium chloride
NALT	Nasopharyngeal associated lymphocyte tissue
NK cell	Natural killer cell
NOD1	Nucleotide-binding oligomerization domain-containing protein 1
NOD2	Nucleotide-binding oligomerization domain-containing protein 2
KO	Knock out
MHC	Major histocompatibility complex
OMV	Outer membrane vesicle
OVA	Ovalbumin
LPS	Lipopolysaccharide
LAL	Limulus amoebocyte lysate
PAS	Periodic acid-Schiff

<b>PAMP</b>	<b>Pattern-associated molecular pattern</b>
<b>PBS</b>	<b>Phosphate-buffered saline</b>
<b>pDC</b>	<b>Plasmacytoid dendritic cells</b>
<b>PRR</b>	<b>Pattern recognition receptor</b>
<b>PSA</b>	<b>Polysaccharide A</b>
<b>qPCR</b>	<b>Quantitative polymerase chain reaction</b>
<b>RBL-assay</b>	<b>Rat basophil leukaemia-assay</b>
<b>RNA</b>	<b>Ribonuclease acid</b>
<b>rpm</b>	<b>Revolutions per minute</b>
<b>RT</b>	<b>Room temperature</b>
<b>SCIT</b>	<b>Subcutaneous allergy immunotherapy</b>
<b>SDS PAGE</b>	<b>Sodium dodecyl sulfate - polyacrylamide gel electrophoresis</b>
<b>SLIT</b>	<b>Sublingual allergy immunotherapy</b>
<b>TCR</b>	<b>T cell receptor</b>
<b>TEM</b>	<b>Transmission electron microscope</b>
<b>Th</b>	<b>T helper</b>
<b>Thf</b>	<b>T helper follicle</b>
<b>TLR</b>	<b>Toll-like receptor</b>
<b>Tregs</b>	<b>Regulatory T cells</b>
<b>TSLP</b>	<b>Thymic stromal lymphopoietin</b>
<b>TNF</b>	<b>Tumour necrosis factor</b>
<b>TriDap</b>	<b>L-Ala-γ-D-Glu-mDAP</b>
<b>WT</b>	<b>Wild type</b>

## 4 Introduction

### 4.1 Allergy

Allergies present the most frequent chronic diseases in Europe, affecting more than 60 million people. In the last half century, allergy shifted from a rare disease to a major public health threat <sup>1</sup>. Allergies involve almost every organ in the body with a wide range of symptoms and phenotypes. One of the major research gaps is a potential therapeutic treatment to prevent or cure allergies <sup>1</sup>.

The typical characteristic of allergic reaction is the induction of T helper (Th) 2 cells and the production of immune globulin (Ig) E antibodies <sup>2</sup>. There are two ways how the immune system takes on the response: i) the immediate hypersensitivity that begins rapidly within antigen challenge and causes major pathological consequences or ii) the late-phase reaction, which is characterised by accumulation of neutrophils, eosinophils, macrophages, and CD4+ Th2 cells. This late-phase reaction is triggered by cytokines, that are produced by the Th2 cells <sup>2</sup>.

Cytokines are responsible for most of the biological effects in the immune system, such as cell mediated immunity and allergic type responses <sup>3</sup>. Cytokines can functionally be distinguished into two groups – inflammatory (which also promote allergic responses) and anti-inflammatory cytokines. One major source of cytokines are T lymphocytes <sup>3</sup>.

Eosinophils are one of the signature cells in allergy and lead to pathogenicity in allergic reactions. They accumulate near sites of inflammation and release toxic products, which can cause tissue damage <sup>4</sup>.

Toll like receptors (TLRs) are vital for the fate of a subsequent pro- or anti-inflammatory immune response. TLRs play a role in innate immune cells by directing the immune response towards e.g., lipopolysaccharide (LPS), double stranded RNA, bacterial DNA, and it was also discovered that they play a role also on tissue cells <sup>1</sup>.

Allergies of the respiratory tract, e.g., asthma and rhinitis, can very frequently coexist in the same patient <sup>5, 6</sup>. Asthma is a chronic inflammatory disease and major global health problem. Recently, 200 million people of all ages suffered from this disease worldwide <sup>7</sup>. Asthma is characterised by airway inflammation and a consistent airflow limitation, leading to cough, wheeze, shortness of breath, and chest tightness. One of the unresolved problems is the difficulty in preventing or treating asthma exacerbations, which can lead to a higher risk of death, severe morbidity, and high cost of treatment <sup>1, 8</sup>. There are two classical types of asthma known, which are clinically defined. Allergic asthma is mostly prevalent among children and approximately 50 % of adults are suffering from it <sup>9</sup>. The disease coincides with allergic sensitization, which is defined by the presence of IgE antibodies or positive skin-prick tests to proteins of common inhaled allergens including fungal spores, animal dander, house dust mite, plant or tree pollen and peanuts <sup>9</sup>. Then there is the nonallergic asthma which is mostly developed later in life and has no obvious involvement of Th2 cells or IgE reactivity to allergens in the serum <sup>9</sup>.

The mechanism of allergic asthma is the activity of cells involved in innate and adaptive immune system together with epithelial cells <sup>9</sup>. Allergens, bacteria, viruses, or pollutants come in contact with the first line of defence, the epithelial cells <sup>1</sup>. In an atopic asthmatic allergy

model, soluble protein allergens enter, and immature dendritic cells (DCs) migrate to a draining lymph node, after the exposure of the allergen peptide or a pattern-associated molecular pattern (PAMP) <sup>1, 10</sup>. Naïve T cells are sensitised through the corresponding processed and presented allergen. The naïve CD4<sup>+</sup> T cells develop further either into adaptive Th2 cells or Th1 cells <sup>1, 10</sup>. CD4<sup>+</sup> cells generate the expression of Th2 cytokines such as IL-4, IL-5, and IL-13 which mediate several features of allergic inflammation <sup>9, 11</sup>. There are two transcription factors that are known to be involved in Th cell development, which is GATA3, highly expressed in CD4<sup>+</sup> Th2 cells or T-bet which is involved in Th1 cell development <sup>11,12, 13</sup>. T-bet was observed to be attenuated in allergic airway inflammation when GATA3 is expressed <sup>11, 12, 13</sup>. Additionally, increased numbers of eosinophils, local and systemic production of IgE antibodies, mucus hypersecretion, and airway hyperresponsiveness (AHR) are observed in allergic subjects <sup>14, 11</sup>.

Allergen-specific IgE binds to a high-affinity IgE receptor on mast cells and the crosslinking leads to release of a variety of inflammatory mediators<sup>15</sup>. Migration of inflammatory cells to allergic tissues takes place and a series of chemokines are produced. Additionally, other effector T cell subsets such as Th9, Th17, and Th22 play also inflammatory roles <sup>1</sup>.

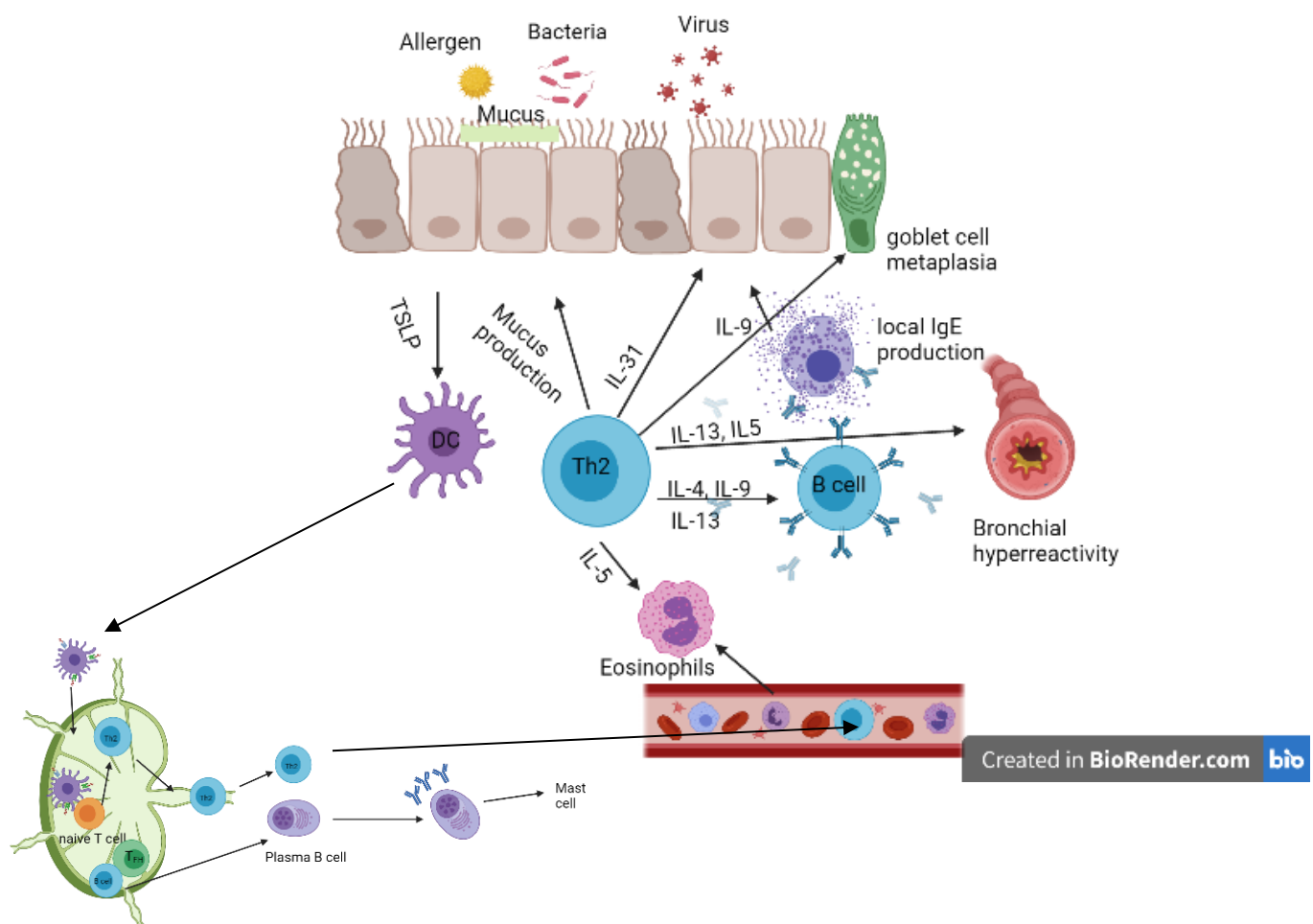


**Figure 1: Schematic depiction of allergic asthma.** Allergens, bacteria, and viruses enter the first line of defence that are epithelial cells. Th2 cells drive expression of different cytokines such as IL-13, Thymic stromal lymphopoietin TSLP, IL-31, IL-4, IL-5, IL-9 and IL-25. IL-5 controls eosinophil development in the bone marrow and IL-13 causes bronchial hyperreactivity and goblet cell metaplasia. DCs acquire entering allergens and immigrated into a lymph node and naïve CD4<sup>+</sup> T cells are sensitised with allergen peptides and these naïve T

cells develop into adaptive Th2 cell or other T helper cells. DCs stimulate Th2 cells to produce IL-5, IL-4, IL-9, and IL-13 and the latter three driving IgE synthesis. Figures were created by using the program BioRender.

## 4.2 Allergy treatment

Preventing the exposure of sensitised individuals to allergens and treating them with the appropriate therapeutics against the disorder are keys in allergy management <sup>16</sup>. Allergen immunotherapy (AIT) is the only approach that is currently known to significantly affect outcome of allergic disease <sup>17</sup>. AIT has been practiced for the last 100 years <sup>18</sup>. Subcutaneous immunotherapy (SCIT) and sublingual immunotherapy (SLIT) <sup>18</sup> are two methods, whereby allergens are administered so that an allergen-specific and long-term clinical and immunological tolerance is induced <sup>19,20</sup>. The SCIT therapy is divided into two phases; the up-dosing phase which is an individual titration of the allergen to build up a tolerance and assessing a sensitivity for the patient, followed by the subsequent maintenance phase when the highest tolerance-dose is reached and given throughout the last phase <sup>18</sup>. SCIT is injected with an adjuvant and needs to be administered by doctors whereas SLIT is available in tablet or drop form and are easier to use for self-treatment at home <sup>18</sup>. A successful AIT is accomplished by a suppression of Th2 cells, basophils, eosinophils, mast cells and neutrophil infiltration in specific target organs <sup>20</sup>. AIT is an effective way to treat allergy, but its remission varies widely depending on the complex interaction between patient, allergy, symptoms and the vaccines that are used <sup>21, 7, 22, 23,24, 25, 26</sup>. AIT is still underused because of the limited access to specialist care, lack of awareness, concerns in terms of safety and effectiveness, and several unmet needs to improve response to AIT <sup>17</sup>.

## 4.3 Probiotic bacteria and allergy

Probiotics are live microorganisms that have a beneficial effect on the host when administered in adequate amounts <sup>27</sup>. These beneficial microorganisms have been studied for the use against diseases of gastrointestinal tract, but there is an evidence that they might also have a beneficial effect in preventing and/or treating chronic airway diseases <sup>27</sup>.

The hygiene hypothesis arose to explain the increase in allergic diseases over the last decades linked by observing a lack of infections and reduction of Type 1 immune responses in westernised countries <sup>28</sup>. This hypothesis proposes that the decrease of infectious disease burden and massive introduction to hygiene measures, vaccines, antibiotics, and declining family size increases the incidences of allergies <sup>28, 29</sup>. It was supported by several studies in murine models that exposure to bacteria, viruses, helminths, and microbe-derived products, could protect from allergy <sup>28</sup>.

There is an evidence that live microbial supplementation can produce positive results in both therapeutic and preventative ways <sup>30</sup>. Most studies on application of probiotic bacteria to prevent atopic diseases were focused on neonates or infants <sup>31</sup>. A study by (author) indicated that *Lactobacillus casei* was effective at preventing atopic eczema in children at-risk <sup>30, 31</sup>.

It was shown in several studies that allergic children from European countries revealed to have a similar microbiota composition and this composition is differing in non-atopic children <sup>32</sup>. Atopic diseases were associated with increased levels of aerobic microbes and decreased levels of anaerobic microbes in the gut <sup>32</sup>. Allergic children had decreased level of

*Bifidobacteria* and *Enterococcus* species and increased levels of *Clostridium* species<sup>33</sup>. Other reports revealed a decreased level of bifidobacterial and gram-positive species in infants suffering from atopic eczema<sup>32, 34, 33</sup>. It shows that an imbalance in microbiota composition (dysbiosis) has a negative impact on the health status<sup>35, 27</sup>. That is why it is believed that probiotics will represent a novel treatment option for chronic allergic diseases<sup>27</sup>. The administration route of probiotics is essential and in most cases the oral route via eating, drinking or intragastric intubation is applied<sup>27</sup>. Alternatively, the intranasal application was investigated in mouse models<sup>36, 37, 38</sup>. *Spacova et al.* showed that intranasal administration of *Lactobacillus rhamnosus* GG attenuated birch pollen-induced asthma in mice<sup>36</sup>. Mechanistically, it has been shown that increased Th2 responses can be regulated by applying of specific probiotic bacteria which shift naïve T helper cells to Th1 type<sup>39</sup>, for example by increased levels of IgG2a antibodies production of IFN- $\gamma$ <sup>40</sup>.

#### 4.4 *E. coli* O83

*Escherichia coli* A0 34/86 (*E. coli* O83; serotype O83:K24:H31) is a commercially available oral live vaccine, known as Colinfant Newborn and was originally isolated from pig faeces. It has been used since 1970 for prevention against diarrhoea and nosocomial infections in infants<sup>41</sup>. *Lodinova et. al*<sup>42, 41, 43, 44</sup> described a variety of beneficial effects through *E. coli* O83 throughout the years. They showed that oral application of *E. coli* O83 to infants which at high risk of developing an atopic disease within the first week of life reduced the prevalence of sensitization within the next 10 to 20 years after treatment within the first week of life<sup>45</sup>.

The application of *E. coli* O83 showed on one hand that it reduces atopic diseases such as atopic skin diseases in later life, but on the other hand it indicated no beneficial effects on respiratory allergies<sup>46, 45</sup>. There was only little knowledge about the strain's immunomodulatory mechanism. That brought *Zwicker et al.* to further investigate different administration routes<sup>47</sup>. By applying *E. coli* O83 via the intranasal route, *Zwicker et al.*, have shown a prevention of allergic diseases in the lung, because the application was navigated directly into the airways<sup>47</sup>.

#### 4.5 Outer membrane vesicles

As part of their natural growth, both pathogenic and commensal gram-negative bacteria produce outer membrane vesicles (OMVs). OMVs are bilayered and spherical membrane nanostructures ranging from 20 nm to 400 nm in diameter<sup>48, 49</sup>, formed by blebbing of the bacterial outer membrane<sup>49</sup>. Via proteomic and biochemical analyses, it was revealed that OMVs contain bacterial components such as RNA, DNA, LPS, proteins, enzymes, and peptidoglycan. OMVs contain a repertoire of bacterial compounds from the parental bacterial strain, but do not replicate<sup>48</sup>. OMVs can be sensed by human intracellular pattern recognition receptors (PRRs) such as nucleotide-binding oligomerization domain-containing protein 1 (NOD1) or extracellular PRRs like TLR2 and TLR4<sup>50</sup>.



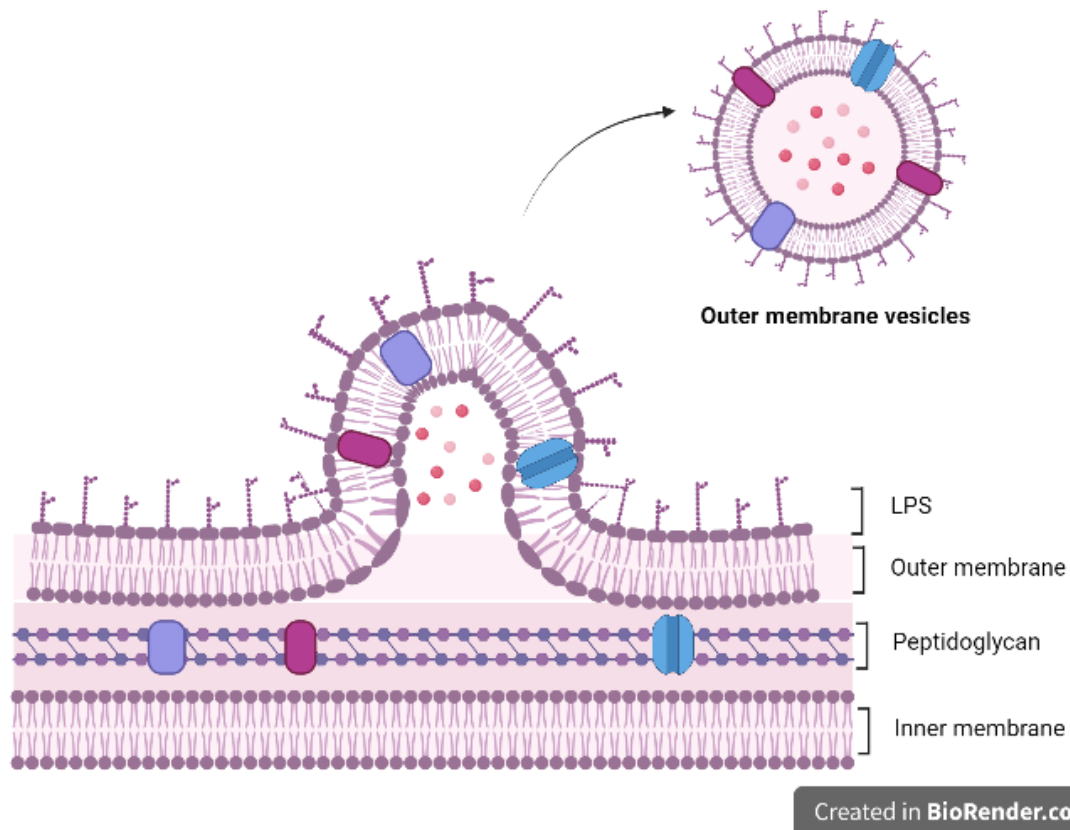


**Figure 2: Forming of outer membrane vesicles by blebbing of the outer membrane.** Figures were created by using the program BioRender.

#### 4.6 Outer membrane vesicles and their immunomodulatory effects

How OMVs interact with the host immune system depends on the bacterium they originate from and what their content is<sup>48</sup>. As it is known that epithelial cells are one of the first defence lines in the host, when OMV enter the host they stimulate epithelial cells<sup>48</sup>. The stimulation happens through microorganism-associated molecular patterns (MAMPs) such as LPS, peptidoglycan, DNA and RNA<sup>50, 51</sup>. These MAMPs induce the production of chemokines, cytokines and a signalling cascade of immune responses and facilitate or limit inflammation and regulate recruitment of inflammatory cells<sup>48</sup>. LPS is one of the MAMPs of OMV and the TLR4 is known to interact with LPS<sup>48</sup>. Furthermore, it is known that OMV of *E. coli* drive TLR4-dependent production of CXCL8 in human epithelial cells through their LPS<sup>52</sup>. When OMVs enter through epithelial cells into submucosa they interact with different immune cells such as neutrophils, macrophages, and DCs<sup>48</sup>.

*Shen et al.* observed that OMVs deriving from *Bacteroides fragilis* containing polysaccharide A (PSA) exhibit therapeutic activity when administered orally to mice in a models of experimental colitis<sup>53</sup>. Mice treated with OMVs showed a very little weight loss compared to control mice. Furthermore, the authors performed studies with bone marrow derived dendritic cells (BMDCs) treated with OMVs. They showed that OMVs are taken up by DCs, induced a tolerogenic DCs which produce IL-10 and drive the development of IL-10-producing Tregs<sup>53</sup>.

## 4.7 Lipopolysaccharide and Toll-like receptor 4

LPS is a major constituent of the outer membrane of gram-negative bacteria, such as *E coli* O83, stimulates the immune system through TLR4 <sup>54</sup>. Several studies on the effect of LPS in experimental models of asthma have produced conflicting results: on one hand beneficial effect and on the other hand exacerbation of allergy <sup>47, 55, 56</sup>. *Rodriguez et al.*, investigated if LPS can suppress asthma-similar responses <sup>57</sup>. It is suggested that the beneficial effect of LPS is mediated by enhanced secretion of Th1 cytokines IL-12 and IFN- $\gamma$  that are known for the down-regulation of allergic responses <sup>58, 59</sup>. Additionally, LPS is known to induce production of nitrite oxide (NO) <sup>60</sup>. The data provided by Rodriguez. et al., showed that NO is induced by LPS signalling via TLR4 and plays a role in the suppression of key factors involved in asthma <sup>57, 61</sup>.

LPS is also involved in the route of vesicular uptake and entry kinetics and efficiency <sup>62</sup>. Lipid A is a conserved part within the outer membrane but there are many species that contain also a highly variable polysaccharide known as O antigen, which is located in the in the outermost region of LPS and indicated to be the most likely region that comes first in contact with the host cells <sup>62, 63</sup>.

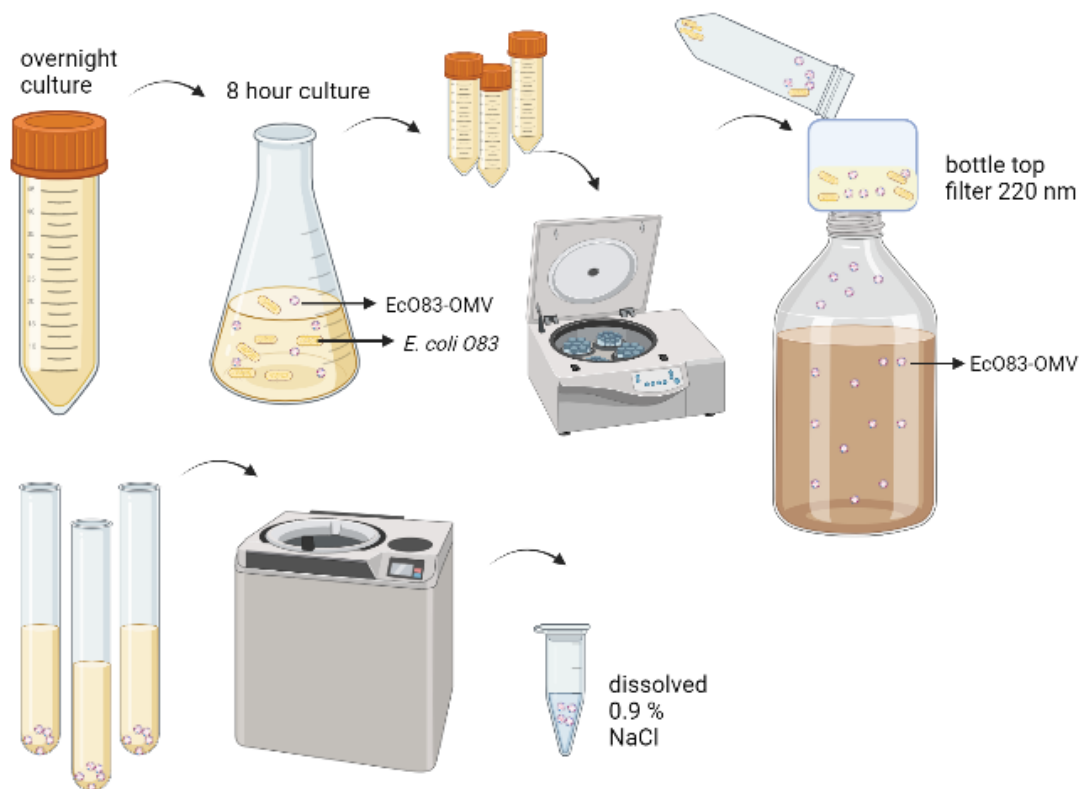
## 5 Aims

- I. Investigate the immunomodulatory effect of EcO83- OMV in different cells *in vitro*
- II. To test whether EcO83-OMV prevent allergy in a mouse model of OVA-induced allergic airway inflammation
- III. To study the interaction of EcO83-OMV with TLR4, TLR2, TLR9, NOD1, and NOD2 *in vitro* and *in vivo*
- IV. To study the role of IL-1 $\beta$  in the interaction of EcO83-OMV with the host immune cells

## 6 Material and Methods

### 6.1 Isolation of EcO83-OMV

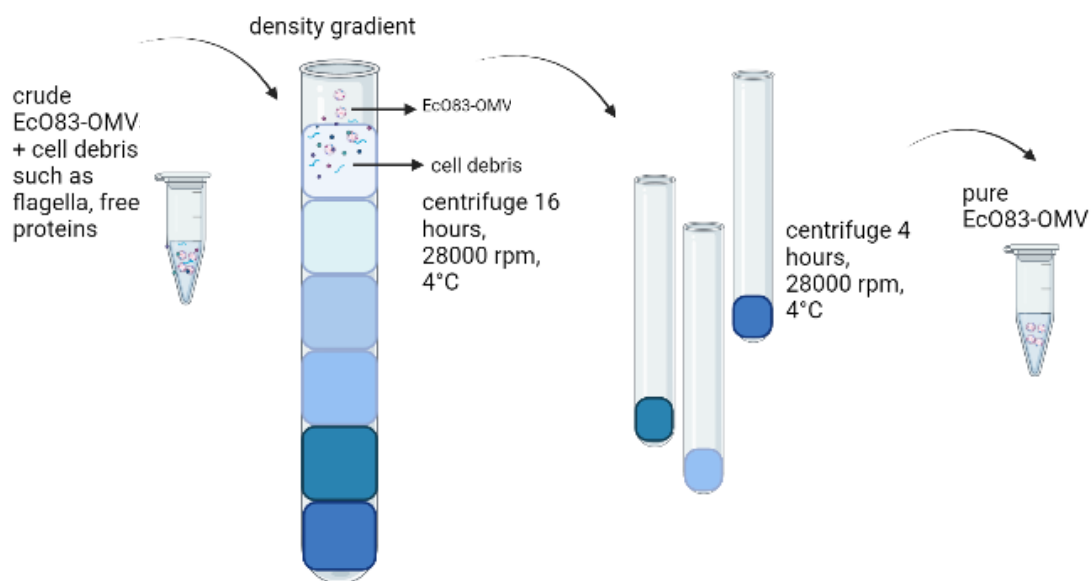
*Escherichia coli* A0 34/86 (*E. coli* O83; serotype O83:K24:H31; an oral live vaccine commercially available from Colinfant Newborn) was stored at -80°C in 10 % glycerol. From this stock, bacteria were scratched with a pipette tip into Brain-Heart-Infusion Medium (BHI; Sigma-Aldrich) and grown overnight at 37°C at 200 rpm and on the next day a dilution was made using 500 ml of BHI medium and 5 ml of the overnight culture, followed by 8 hours of incubation at 37°C at 200 rpm (**figure 3**). Culture was split into Falcon tubes and centrifuged for 20 minutes at 3000 rpm and the supernatant was sterile filtrated through a 220 nm bottle top filter (Sigma-Aldrich) (**figure 3**). The filtrated supernatant was centrifuged in an ultracentrifuge (Beckman Coulter, 45 TI rotor) for 4 hours at 4°C at 28000 rpm (**figure 3**). The supernatant was discarded and the pellet (containing the crude EcO83-OMV) was suspended in 0.9 % NaCl (B. Braun) (**figure 3**). EcO83-OMV were further centrifuged by gradient ultracentrifugation (**figure 4**). The gradients were formed in a centrifuge tube using 60 % - 30 % of Iodixanol (OptiPrep™ Density Gradient Medium, Sigma-Aldrich). The crude vesicles were added to the tube and ultracentrifuged for 16 hours at 4°C at 28000 rpm (**figure 4**). Every fraction was separated and again centrifuged for 4 hours at 4°C at 28000 rpm (**figure 4**). The supernatant was discarded and the pellet was suspended in 0.9 % NaCl (**figure 4**). To determine the protein concentration of the fractions a Bicinchoninic acid assay (BCA, Thermo Scientific™ Pierce™ BCA Protein Assay Kit) was performed, followed by sodium-dodecyl sulphate polyacrylamide-gel electrophoresis (SDS-PAGE).



Created in BioRender.com bio

**Figure 3: Isolation of crude EcO83-OMV.** *E. coli* O83 was cultured over night at 37°C at 200 rpm. The overnight culture was then used in a 1:10 dilution for an 8-hour culture. The *E. coli* O83 culture was further distributed into Falcon tubes and centrifuged for 20 minutes at RT at 3000 rpm. The supernatant was filtered using a 220 nm bottle top filter. The supernatant was further divided into ultracentrifuge tubes (Beckman Coulter) and spun

down for 4 hours at 4°C at 28000 rpm. The supernatant was discarded and the pellet of crude EcO83-OMV was dissolved in 500 µl of 0.9 % NaCl. Figures were created by using the program BioRender.



Created in BioRender.com 

**Figure 4: Gradient ultracentrifugation of crude EcO83-OMV.** Crude EcO83-OMV suspended in 0.9 % NaCl were pipetted into a tube with a density gradient through a 30 % - 60 % Iodixanol solution to separate the vesicles from all remaining cell debris, free proteins, and flagella. The sample was centrifuged for 16 hours at 4°C at 28000 rpm, each gradient section was divided into another tube and centrifuged again for 4 hours, at 4°C, at 28000 rpm, followed by discarding the supernatant and suspending the collected EcO83-OMV pellet in 500 µl of 0.9 % NaCl. Figures were created by using the program BioRender.

## 6.2 Bicinchoninic acid assay

The amount of protein in EcO83-OMV was measured by Bicinchoninic acid assay according to the manufacturer's protocol. 25 µl of the BCA standard (working range = 20-2000 µg/ml) and of EcO83-OMV suspension (EcO83-OMV samples were diluted by working reagent in ratio of 1:20) was used. 200 µl of the working reagent was added to each well and the microplate was mixed thoroughly on a plate shaker for 30 seconds and then incubated for 30 minutes at 37 °C, covered with a foil. The plate was cooled down to room temperature (RT) and the absorbance was measured at 562 nm on TECAN Spark™<sup>10</sup>M microplate reader.

## 6.3 Limulus Amoebocyte Lysate assay

The QCL-1000™ Endpoint Chromogenic Limulus Amoebocyte Lysate (LAL) assay (Lonza) was used to measure the level of endotoxin. For this procedure, a 96-well cell culture plate was pre-warmed on a thermo block at 37°C and covered with a foil. The standard was prepared according to the manufacturer's protocol, the EcO83-OMV samples were diluted (1:10, 1:100, and 1:1000) with reagent water. 50 µl of each standard and sample were added in duplicates to the plate, followed by 50 µl of LAL solution into all wells. The plate was incubated for 10 minutes at 37°C at 300 rpm and then 100 µl of pre-warmed substrate solution was added to

the wells and after 6 minutes the reaction was stopped by 100 µl of 25 % acetic acid. The plate was measured by a plate reader at 405-410 nm (TECAN Spark™10M microplate reader).

#### **6.4 Sodium-dodecyl sulfate-polyacrylamide gel electrophoresis**

10 µl of the isolated pure EcO83-OMV were heated for 10 minutes at 95°C with 3 µl 5 x SDS loading dye (Boster Bio), loaded on a Sodium-dodecyl sulfate (SDS)-polyacrylamide gel (NU-PAGE™ 4-12 % Bis-Tris gel, Invitrogen), and run for 30 minutes at 250 V. The gels were rinsed three times in distilled water for 5 minutes and stained with SimplyBlue™ SafeStain (Invitrogen) for one hour and then washed twice with distilled water for one hour.

#### **6.5 Nanoparticle tracking analysis**

The nano particle tracking analysis (NTA) of the EcO83-OMV was performed by size distribution of particles in EcO83-OMV samples via the LM10 Nanosight (Malvern Panalytical) in a collaboration with Dr. Taras Afonyushkin from the Research Center of Molecular Medicine of the Austrian Academy of Sciences. First, a calibration was done with silica beads (Microspheres-Nanospheres, SpecNano™), followed by diluting all samples 1:200 in PBS. During measurements, several 30 second videos were recorded. Data analysis was done by Nanosight Tracking Analysis software (NTA 2.3).

#### **6.6 Transmission electron microscopy**

Transmission electron microscopy (TEM) was done through a collaboration with Dr. Katy Schmidt from the Center for Anatomy and Cell Biology at the Medical University of Vienna. 3 µl of EcO83-OMV suspension (6.5 µg/µl) were applied on formvar-coated grids freshly coated with a thin layer of carbon. After 30 seconds of waiting until EcO83-OMV adhered, uranylacetate (1 %) for negative staining was applied in two steps. The dried grids were imaged using a FEI Tecnai20 electron microscope (Thermo Scientific) with a 4K Eagle-CCD camera. All images were edited by Adobe Photoshop Elements.

#### **6.7 *In vivo* and *in vitro* studies**

##### **6.7.1 OVA-induced mouse models**

C57BL/6J wildtype (WT) mice, interleukin-1β (IL-1β) knockout (KO) mice strain on the C57BL/6J background and Toll-like receptor 4 (TLR4) KO mice on the BALB/c background were provided by Dr. Miloslav Kverka from the Laboratory of Molecular and Cellular Immunology, Institute of Microbiology of the Czech Academy of Science, Czech Republic. BALB/c mice were obtained from Charles River (Sulzfeld, Germany). All mice were kept at the animal house of the Medical University of Vienna. And were provided with water and food *ad libitum*. Every experiment was approved by the Animal Experimentation Committee of the Medical University of Vienna and the Austrian Federal Ministry of Education, Science and Culture (BMBWF-66.009/0277-V/3b/2019).

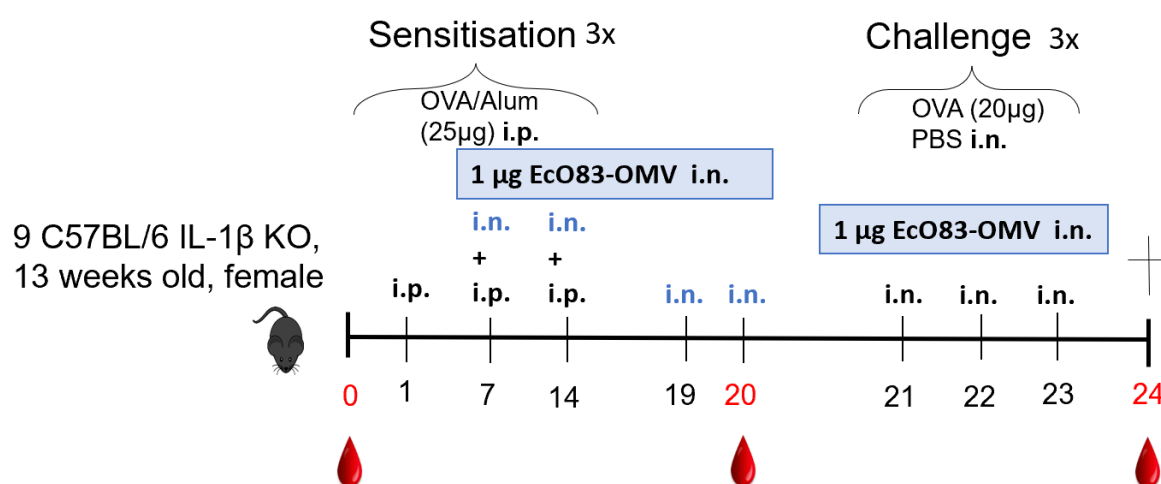


**Figure 5: Experimental set up of OVA-induced allergic IL-1 $\beta$  KO mice and the treatment of EcO83-OMV.** Mice (IL-1 $\beta$  KO C57BL/6; n=9) were sensitised i.p. with 150  $\mu$ l OVA/alum mix (25  $\mu$ g OVA + 25  $\mu$ l PBS + 100  $\mu$ l alum) on day 1, 7 and 14. Mice were treated i.n. with 30  $\mu$ l (1  $\mu$ g) EcO83-OMV or 30  $\mu$ l NaCl on day 7, 14, 19 and 20 (30 minutes before i. p. sensitisation). Blood was taken on day 0, 20 and 24. The challenge was performed on day 21, 22 and 23 with OVA/PBS (2  $\mu$ l OVA + 28  $\mu$ l PBS) followed 30 minutes later by retreatment with either 30  $\mu$ l NaCl or 30  $\mu$ l (1  $\mu$ g) EcO83-OMV i.n.

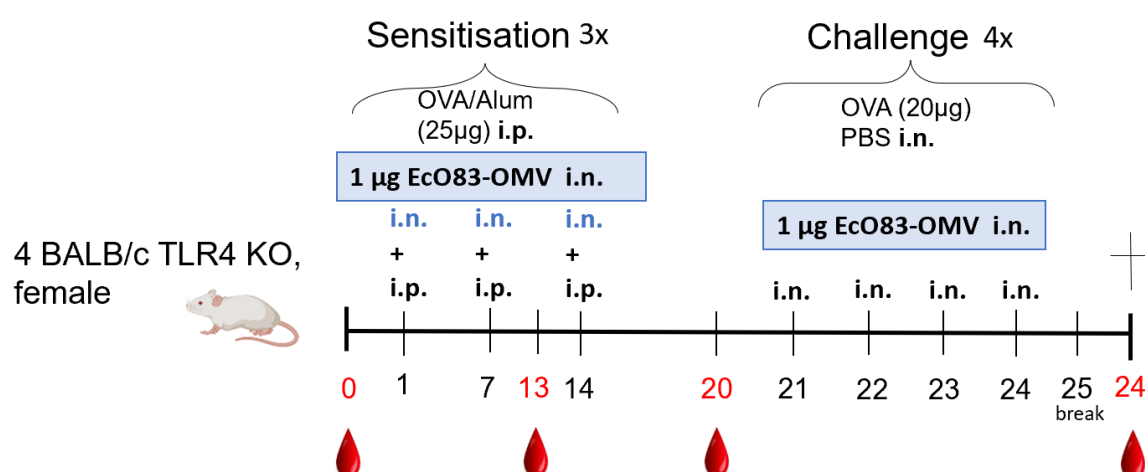


**Figure 6: Experimental set up of OVA-induced allergic TLR4 KO mice and the treatment of EcO83-OMV.** TLR-4 KO mice were all sensitised with an OVA/alum mix (10  $\mu$ g OVA + 40  $\mu$ l PBS + 100  $\mu$ l alum) i.p. on day 1, 7 and 14 and on the same day they were treated 30 minutes prior with either 30  $\mu$ l NaCl or 30  $\mu$ l (1  $\mu$ g) EcO83-OMV i.n. The mice were four times challenged i.n. on day 21, 22, 23 and 24 with 30  $\mu$ l OVA/PBS (100  $\mu$ g OVA in 30  $\mu$ l PBS) and prior intranasally treated either with 30  $\mu$ l of NaCl or 30  $\mu$ l (1  $\mu$ g) EcO83-OMV. The blood was taken on day 0, 13, 20 and 27.

To study the immunomodulatory effect of EcO83-OMV on the host immune system, the experimental model of allergic airway inflammation was established in C57BL/6J WT and IL-1 $\beta$  KO (**figure 5, table 1**) and in the BALB/c WT and TLR4 KO (**figure 6, table 2**) strains. In the first experiment (**figure 5, table 1**), mice (n=10) were divided in sham-treated (30  $\mu$ l NaCl) EcO83-OMV group (n=4) and 1  $\mu$ g EcO83-OMV treated group (n=5) (**figure 5, table 1**). 30 minutes before sensitisation was performed intraperitoneally (i.p.) (day 1, 7, 14) using 25  $\mu$ l OVA (Grade V, Sigma-Aldrich; Stock: 1 mg/ml) + 25  $\mu$ l PBS + 100  $\mu$ l of alum, on day 7, 14, 19 and 20 the mice were treated intranasally (i.n.) either as sham-group (30  $\mu$ l NaCl) or with 1  $\mu$ g EcO83-OMV in 30  $\mu$ l NaCl. The challenge was done on day 21, 22 and 23 using 30  $\mu$ l of OVA/PBS (2  $\mu$ l OVA (Stock: 10 mg/ml)+ 28 $\mu$ l PBS) i.n. and 30 minutes before starting the challenge, the mice were treated either with 30  $\mu$ l of NaCl or 1  $\mu$ g EcO83-OMV in 30  $\mu$ l NaCl via i.n. administration. For the second experiment (**figure 6, table 2**), the group setting can be seen in **table 2** below and the treatment was similar to experiment 1 except that the respective

groups that were treated with EcO83-OMV were treated starting on day 1 and challenged 4 times instead of 3 times.

**Treatment groups first *in vivo* experiment**

Group	Sensitization i.p.	Challenge i.n.	Treatment i.n.
<b>OVA</b> (female IL-1 $\beta$ KO; n=4)	OVA/Alum	OVA in PBS	30 $\mu$ l NaCl
<b>OVA/EcO83-OMV</b> (female IL-1 $\beta$ KO; n=5)	OVA/Alum	OVA in PBS	1 $\mu$ g EcO83-OMV in 30 $\mu$ l NaCl

**Table 1: Specific treatment of IL-1 $\beta$  KO mice.**

**Treatment groups second *in vivo* experiment**

Group	Sensitization i.p.	Challenge i.n.	Treatment i.n.
<b>OVA</b> (female TLR4 KO; n=2)	OVA/Alum	OVA in PBS	30 $\mu$ l NaCl
<b>OVA/EcO83-OMV</b> (female TLR4 KO; n=2)	OVA/Alum	OVA in PBS	1 $\mu$ g EcO83-OMV in 30 $\mu$ l NaCl

**Table 2: Specific treatment of TLR4 KO mice.**

## 6.7.2 Bronchoalveolar lavage

A tiny incision was made in the center of the trachea using microscissors to make a hole to thread the needle. The airways were lavaged twice with 500  $\mu$ l of ice cold PBS and collected in a tube. Bronchoalveolar lavage (BAL) fluid was spun down for 5 minutes at 2000 rpm, the supernatant was stored at -20°C, and the pellet suspended in 200  $\mu$ l PBS. The BAL cells were counted in Bürker-Türk counting chambers (Neubauer). After adjusting the cells to  $4 \times 10^4$ , the cell suspension was spun unto a glass microscope slide (VWR) and centrifuged by the Shandon Cytospin 4 centrifuge (Thermo Scientific) in combination with Shandon filter cards (Thermo Scientific). To wet the filters first, 100  $\mu$ l of PBS were spun on the slides for 3 minutes at 850 rpm, followed by the cell suspension using the same settings. The glass slides were taken out and air dried for 20 minutes and stained using the Hemacolor® staining kit (Merck) according to manufacturer's protocol. The slides were fixed for 30 seconds, stained in eosinophil reagent for 6 seconds followed by the hematoxylin staining for 4 seconds. After staining, the slides were rinsed in distilled water for 45 seconds.

## 6.7.3 Lung cell isolation and single cell suspension

Lungs were isolated from mice at sacrifice and placed on a cell strainer in a 6-well plate in wash medium (RPMI 1640 medium, Biowest®; with 1 ml of Gentamycin, Thermo Scientific) with Liberase (10  $\mu$ l/ml, Sigma-Aldrich) and DNase (0.5 mg/ml, Sigma-Aldrich). The tissue was minced into small pieces and incubated for 45 minutes at 37°C in the 5 % CO<sub>2</sub> incubator. The lung chunks were pressed through a 70  $\mu$ m cell strainer using the plunger of a 3 ml syringe.



The suspension was washed with 10 ml of fresh wash medium. Cell suspension was centrifuged for 6 minutes at 4°C at 1300 rpm (Eppendorf Centrifuge 5810 R). Remaining erythrocytes were removed by adding 3 ml of hemolysis buffer (ACK Lysing Buffer, Lonza) for 90 seconds. The reaction was stopped with 10 ml wash medium and centrifuged for 5 minutes at 1300 rpm. The supernatant was discarded and the pellet was suspended in 1 ml of RPMI complete medium and counted using Trypan blue (Thermo Scientific) to exclude dead cells. The cell suspension was adjusted to  $5 \times 10^6$  cells/ml. The single cell suspension was re-stimulated with OVA (100 µl/well) in a 96 well plate. As control, cells were cultured with media only or with ConA (100 µl/well). The re-stimulated cell suspension was incubated for 72 hours, at 37°C in 5 % CO<sub>2</sub> and the supernatant was stored at -20°C and used to perform cytokine ELISA. In parallel, non-stimulated cells were analysed by fluorescence-activated cell sorting (FACS) analysis.

#### **6.7.4 Spleen cells isolation and single cell suspension**

Spleens were isolated and collected in wash medium. The tissue was pressed through a metal net using the plunger of a 3 ml syringe. After resting for 10 minutes, the minced spleen was pushed through a 70 µm cell strainer into 10 ml of wash medium and centrifuged for 7 minutes at 4°C at 1300 rpm. The supernatant was discarded and the pellet suspended in 3 ml of hemolysis buffer. The reaction was stopped after 90 seconds with wash medium. Sample was centrifuged and the pellet was resuspended in 5 ml of RPMI complete medium. 2 µl of Acridine orange/propidium iodide (Thermo Scientific) staining was added to 18 µl of the cells to exclude dead cells. The counting was performed with a fluorescence cell counter (Luna™ Du-al Fluorescence Cell Counter, Logos Biosystems). The cell suspension was adjusted to  $5 \times 10^6$  cells/ml. This cell suspension was re-stimulated with OVA, medium or ConA (concentrations as above) and incubated for 72 hours, at 37°C in 5 % CO<sub>2</sub>. As above, the supernatant was stored at -20°C.

#### **6.7.5 Bronchial lymph nodes**

Bronchial lymph nodes (BLN) were pushed through a metal net in a petri dish. After resting for 10 minutes, the minced tissue was collected into a tube through a cell strainer. The cell suspension was centrifuged for 7 minutes at 4°C at 1300 rpm. The supernatant was discarded and the pellet resuspended in 3 ml haemolysis buffer, followed by stopping the reaction with wash medium (**table 6**). After centrifuging the suspension, 1 ml of RPMI complete medium was added and the cells were counted by acridine orange/propidium iodide as mentioned above. All further steps were done according to the spleen protocol above.

#### **6.7.6 Cytokine ELISA**

Detection of cytokines was performed by eBioscience™ ELISA-Ready-Set-Go! Kit (Thermo Scientific), according to the manufacturer's protocol (Thermo Scientific,). 96 well plates were coated with capture antibody in a coating buffer sealed, and incubated overnight at 4°C. On the second day the plate was washed using the ELISA wash buffer (**table 10**), followed by blocking for 1 hour at RT with an assay diluent and a repeated washing step. Then the standards and the samples (diluted depending on the origin of the sample and the cytokine) were applied on the plate (50 µl/well) and incubated over night at 4°C. On day 3, the washing step was repeated, followed by applying the detection antibody (100 µl/well) and then incubated for one hour at RT. After repeating the washing step, 100 µl/well of Avidin-

Horseradish Peroxidase (Avidin-HRP) was added and incubated for 30 minutes at RT. After another washing step, 3,3',5,5'-Tetramethylbenzidine (TMB) was applied (100 µl/well) for 5-15 minutes and the reaction was stopped with 0.18M H<sub>2</sub>SO<sub>4</sub> (50 µl/well, Sigma-Aldrich). The plate was measured at an absorbance range of 450/570 nm (TECAN Spark™ 10M microplate reader).

### **6.7.7 Histology of lung tissue**

One lobe of the lung was stored in 4 % formaldehyde (SAV liquid production GmbH). The fixed tissue was dehydrated in increasing concentrations of ethanol (30 % - 100 %, Sigma-Aldrich), followed by fixation in xylene (Sigma-Aldrich). Afterwards, the tissue was embedded in paraffin and cut in 4 µm slices using the semi-automated Rotary Microtome Microm HM 340E Thermo Scientific and placed on a glass microscope slide. Samples were incubated for 30 minutes at 56°C and then rehydrated in decreasing concentrations of ethanol (100 % - 30 %) and finally washed in distilled water.

### **6.7.8 Haematoxylin and Eosin staining**

The lung tissue sections were removed from the distilled water and stained with Hämalau (Mayer) for 10 minutes, followed by 2-3 washes in distilled water. After immersion of slides into 1% HCL (Sigma-Aldrich) in 70 % ethanol, samples were rinsed in running tap water for 7 minutes. Afterwards, the slides were stained by eosin working solution (5 %, Sigma-Aldrich) for 15 seconds and washed in distilled water. The tissue sections were dehydrated in increasing concentrations of ethanol (80 %, 96 %, and 99 %) by dipping into each concentration 2-3 times and incubated in xylene for 5 minutes. One drop of mounting medium (Histomount, Life Technologies) was added to the slides, covered with a cover slips and dried overnight. To record all the sections digitally the Tissue FAXSi PLUS (TissueGnostics) software was used.

### **6.7.9 Periodic Acid-Schiff staining**

The lung sections were dehydrated as described above and incubated in periodic acid solution (1%, Sigma-Aldrich) for 10 minutes followed by washing in distilled water for several times. Afterwards the slides were incubated for 20 minutes in Schiff's reagent (Periodic acid-Schiff (PAS) kit; Sigma-Aldrich) and then rinsed for 5 minutes in tap water, followed by counterstaining with haematoxylin solution for 90 seconds. The samples were rinsed, dehydrated, and mounted in (Histomount, Life Technologies) medium was applied, and all sections were covered with cover slips.

### **6.7.10 Isolation, cultivation, and stimulation of bone marrow derived**

#### **dendritic cells**

Femur and tibia were isolated from mice and put into ice cold PBS. The bones were washed in 70% ethanol for 1 minute and then rinsed with PBS twice. Both ends of the femur and tibia were cut off and with the help of a needle, the bone marrow was flushed out with 2.5 ml dendritic cell (DC) medium (RPMI 1640, FBS, Pen/Strep, Glutamine) into a cell strainer and collected in a Falcon tube, followed by another 5 ml of DC medium. The cell suspension was spun down for 7 minutes at 4°C at 1300 rpm. The supernatant was discarded, and the pellet was suspended in 10 ml of DC medium. The cells were counted by trypan blue (Thermo Scientific) and adjusted to 1 x 10<sup>7</sup> cells/ml by using DC medium containing 20 ng/ml

granulocyte macrophage-colony stimulating factor (GM-CSF, Invitrogen). For the cultivation, 10 ml of DC medium were pipetted on petri dishes and 200 µl of cells suspension was dropwise added to the centre of the petri dish. On the third day, 10 ml of DC medium was added to each petri dish and on day six, 9 ml of the old medium were removed, and 10 ml of fresh medium were added. On day eight, the cells were harvested, counted and adjusted to  $2 \times 10^5$ , and stimulated (500 µl/well), followed by incubation for 24 hours at 37°C in 5 % CO<sub>2</sub>. Medium only was used as negative control, Pam3CSK4 (1 µg/ml, InvivoGen), LPS (10 ng/ml, 100 ng/ml, 1 µg/ml or 10 µg/ml, InvivoGen), *E. coli* OMVs InvivoFit™ InvivoGen (1-100 ng/ml concentration), and EcO83-OMV (1-100 ng/ml concentration). 500 µl/well of each stimulus were added. The supernatants were stored at -20°C.

### 6.7.11 Flow cytometry – Fluorescence activated cell sorting (FACS)

After lung digestion (see above) the cells were spun down for 7 minutes at 4°C at 1300 rpm and then adjusted to  $5 \times 10^6$  cells/ml. 200 µl/well of cell suspension was added to a 96 well plate (V-bottom, BRANDplates®). Plates were centrifuged for 5 minutes at 1300 rpm and the supernatant was discarded. 200 µl of PBS were added to each well and thoroughly resuspended. After another spinning step, the supernatant was discarded and the washing step with PBS was repeated. After that 0.1 µl Fc block (Anti-Mouse CD16/CD32, eBioscience) and 1 µl of viability dye (Fixable Viability Dye eFluor™ 506, eBioscience) (**Table 3**) were diluted in 48.9 µl PBS, added to the cells and incubated for 15 minutes, in the dark on ice.

ef 506	live/dead	1:1000	Invitrogen
-	Fc-Block	1:100	Invitrogen

Table 3: Fluorophores and antibody surface markers for live/dead and Fc-Block staining.

The prepared antibody mix and the prepared FMO control mix (fluorescence minus one control) for each antibody (50 µl/well, dilutions and fluorophores are listed in **table 4 and 5**) were added to the cells and incubated for 30 minutes, in the dark on ice.

FITC	Ly6G	1:400	eBioscience
PE	CD11c	1:200	eBioscience
PerCP-Cy5.5	CD11b	1:600	eBioscience
PE-Cy7	MHCII	1:800	eBioscience
AF 647	Siglec F	1:100	eBioscience
APC Cy7	Ly6C	1:400	eBioscience
eFluor450	CD103	1:100	eBioscience

Table 4: Myeloid panel with fluorophores and antibody surface markers.

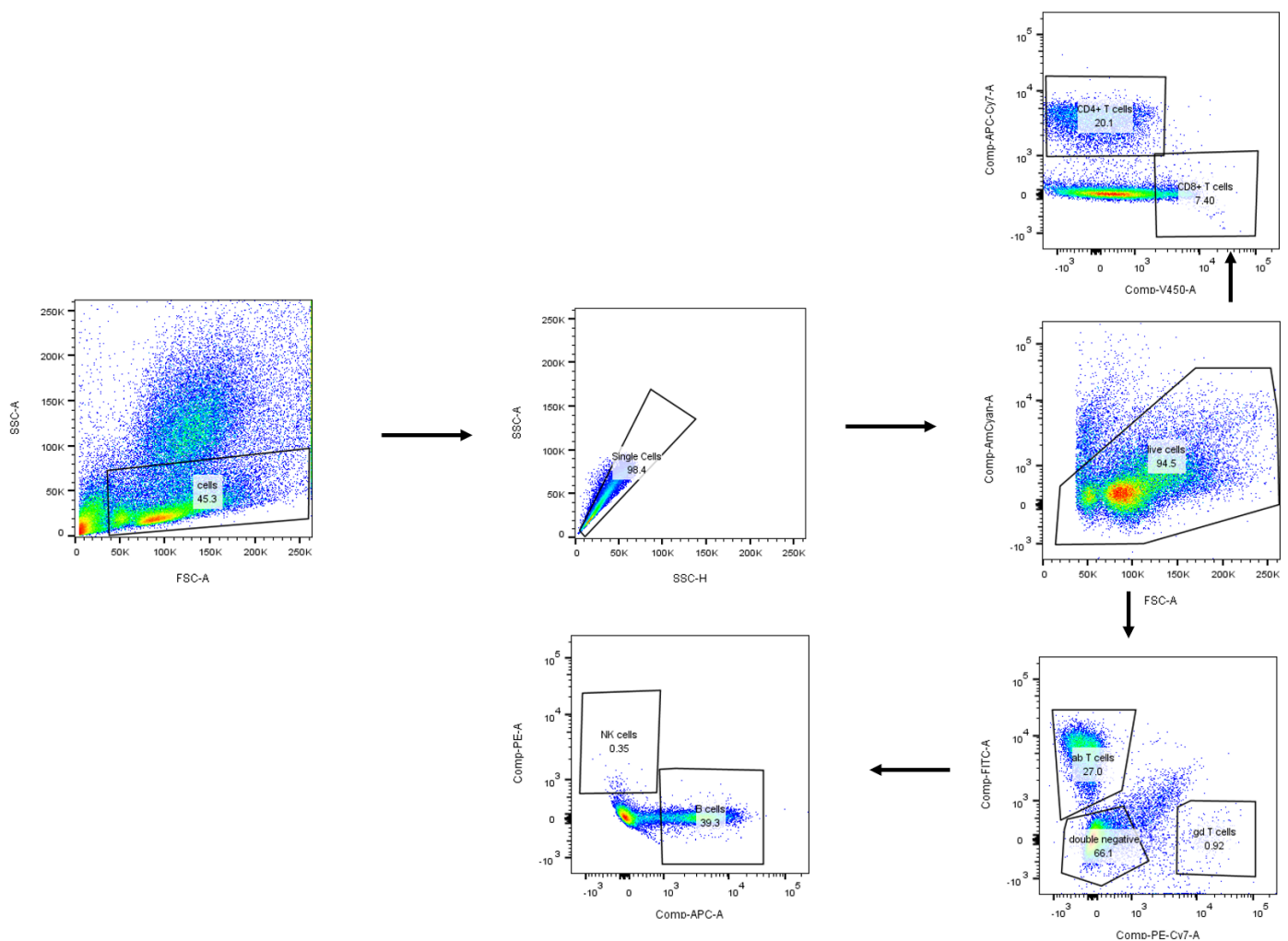
FITC	TCR beta	1:300	eBioscience
PE	Pan NK	1:200	Pharmingen
PE-Cy7	TCR gamma delta	1:200	eBioscience
APC	CD19	1:200	eBioscience
APC Cy7	CD4	1:400	BD
eFluor450	CD8a	1:200	eBioscience

Table 5: Lymphocyte panel with fluorophores and antibody surface markers.

The washing step with PBS was repeated twice and then 300 µl of PBS were added to the wells, resuspended and the cell suspension was then transferred to FACS tubes. Compensation beads (UltraComp eBeads™, Invitrogen) were used for compensation. For each fluorophore

one drop of beads was added into a microtube and dependent on each respective fluorophore, different volumes of FACS buffer (**table 10**) were added to these tubes and 1  $\mu$ l of each fluorophore, followed by 5 minutes of incubation in the dark and on ice. After centrifugation (using the same settings as above), discarding the supernatant, and repeating the washing step, 300  $\mu$ l of FACS buffer was added to wells, mixed and transferred to FACS tubes. All samples were measured with FACS Canto II (BD) and the data was analysed via FlowJo (BD).

### 6.7.12 Gating strategy



**Figure 7: Gating strategy for the lymphoid panel and the corresponding cell populations.** Lung cells were stained with surface antibody fluorophore markers. First, the main population of cells was gated, followed by choosing the single cells and excluding the dead cells. Next, the CD4+ T cell, CD8+ T cell,  $\alpha$ - and  $\beta$ -T cell,  $\gamma$ -/ $\delta$ - T cell populations were gated and furthermore the double negative cells were closely determined into NK cell and B cell populations.

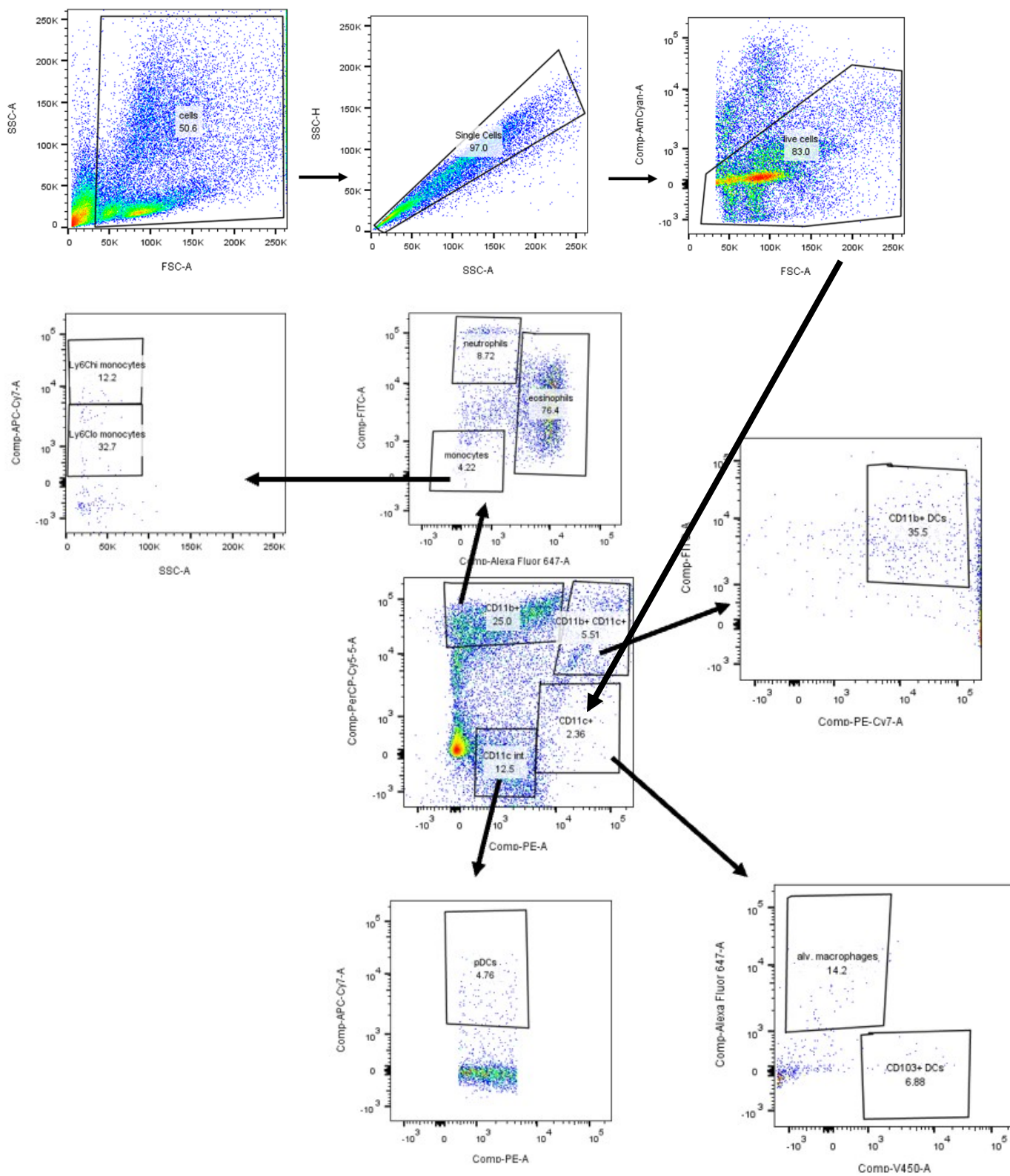


**Figure 8: Gating strategy for the myeloid panel and the corresponding cell populations.** Lung cells were stained with surface antibody fluorophore markers. After narrowing down to the single cells, excluding the dead cells, the cells were separated by being CD11b+ or CD11c+ cells or double positive. CD11b+ population was further divided into neutrophils, eosinophils and monocytes. The monocytes were distinguished between Ly6Clo monocytes (expressing low level of Ly6C) and Ly6Chi monocytes (expressing high level of Ly6C). The CD11c+ cell population was further characterised into CD11b+ DCs that expressed also MHCII. The CD11b+ cell population was separated into alveolar macrophages and CD103+ DCs. The CD11c+int. (internal) cells were further characterised into pDCs (plasmacytoid dendritic cells) when expressing Ly6C.

### 6.7.13 Rat basophil leukaemia cells assay

Rat basophil leukaemia (RBL) cells were cultured in RBL medium (**table 10**) and incubated for two days at 37°C in 5 %. On the third day, 3 ml of Trypsin/EDTA (**table 10**) was added for 1 minute to detach the adherent cells, which were then collected in a tube and centrifuged for 5 minutes at RT at 1300 rpm. After discarding the medium, cells were counted and adjusted to  $4 \times 10^5$  cells/ml and 100 µl were pipetted into a 96-well flat bottom tissue culture plate and incubated for 24 hours at 37° in 5 % CO<sub>2</sub>. The supernatants were removed and 40 µl of sera were added (dilution 1:10) and 40 µl of RBL medium/well were used for the last two lanes for positive and negative controls, respectively. The plate was incubated for 2 hours at 37°C in 5 % CO<sub>2</sub> and afterwards washed twice with 200 µl/well Tyrode's buffer (**table 10**). 100 µl/well of 0.3 µg/ml OVA (diluted in Tyrode's buffer) was added to the plate, except for the positive control and incubated for 30 minutes at 37°C. As a positive control, cells were treated with 10 µl/well of 10 % Triton X-100 (Honeywell Fluka™). The plate was then centrifuged for 5 minutes at 1300 rpm and 50 µl of the suspension was transferred to a 96-well ELISA plate. Another 50 µl of assay solution (**table 10**) was added to the wells, followed by an incubation for 1 hour at 37°C. The reaction was stopped by adding 100 µl/well of glycine buffer (**table 10**). The measurements were performed by the ELISA reader at an absorption range of 360 nm – 465 nm.

### 6.7.14 Antibody ELISA

Levels of antibodies were determined by ELISA. 96-well plates were coated with a carbonate buffer (**table 10**) and 5 µg/ml OVA at 4°C overnight. On the second day, the plate was washed with 200 µl/well ELISA wash buffer (**table 10**) and blocked with antibody ELISA blocking (**table 10**) for 2 hours at 37°C. After discarding the blocking solution, the sera samples were diluted according to the specific antibodies (IgE 1:10, IgG1 1:1000, IgG2a 1:500, and IgG2c 1:500), with antibody ELISA sample dilution buffer (**table 10**) at 4°C overnight. BAL fluid was tested undiluted. On day 3, a repeated washing step was done and then 100 µl/well of all the respective rat anti-mouse antibodies (Thermo Scientific) were added (IgE; IgA; IgG2a; IgG1; 1:500, and IgG2c 1:4000) and incubated for 2 hours at 37°C. After another washing step, 100 µl/well of mouse anti-rat IgG (peroxidase (POX)-conjugated mouse-anti-rat antibody, Dianova) was added, followed by 2 hours of incubation at RT. After incubation the washing step was repeated and TMB was used for detection (see above Cytokine ELISA). The optical density (O. D.) of the antibody level was measured at an absorption scale from 405-490 nm via the ELISA reader.

### 6.7.15 Cultivation and stimulation of HEK 293 transfected with NOD1, NOD2, TLR2, TLR2/CD14 and TLR4/CD14/MD2

HEK 293 NOD1, HEK 293 NOD2, HEK 293 TLR2, HEK 293 TLR2/CD14, and TLR4/CD14/MD2 (cells were provided by Dr. Martin Schwarzer, Institute of Microbiology of the Czech Academy of

Sciences) were seeded with 5 ml prepared medium (**table 10**) in a 25 cm<sup>2</sup> flask (Sarstedt AG & Co.) HEK TLR4 cells were seeded into a flask for sensitive adherent cells. Cells were incubated for 4 days at 37°C in 5 % CO<sub>2</sub>. The cell growth was monitored by light microscope (Zeiss), medium was discarded and cells washed with PBS. The cells were then incubated for 1 minute with 500 µl of Trypsin/EDTA. In the case of cells transfected with TLR4, only PBS was used. Cell were washed with 10 ml of cell medium (**table 10**), the cells were collected in a tube and spun down for 5 minutes at 1300 rpm. They were transferred to a 75 cm<sup>2</sup> flask and incubated for another 2 days at 37°C in 5 % CO<sub>2</sub>. On day 6 the cells were harvested and counted as described above, and then adjusted to 4 x 10<sup>5</sup> cells/ml. 100 µl of suspension was pipetted on a 96-well plate (flat bottom) and incubated for 24 hours at 37°C in 5 % CO<sub>2</sub>. On the next day the supernatant was discarded and 100 µl/well of the corresponding stimuli (**table 6**) were added to the cells and stimulated for 24 hours at 37°C in 5 % CO<sub>2</sub>. The supernatant was then taken up and stored at -20°C for further use.

<b>HEK 293 cells</b>	
<b>Stimulus</b>	<b>Company</b>
Medium	<b>Table 10</b>
TriDap	InvivoGen
MDP	InvivoGen
LPS 10 – 1000 ng/ml	InvivoGen
Pam3CSK4	InvivoGen
Endotoxin	Lonza
<i>E. coli</i> O83 10 <sup>6</sup> , 10 <sup>7</sup> , 10 <sup>8</sup>	Institute batch
<i>E. coli</i> OMVs 1 – 1000 ng/ml	institute batch
Heat inactivated EcO83-OMV 1 – 10000 ng/ml	Institute batch

**Table 6: Stimulation settings of HEK 293 cells transfected with NOD1, NOD2, TLR2, TL2/CD14, and TLR4/CD14/MD2.**

### 6.7.16 RNA isolation and reverse transcription

Isolation of mRNA from lung and NALT (nasal-associated lymphoid tissue), was done using the RNeasy® Mini Kit (Qiagen) according to the manufacturer's protocol. Less than 30 mg of the tissue were placed into a tube with homogenisation beads (PeqLab), 600 µl of a mix of RLT buffer (Qiagen) and β-mercaptoethanol (β-ME, Sigma-Aldrich) and homogenised for 1 minute at 5500 rpm (Precellys® Evolution, Bertin Instruments). 600 µl of 70% Ethanol were added to the lysates the suspension was transferred to a RNeasy Mini spin column which was placed in a 2 ml collection tube and centrifuged for 15 seconds at 3000 rpm. The flow-through was then discarded. Afterwards 700 µl of RW1 Buffer (Qiagen) were added to the column and centrifuged for 15 seconds at 3000 rpm and flow-through was discarded. Then, 500 µl of RPE

Buffer were pipetted into the column and again centrifuged for 15 seconds at 3000 rpm and this step was repeated again. The RNeasy spin columns were centrifuged another time to with 3000 rpm to dry the membrane. The spin column was placed in a new 1.5 ml collection tube and 30  $\mu$ l of RNase-free water was added on the spin column membrane to elute the RNA. The tube was then spun down for 1 minute at 3000 rpm. For the lung lobes, the last step was repeated with another 30  $\mu$ l of RNase-free water. NanoDrop 2000 (PreqLab) was used to measure the amount and purity of RNA in the sample.

### 6.7.17 Reverse transcription and real time quantitative polymerase chain reaction

The isolated mRNA samples were further transcribed into cDNA by using the iScript cDNA synthesis Kit (Bio-Rad). For each sample 4  $\mu$ l of 5x iScript Reaction Mix and 1  $\mu$ l of iScript Reverse Transcriptase were mixed with 1000 ng of mRNA samples and the respective amount of nuclease-free water (dependent on the mRNA concentration). The complete mix was incubated in a Thermal cycler (Bio-Rad) further described in the table below.

Priming	5 minutes at 25°C
Reverse transcription	20 minutes at 46°C
Reverse transcription – inactivation	1 minute at 95°C
Optional step	Hold at 4°C

**Table 7: Reaction step for reverse transcriptase.**

The cDNA was further used for real-time (RT) – quantitative polymerase chain reaction (qPCR). The components for the qPCR are listed in **table 8**. The RT qPCR mix was prepared in a 96-well TW-MT plate (Biozym) and the cDNA was replicated in the PqLab Kapa Sybr FAST Light Cyclor 480. The reaction set up is listed in **table 9**.

Mastermix (LightCycler® 480 SYBR Green I Master, Roche)	7.5 $\mu$ l
Forward primer (Eurofins Genomics)	0.5 $\mu$ l
Reverse primer (Eurofins Genomics)	0.5 $\mu$ l
Nuclease free water (LightCycler® 480 SYBR Green I Master, Roche)	4.5 $\mu$ l
cDNA	2 $\mu$ l

**Table 8: Master mix for cDNA real time qPCR.**



Denaturation	95°C	4 minutes
Amplification	95°C	30 seconds
	60°C	30 seconds 40x
	72°C	3 seconds
Melt	95°C	5 seconds
	65°C	1 minutes
	97°C	continuous

**Table 9: Reaction steps for real time qPCR.**

## 6.8 Statistic

All data in this thesis was statistically analysed by using GraphPad Prism software version 7.0 and 4.0 by applying a multiple T test. The entire data was shown as a mean including +- standard error of the mean (SEM). Significance was determined by applying the Holm-Sidak method with P values starting at < 0.05 up to < 0.0001 (\*p< 0.05, \*\*p< 0.01, \*\*\*p< 0.001, \*\*\*\*p< 0.0001).

## 6.9 Media and Solutions

Media and Solution	Company
<b>Carbonate Buffer (pH 5.8-9.8)</b>	
Na <sub>2</sub> CO <sub>3</sub> 3.93 g	Sigma-Aldrich
NaHCO <sub>3</sub> 5.29 g	Sigma-Aldrich
dH <sub>2</sub> O 1 l	
<b>Tyrodé's Buffer</b>	
dH <sub>2</sub> O 1 l	
Tyrodé's Salts 1x	Sigma-Aldrich
NaHCO <sub>3</sub> 1 g	Sigm-Aldrich

HEPES 10 ml	Gibco™
BSA (bovine serum albumin fraction γ) 0.1 %	Roth
<b>Citrate Buffer (pH 4.5)</b>	
dH <sub>2</sub> O 500 ml	
Citric acid 10.5 g	Sigma-Aldrich
<b>Assay solution</b>	
Citrate buffer 5 ml	
4-MUG 80 µl	Sigma-Aldrich
<b>Wash medium</b>	
RPMI 1640 500 ml	Biowest
Gentamycin 1 ml	Thermo Scientific
<b>Complete medium</b>	
RPMI 1640 500 ml	
FCS 50 ml	
Glutamine 5 ml	Sigma-Aldrich
β-mercapthoethanol 50 µl	
Gentamycin 20 µl	
<b>Stop solution (ELISA)</b>	
H <sub>2</sub> SO <sub>4</sub> 10 ml	Sigma-Aldrich
dH <sub>2</sub> O 90 ml	
<b>ELISA wash buffer</b>	
dH <sub>2</sub> O 1 l	
10x PBS 10 ml	
Tween 500 µl	Roth
<b>Blocking buffer (ELISA)</b>	
10x PBS 10 ml	

dH <sub>2</sub> O 1 l	
BSA 1 %	Roth
Tween 0.05 %	
<b>Antibody ELISA sample dilution buffer</b>	
10 x PBS 10 ml	
dH <sub>2</sub> O 1 l	
BSA 0.5 %	
Tween 0.05 %	
<b>Murine DC medium</b>	
RPMI 1640 500 ml	
FBS (heat inactivated) 50 ml	
Pen/Strep 5 ml	Sigma-Aldrich
Glutamine 5 ml	
GM-CSF 2 µl/10 ml	
<b>RBL medium</b>	
RPMI 1640 500 ml	
FCS (heat inactivated) 50 ml	
Glutamine 10 ml	
Sodium Pyruvate 10 ml	Biochrom
HEPES 5 ml	
β-mercapthoethanol 50 µl	
Pen/Strep 5 ml	
<b>HEK 293 NOD1 and HEK 293 NOD2 medium</b>	
DMEM 500 ml	Gibco™
FCS (heat inactivated) 50 ml	
Blasticidin 550 µl	InvivoGen

Normocin 1.1 m l	InvivoGen
Pen/Strep 2.75 ml	Sigma-Aldrich
<b>HEK 293 TLR2 medium</b>	
DMEM 500 ml	
FCS (heat inactivated) 50 ml	
Puromycine 500 µl	Sigma-Aldrich
Gentamycin 1 ml	
<b>HEK 293 TLR2/CD14 medium</b>	
DMEM 500 ml	
FCS (heat inactivated) 50 ml	
Pen/Strep 5 ml	
Blasticidin 550 µl	
Hydrogold 275 µl	Thermo Scientific
<b>HEK 293 TLR4/CD14/MD2 medium</b>	
DMEM 500 ml	
FCS (heat inactivated) 50 ml	
Gentamycin 1 ml	
Blasticidin 550 µl	
Hydrogold 275 µl	
<b>BHI medium</b>	
BHI broth power 37 g	
dH <sub>2</sub> O 1 l	
<b>Eosin working solution</b>	
Eosin 300 ml	Sigma-Aldrich
Acetic acid 100 µl	
dH <sub>2</sub> O 600 ml	

<b>FACS buffer</b>	
BSA 1 g	
Na-azid 1 g	
EDTA 2.5 ml	
1x PBS 1 l	

**Table 10: List of all media and solution that were used for the experiments.**

## 7 Results

### 7.1 Characterisation of EcO83-OMV

#### 7.1.1 Transmission electron microscopy

To confirm the presence of vesicle in the sample after purification steps, crude and purified vesicles were analysed by TEM. Images of the crude preparation show a spherical character of vesicles and the presence of cell debris and fragments of flagella, which were not removed by gradient ultracentrifugation (**figure 9 A**). The fraction collected after density gradient centrifugation contained smaller and more homogenous spherical vesicles compared to crude vesicles (**figure 9 B**).

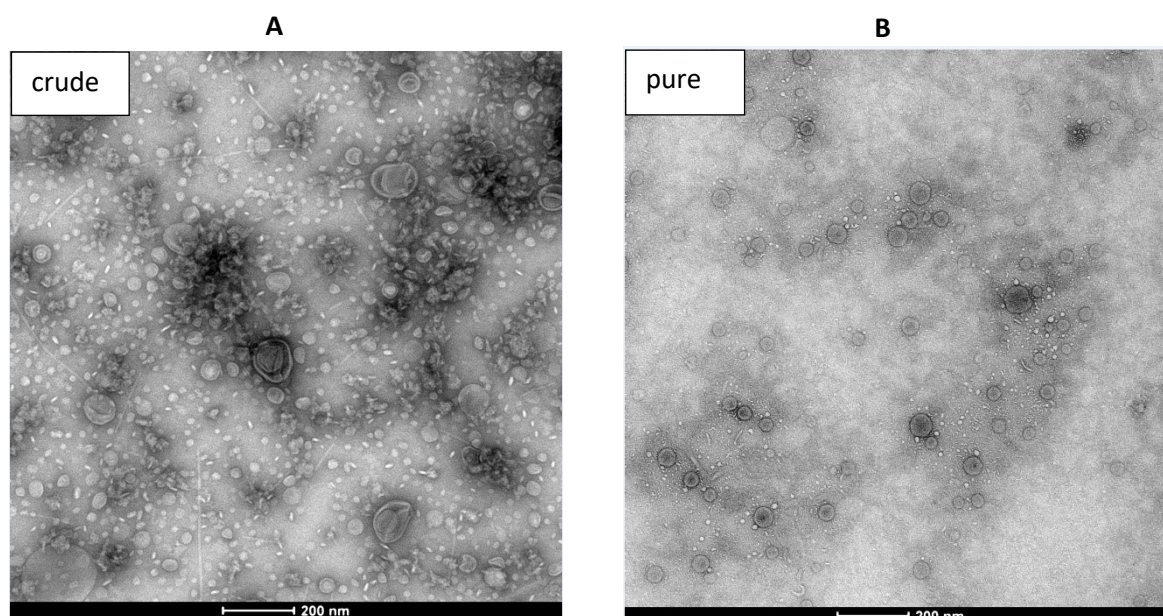


**Figure 9: Characterisation of EcO83-OMV using TEM.** Images of crude (A) and pure (B) EcO83-OMV. The picture was taken with FEI Tecnai20 electron microscope.

#### 7.1.2 Nanoparticle tracking analysis

Crude and pure EcO83-OMV were analysed using NTA. **Figure 10** depicts their size distribution and concentration. Both crude and pure samples were polydispersed in size, with a diameter ranging from ~ 50 to 400 nm and median sizes of ~ 100 nm.

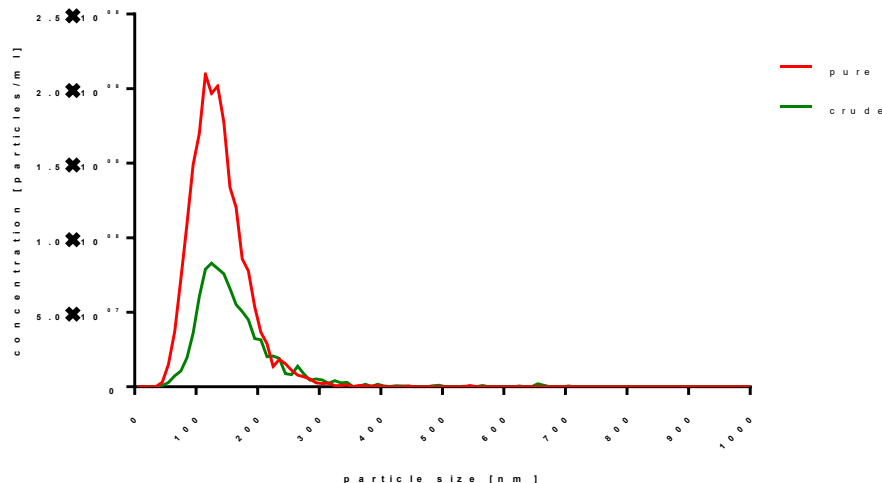


**Figure 10: NTA analysis of EcO83-OMV.** The crude (green line) and pure (red line) vesicles were analysed by NTA. The concentration of particles/ml is shown on the y axis and the size distribution of vesicles on the x axis.

### 7.1.3 Measuring the endotoxin levels and protein content

The LAL assay was performed to determine the endotoxin level in crude and in pure EcO83-OMV. One litre of *E. coli* O83 culture yielded 6500 µg/ml (6 mg/ml), as measured by BCA. In the crude fraction, 100 pg of protein contained 1 EU endotoxin. In the pure fraction, the protein concentration was 1000 mg/ml and 1.2 EU endotoxin per 100 pg vesicle protein were measured.

## 7.2 Stimulation of mouse splenocytes derived from wild type and TLR4-deficient mice with EcO83-OMV

The splenocytes of WT and TLR4 KO BALB/c mice were isolated and prepared as a single cell suspension. Stimulation of cells derived from TLR4 KO mice with LPS led to lower production of IL-6 and TNF-α (**figure 11**) compared to stimulation of cells from WT controls (**figure 11**). The level of IL-1β, IL-17, IL-10, and IFN-γ induced by LPS was comparable between KO and WT cells (**figure 11**). Stimulation by Pam3CSK4 led to comparable levels of IL-6, TNF-α, IL-1β, IL-10, and, IFN-γ in WT and TLR4 KO cells (**figure 11**). The production of IL-17 and IFN-γ induced by the parent bacterial strain *E. coli* O83 was significantly higher in the TLR4 KO cells compared to the WT cells and no difference was observed for the other cytokines (**figure 11**). In all cytokines, except for IL-1β, there was no dose dependent effect to observed between the three different concentrations of EcO83-OMV in both KO and WT mice (**figure 11**). The production of TNF-α induced by 10 ng/ml EcO83-OMV showed a significant reduction in the KO strain compared to the WT strain and for the other concentrations a trend of reduction was seen (**figure 11**). IL-6 production induced by all three concentrations of EcO83-OMV was reduced in the KO strain compared to the WT strain (**figure 11**). The level of production in all other cytokines induced by 1 ng/ml, 10 ng/ml and 100 ng/ml of EcO83-OMV showed no significant difference between the two mouse strains (**figure 11**). This experiment was performed one time, n=2. Due to the COVID-19 pandemic, it was not possible to obtain additional TLR4 KO mice to repeat the experiment.

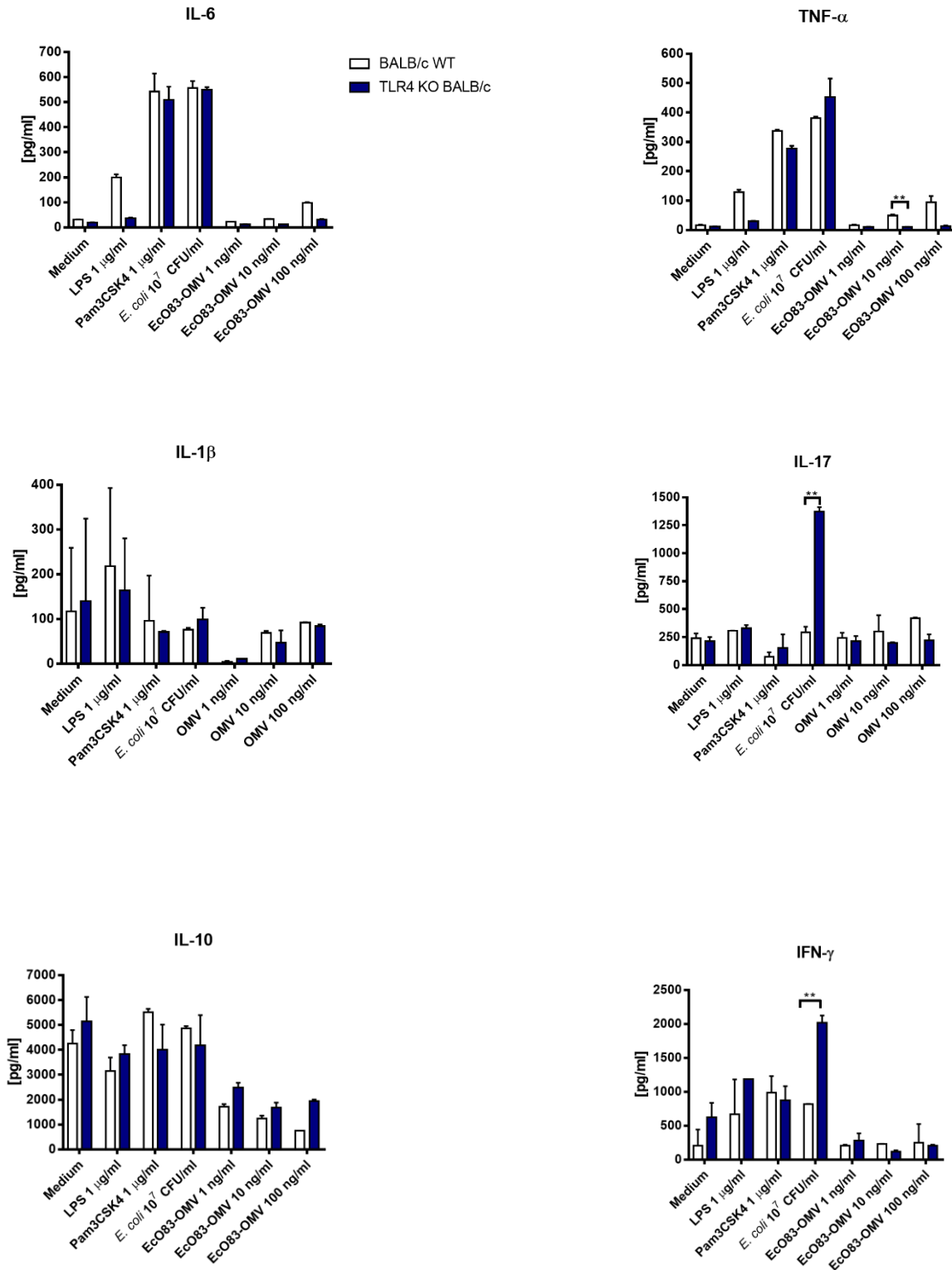


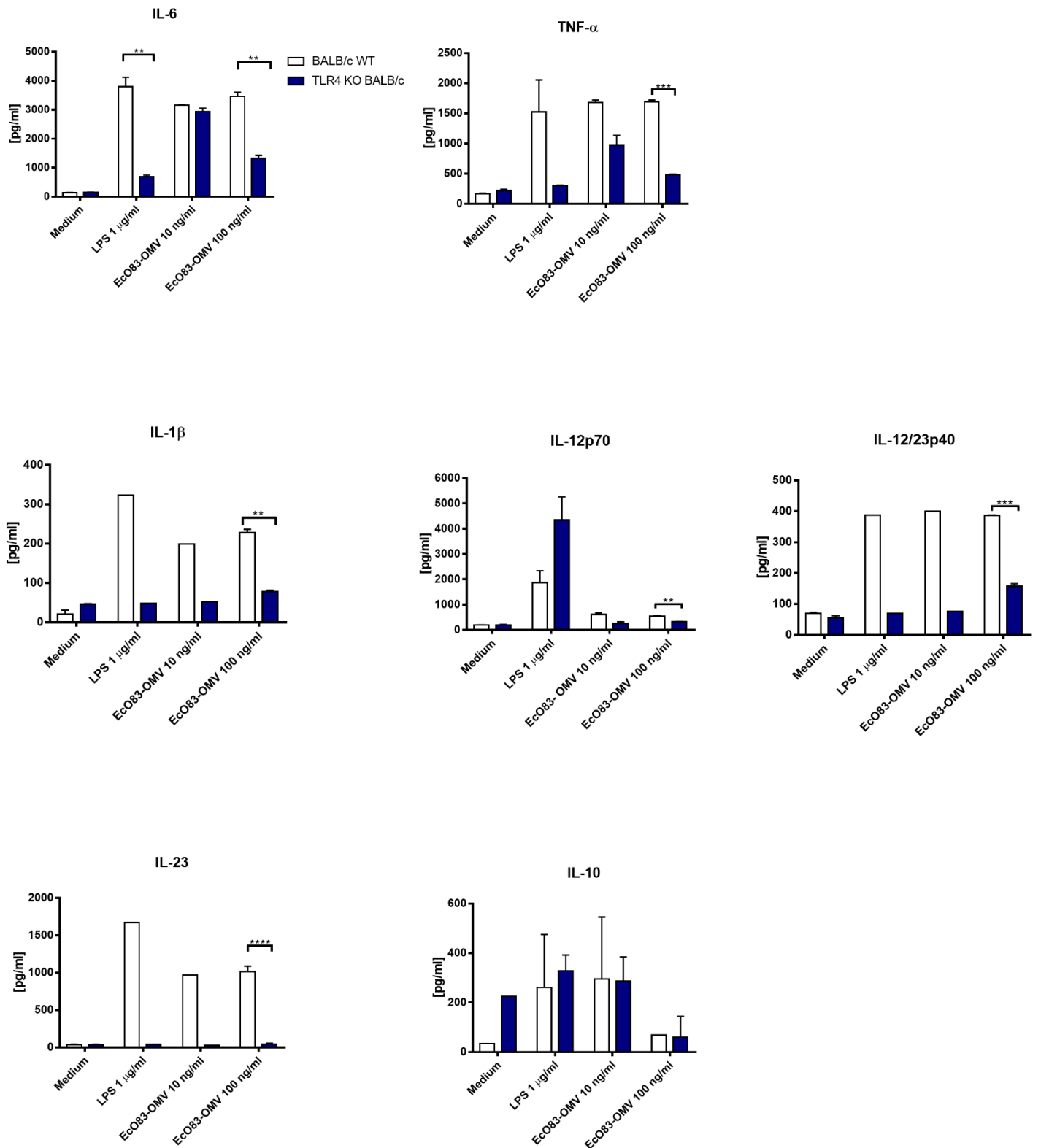
**Figure 11: Production of cytokines in mouse splenocytes derived from WT and TLR4 KO BALB/c mice.** Splenocytes were cultured with medium only or stimulated with LPS (1  $\mu$ g/ml), Pam3CSK4 (1  $\mu$ g/ml), *E. coli* O83 (1  $\times$  10<sup>7</sup> CFU/ml) and EcO83-OMV (1 ng/ml, 10 ng/ml and 100 ng/ml) for 72 hours. Supernatants were collected and levels of cytokines were measured by ELISA. The statistical analysis was done by using a multiple t test. \*\*p < 0.01. n=2. Groups: WT BALB/c and TLR4 KO BALB/c.



### 7.3 Stimulation of mouse bone marrow derived dendritic cells derived from wild type and TLR4-deficient mice with EcO83-OMV

We have shown previously that EcO83-OMV induce signalling via TLR4 (*Schmid et al.* 2020). Here, we isolated BM from BALB/c WT and TLR4 KO mice and generated BMDCs. The stimulation of WT cells with LPS and EcO83-OMV led to the production of IL-6, TNF- $\alpha$ , IL-1 $\beta$ , IL-12/23p40, IL-12p70, IL-23 and IL-10. The levels of IL-6, TNF- $\alpha$ , IL-1 $\beta$ , IL-12p70, IL-12/23p40, and IL-23 induced by 10 ng/ml and 100 ng/ml EcO83-OMV in WT mice were comparable (**figure 12**).

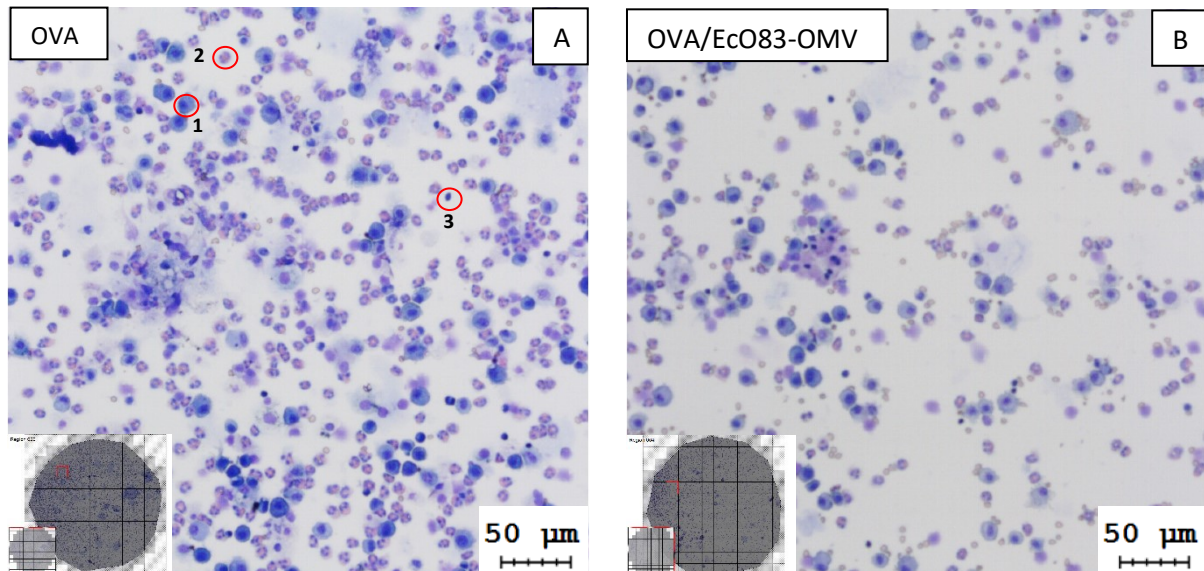
As expected, LPS-induced levels of IL-6, TNF- $\alpha$ , IL-1 $\beta$ , IL-12/23p40, and IL-23 were reduced in the cell cultures derived from TLR4 KO mice in comparison to levels observed in WT cells (**figure 12**). Except IL-10, the level of all cytokines induced by 100 ng/ml of EcO83-OMV were significantly reduced in KO mice compared to WT mice (**figure 12**). Though not significant, the levels of IL-6, TNF- $\alpha$ , IL-1 $\beta$ , IL-12p70, IL12/23p40, and IL-23 induced by 10 ng/ml of EcO83-OMV were partially reduced in TLR4 KO mice relative to WT controls (**figure 12**). This experiment was performed one time with n=2. Due to the COVID-19 pandemic, it was not possible to obtain additional KO mice; therefore, it was not possible to repeat the experiment.



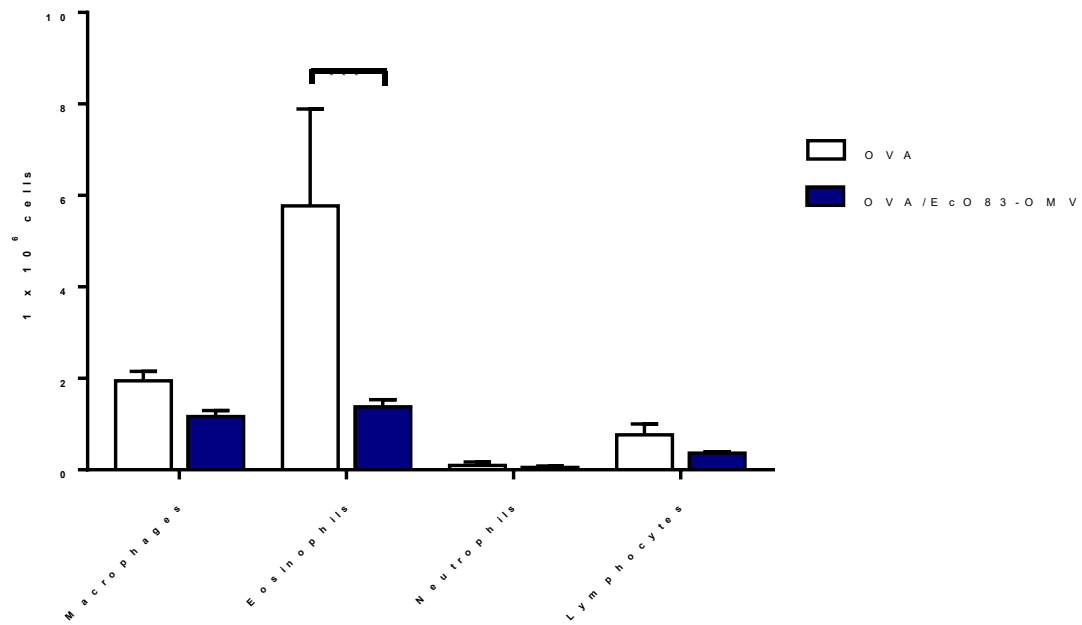
**Figure 12: Production of cytokines in mouse BMDC derived from WT and TLR4 KO BALB/c mice.** BMDC were cultured with medium only or stimulated with LPS (1  $\mu$ g/ml) and Eco83-OMV (10 ng/ml or 100 ng/ml) and incubated for 24 hours. Supernatants were collected and levels of cytokines were measured by ELISA. The statistical analysis was done by using a multiple t test. \*\* $p < 0.01$ , \*\*\* $p < 0.001$ , \*\*\*\* $p < 0.0001$ .  $n=1$ . Groups: WT BALB/c and TLR4 KO BALB/c.

## 7.4 The role of TLR4 in the recognition of EcO83-OMV in the mouse model of OVA-induced allergy

Previously, we have shown that intranasal application of *E. coli* O83 reduced allergic airway inflammation in mice and this effect was abolished in TLR4 KO mice <sup>47</sup>. Along these lines, Schmid *et al.* have shown that EcO83-OMV reduce the development of allergic airway inflammation in wild type BALB/c mice <sup>64</sup>. As shown above, level of EcO83-OMV-induced cytokines by spleen and dendritic cells *in vitro* was partially TLR4-dependent. Therefore, we tested whether EcO83-OMV can prevent the development of allergy in TLR4-deficient mice. The TLR4 KO mice were sensitised and challenged with OVA as shown in **figure 6**. The BAL fluid was isolated and cells collected. **Figure 13** shows that, the infiltration of inflammatory, especially eosinophils, to the lungs is reduced in the OVA/EcO83-OMV group in comparison to OVA controls. The results shown by the microscope image is supported by the results in **figure 14** showing that the numbers of eosinophils were significantly decreased in the OVA/EcO83-OMV group in comparison to the OVA controls.



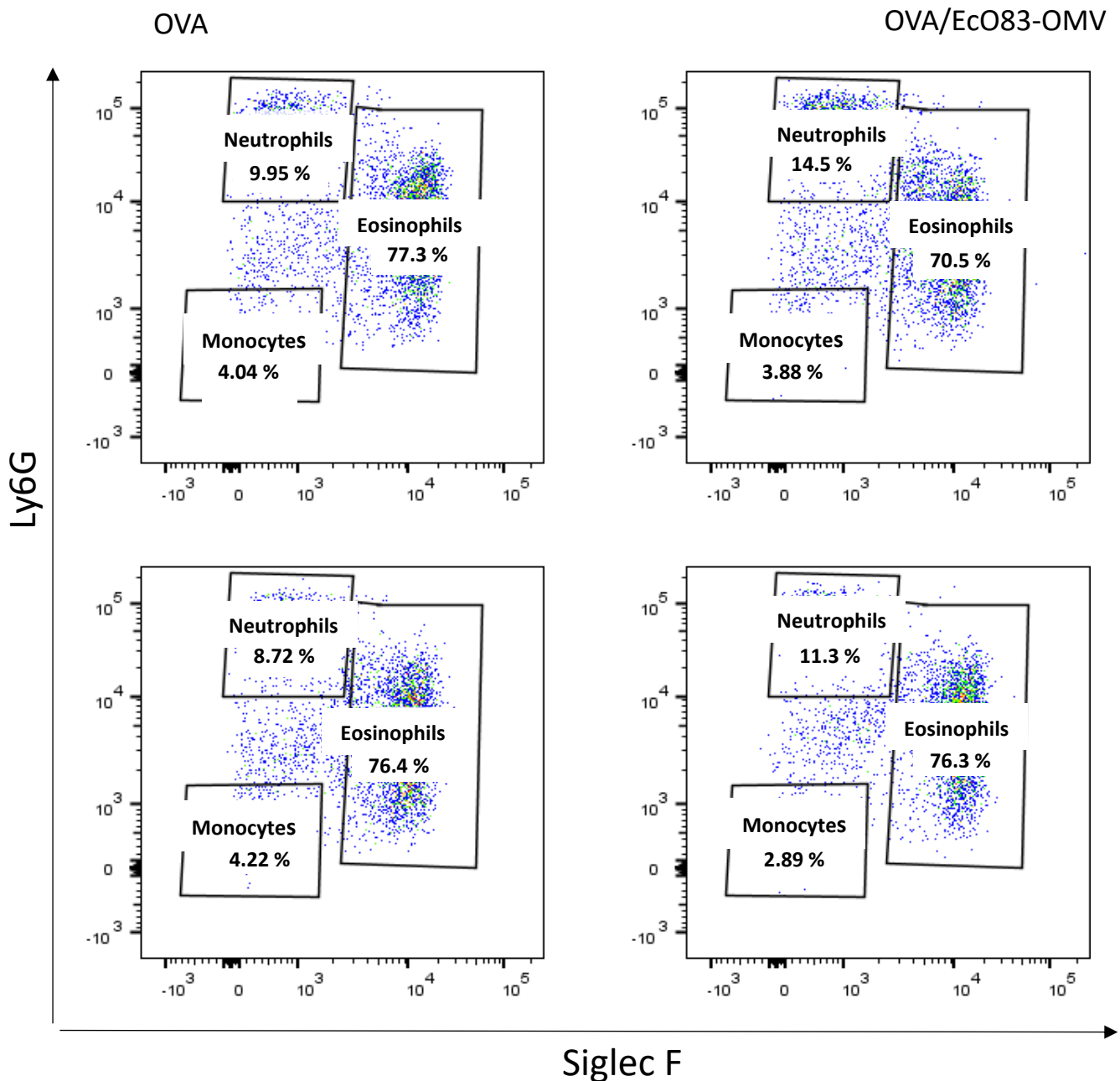
**Figure 13: Microscope images of stained BAL fluid cells.** The BAL fluid cells collected from (A) OVA and (B) OVA/EcO83-OMV group were stained by using the Hemacolor® staining kit and imaged with FAXSi PLUS. In the left corner the whole image of the stained cells is shown, and the red lines depict the specific spot from where the zoomed picture was taken. The red circle indicates the individual cells. 1=macrophages, 2=eosinophil, 3=lymphocyte.

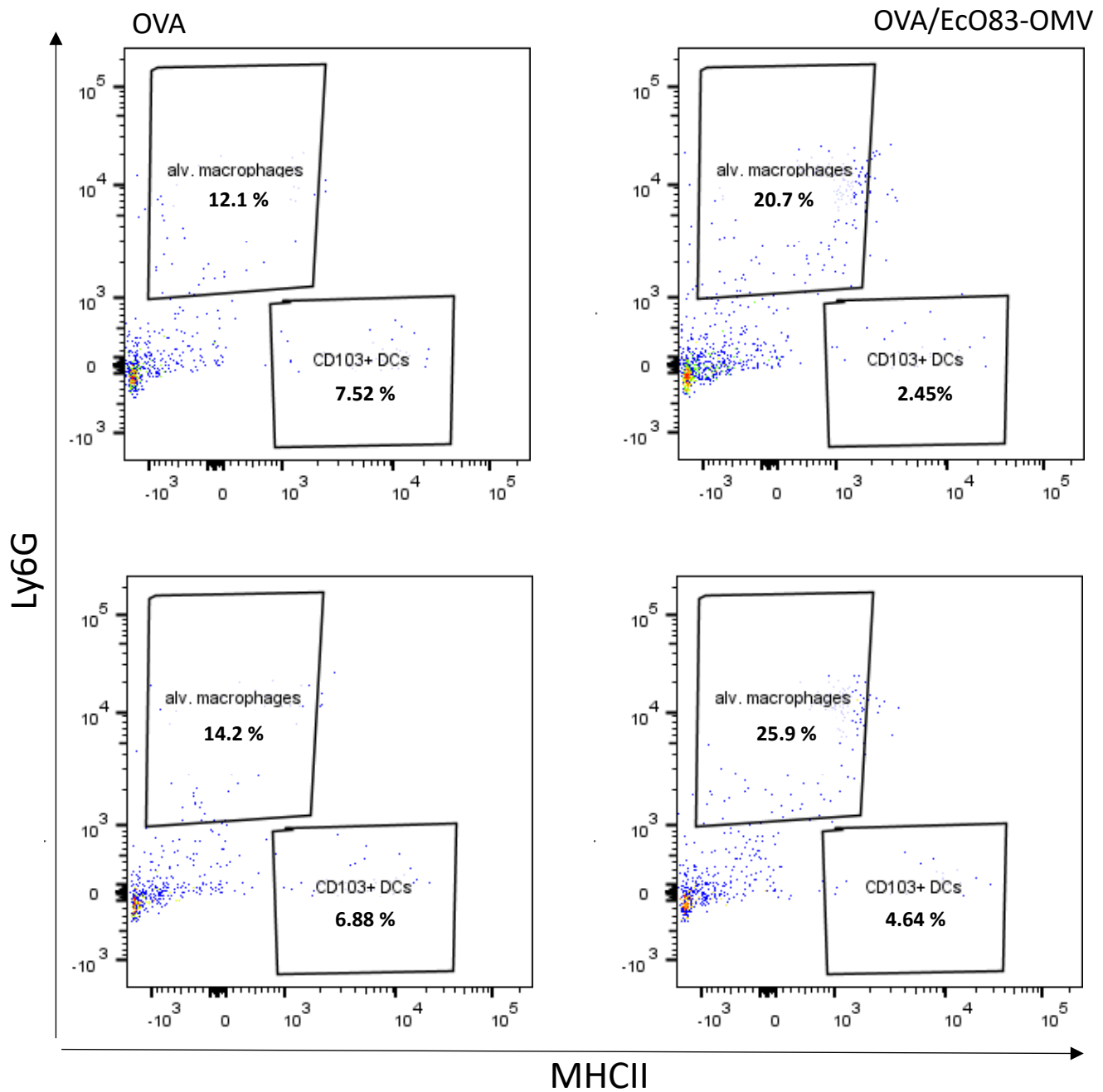


**Figure 14: Absolute numbers of cell populations in BAL fluid of TLR4 KO mice.** (A) OVA and (B) OVA/EcO83-OMV groups. The statistical analysis was done by using a multiple t test. \*\*\* $p < 0.001$ .

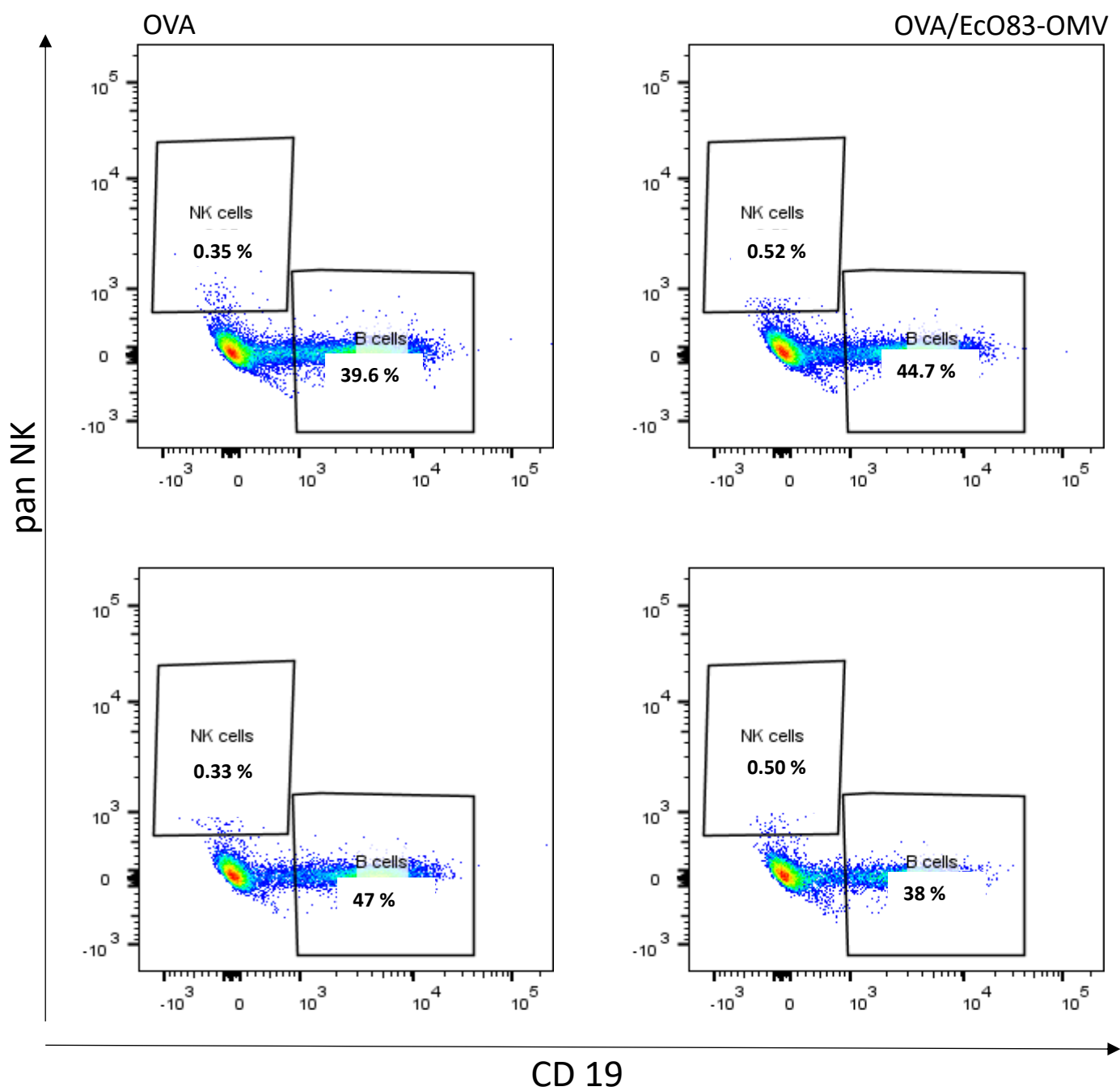
### 7.4.1 Lung cell population analysis

Additionally, part of the lung single cell suspension was used to perform FACS analysis to determine the specific cell populations and to see if there was a difference between the two treatment groups: OVA and OVA/EcO83-OMV. As displayed in **figure 15**, the numbers of neutrophils, monocytes, and eosinophils do not differ between OVA and OVA/EcO83-OMV groups. Eosinophils were the most abundant population in both groups. The percentage of alveolar macrophages abundance in percentage in the OVA/EcO83-OMV group than in the OVA group (**figure 15**). The number of NK cells (**figure 16**) were low in both groups. The number of the B cells,  $\alpha\beta$  and  $\gamma\delta$  T cells were similarly distributed in both EcO83-OMV-treated and control TLR4 KO mice (**figure 16**).





**Figure 15: FACS analysis of myeloid cells in lung cells derived from TLR4 KO BALB/c mice.** Cells were analysed by FACS Canto II and FlowJo. The percentage of each cell population is given. On the inside of the scale the surface marker is listed and on the outside the cell population. Both treatment groups are represented: OVA and OVA/EcO83- OMV. n=4



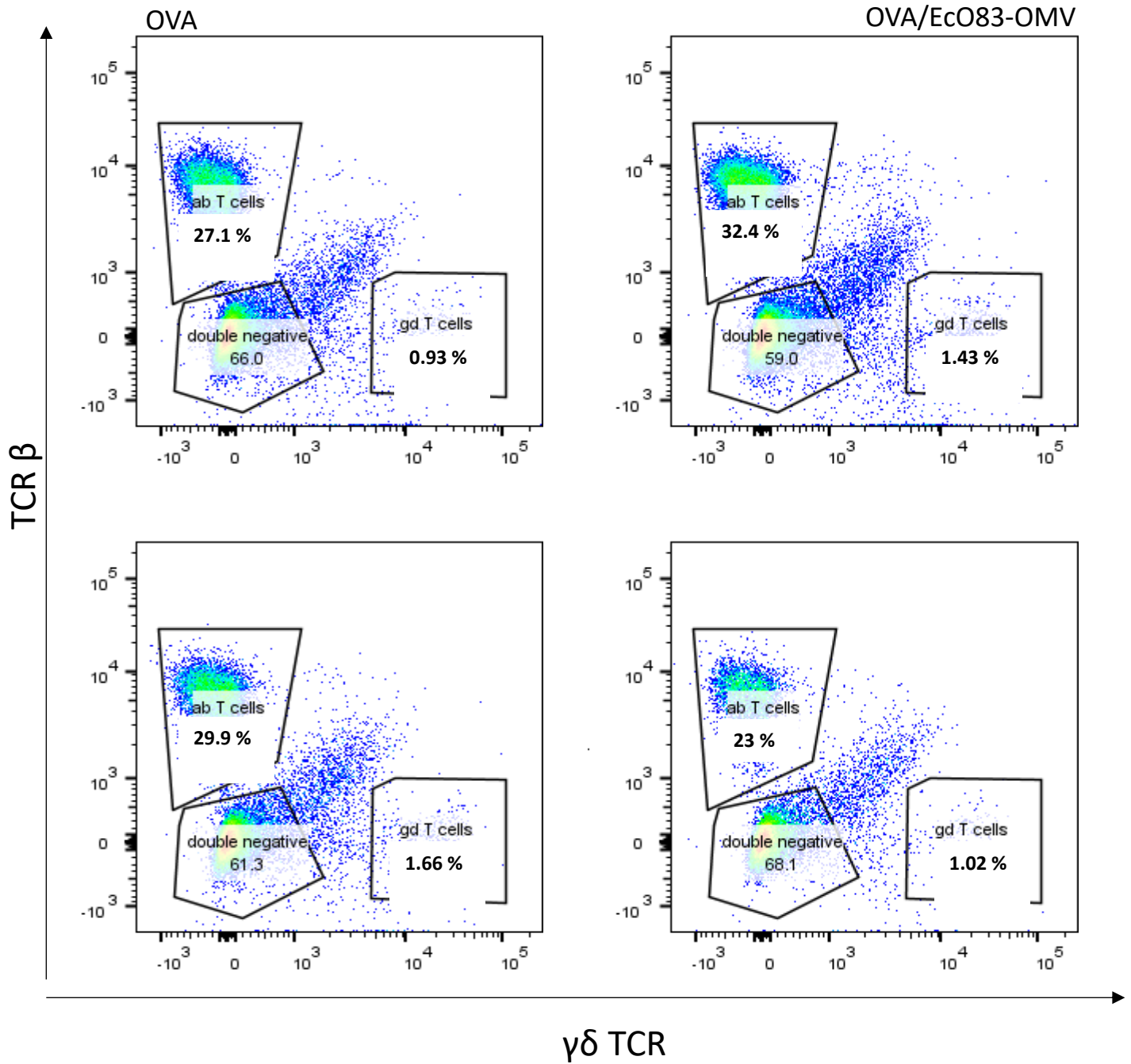


**Figure 16: FACS analysis of lymphoid cells in lung cells derived from TLR4 KO BALB/c mice.** Cells were analysed by FACS Canto II and FlowJo. The percentage of each cell population is given. On the inside of the scale the surface marker is listed and on the outside the cell population. Both treatment groups are represented: OVA and OVA/EcO83-OMV. n=4.



#### **7.4.2 *Ex vivo* stimulation of lung and spleen cells derived from sensitised and challenged TLR4 KO BALB/c mice**

Lung and splenocyte single cell suspensions from OVA-sensitised and challenged TLR4 KO mice were stimulated and supernatants were analysed to measure levels of cytokines. In the lung cells (**figure 17**), the level of IL-4, IL-5 IL-10 and IFN- $\gamma$  upon OVA re-stimulation did not differ between the two treatment groups (OVA and OVA/EcO83-OMV). However, the level of IL-13 was reduced by EcO83-OMV-treatment in comparison to sham-treated mice (**figure 17**). The production of IL-4, IL-5, and IL-13 was comparable in both treatment groups after stimulation by ConA, whereas EcO83-OMV-treatment reduced the levels of IL-10 and IFN- $\gamma$  (**figure 17**). In spleen cell cultures, the levels of OVA-specific IL-4, IL-5, and IL-10 were significantly reduced by EcO83-OMV in comparison to the OVA group (**figure 18**). The level of IFN- $\gamma$  was comparable between both OVA and OVA/EcO83-OMV groups (**figure 18**). Stimulation by ConA led to reduced levels of IL-5 and IL-10 in cells derived from EcO83-OMV-treated mice compared to OVA group, and also IL-4 showed a trend of reduction in the EcO83-OMV group relative to the OVA group (**figure 18**). IFN- $\gamma$  cytokine production induced by ConA showed no significant difference between cells from the two treatment groups (**figure 18**).

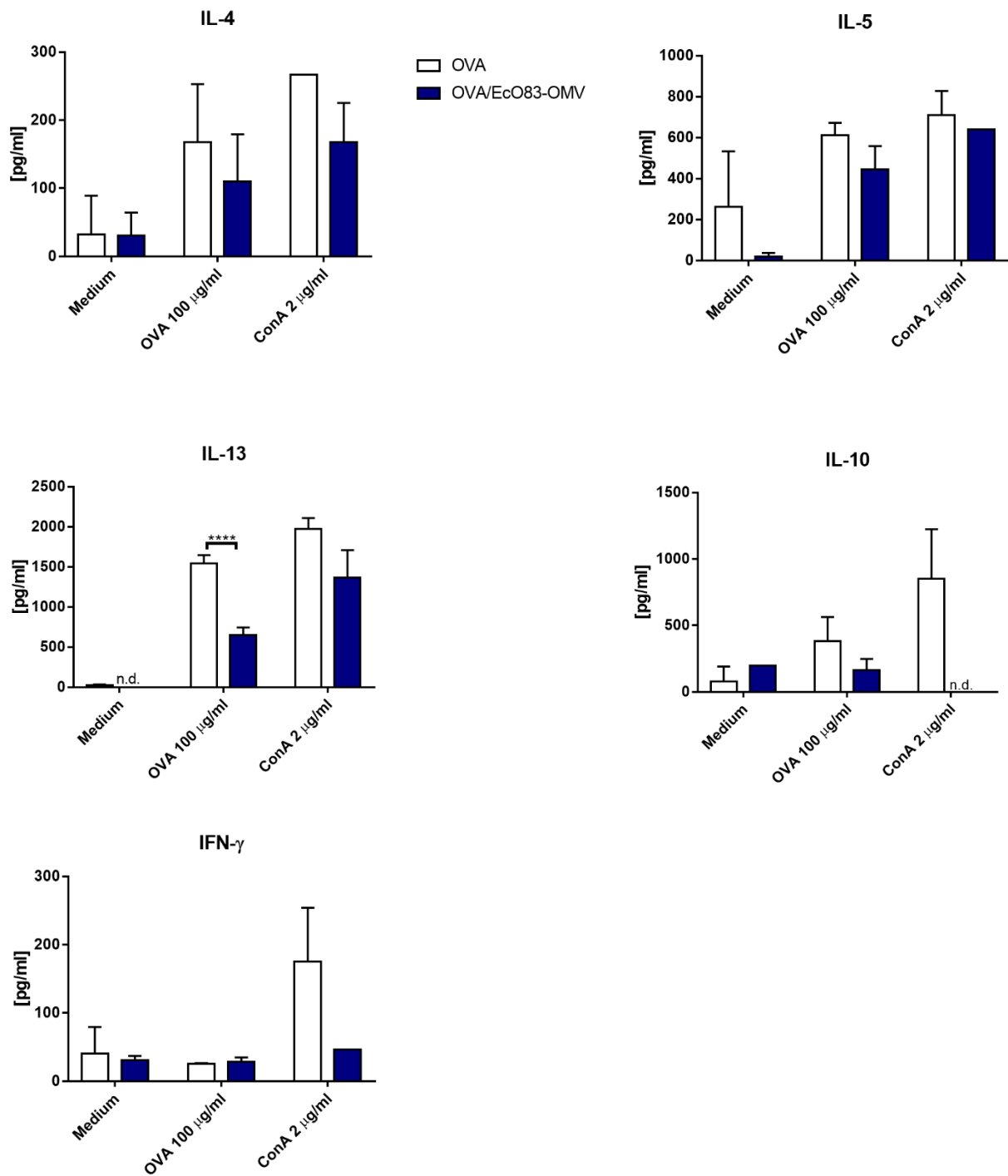


**Figure 17: Cytokine production of lung cells derived from allergic TLR4 KO BALB/c mice** Lung cells were cultured with medium only or stimulated with OVA (100  $\mu$ g/ml) and ConA (2  $\mu$ g/ml) for 72 hours. Both treatment groups are represented: OVA and OVA/EcO83-OMV. Supernatants were collected and levels of cytokines were measured by ELISA. The statistical analysis was done by using a multiple t test. \*\*\*\* $p < 0.0001$ . n. d. = not detected

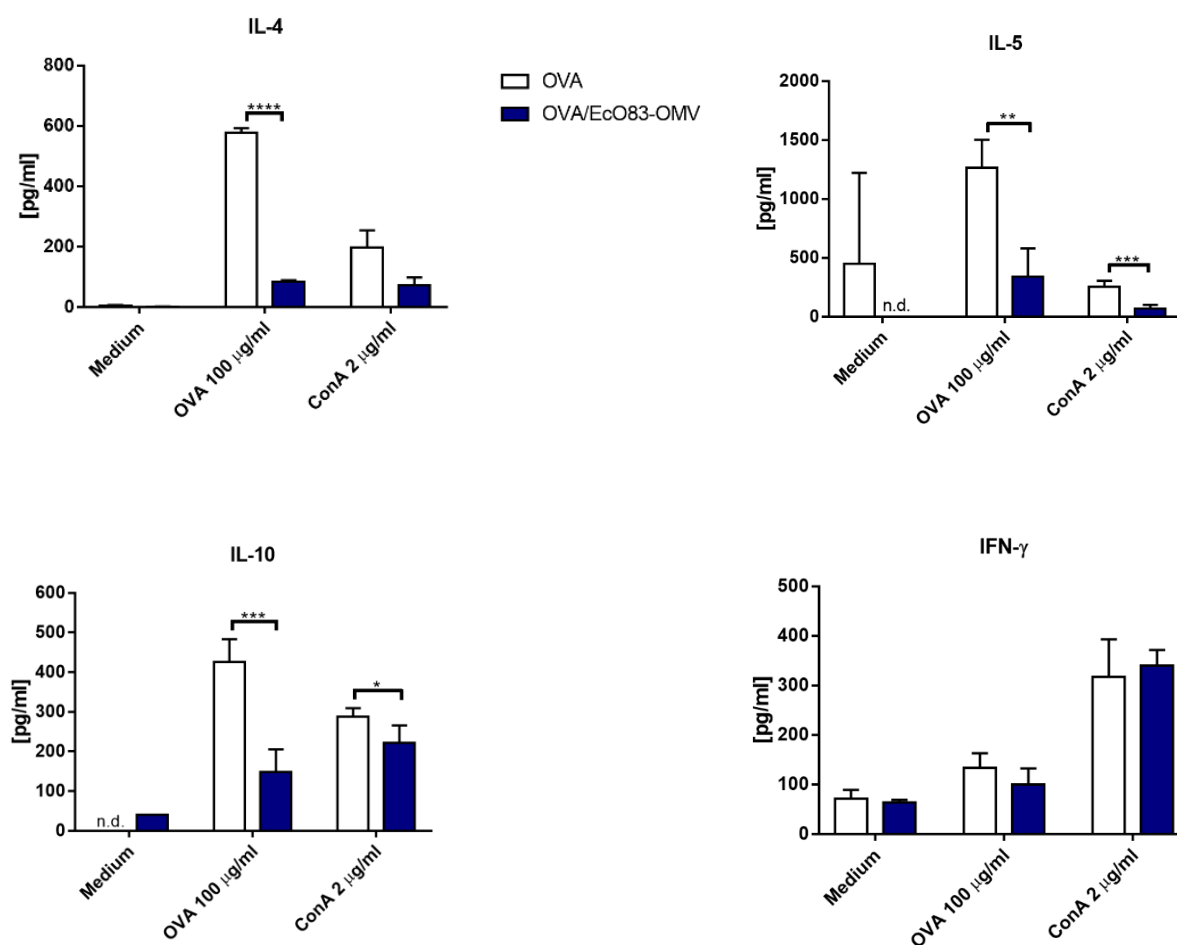


**Figure 18: Cytokine production of splenocytes derived from allergic TLR4 KO BALB/c mice.** Lung cells and splenocytes were cultured with medium only or stimulated with OVA (100 μg/ml) or conA (2 μg/ml) for 72 hours. Both treatment groups are represented: OVA and OVA/EcO83-OMV. Supernatants were collected and levels of cytokines were measured by ELISA. The statistical analysis was done by using a multiple T test. \* $p < 0.05$ , \*\* $p < 0.01$ , \*\*\* $p < 0.001$ , \*\*\*\* $p < 0.0001$

### 7.4.3 Production of OVA-specific antibodies

The blood from TLR4 KO BALB/c mice was taken on four different days. **Figure 19** shows that level of OVA-specific IgG1 is comparable between OVA and OVA/EcO83-OMV groups as measured in samples collected on day 0, 13, 20, and 26. Levels of OVA-specific IgG2a and the levels of IgE expressed as the release of hexaminidase in RBL assay were decreased in OVA/EcO83-OMV group in sera collected on day 26 in comparison to controls (**figure 19**).

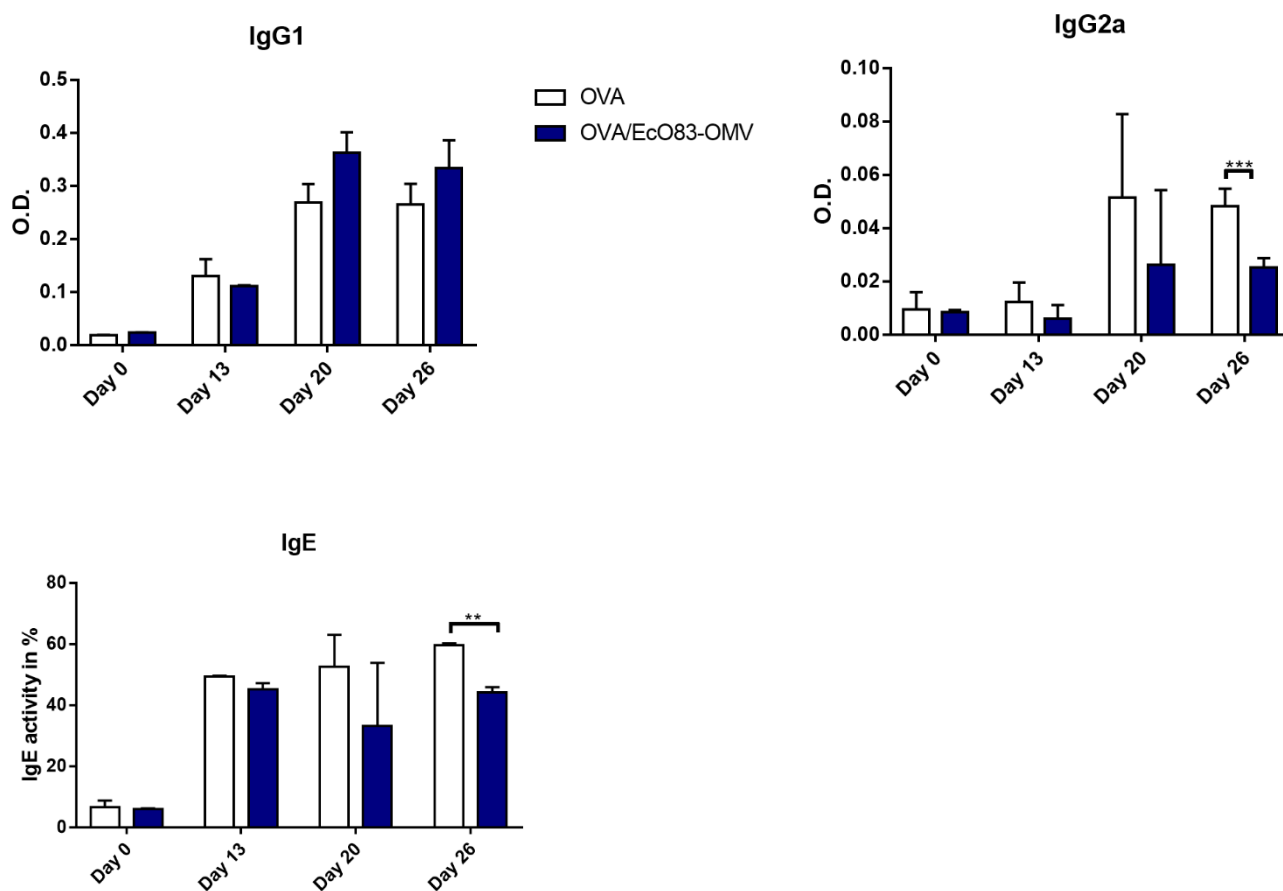


**Figure 19: Level of OVA-specific antibody production in TLR4 KO BALB/c mice.** The levels of OVA-specific IgG1 and IgG2a in sera collected on day 0, 13, 20 and 26 were measured by ELISA. The RBL cell assay was used to measure the level of OVA-specific IgE antibodies. The data was statistically analysed by using a multiple t test. \*\*\* $p < 0.001$ , \*\* $p < 0.01$ .

## 7.5 The suppression of allergy by the intranasal application of EcO83-OMV IL-1 $\beta$ independent

Previously we have shown that intranasal application of EcO83-OMV reduced the development of allergic airway inflammation in mice <sup>64</sup>. In parallel, we have shown that the parent strain, as well as EcO83-OMV, induce high levels of IL-1 $\beta$  *in vitro* in BMDCs and splenocytes. We tested its role *in vivo*, in a mouse model of OVA-induced airway inflammation in IL-1 $\beta$  KO mice.

BAL fluid was collected and haematoxylin and eosin-stained cells were analysed by light microscopy (**figure 20**). The differential counting indicates that allergic control mice exhibit high levels of infiltration of eosinophils into the lung, which was reduced by EcO83-OMV treatment (**figure 21**). Although the counts of macrophages and lymphocytes were not influenced by EcO83-OMV, the numbers of neutrophils were increased by EcO83-OMV (**figure 21**).

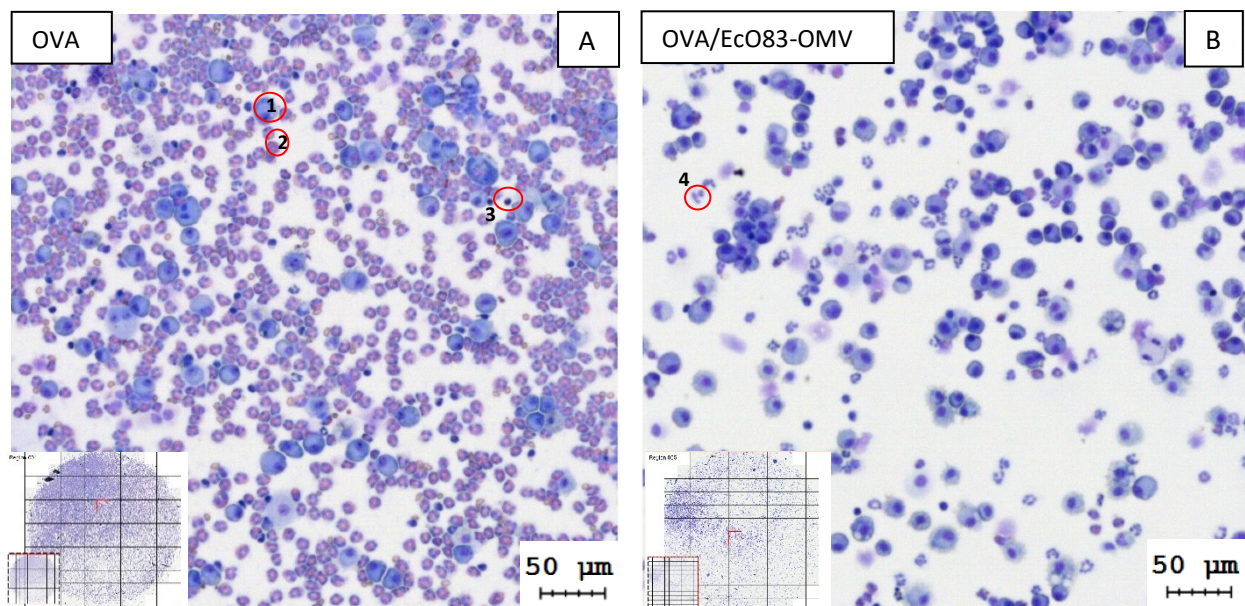


**Figure 20: Microscope images of stained BAL fluid cells.** BAL fluid cells were stained and imaged via FAXSi PLUS. Both groups of treatment are represented (OVA and OVA/EcO83-OMV). The red circle indicates individual cells. 1=macrophages, 2=eosinophils, 3=lymphocytes, 4=neutrophils.

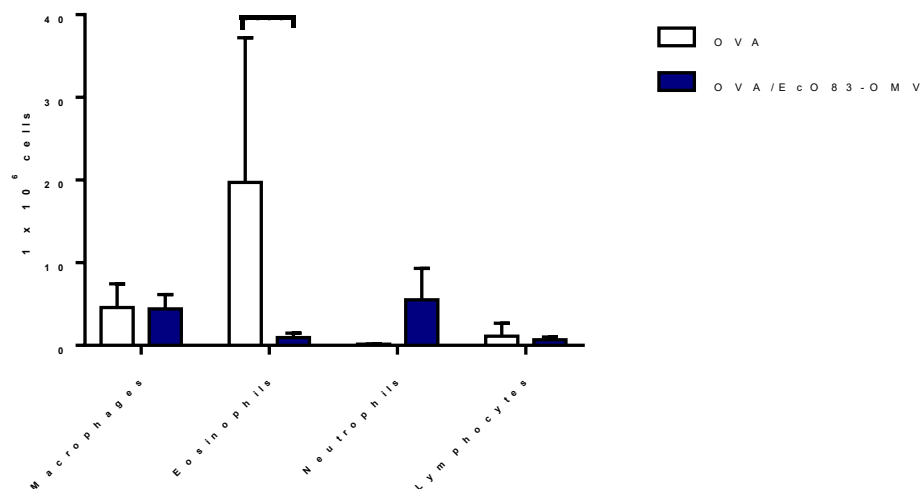


**Figure 21: Absolute numbers of cell populations in BAL fluid of IL-1 $\beta$  KO C57BL/6J mice.** BAL fluid cells were stained with H&E, imaged via FAXSi PLUS and counted (figure 19, (A and B)). Absolute cell count of macrophages, eosinophils, neutrophils and lymphocytes is shown. The statistical analysis was done by using a multiple t test. \*\*\* $p < 0.0001$ .

### 7.5.1 Lung cell populations in IL-1 $\beta$ KO C57BL/6J mice with and without EcO83-OMV treatment

In figure 22 lung tissue stained with H&E is depicted (A) and (B) showing the infiltration of cells to the lung in both groups. Furthermore, samples stained by PAS did not detect mucus production in any of the treatment groups (figure 22 C and D).



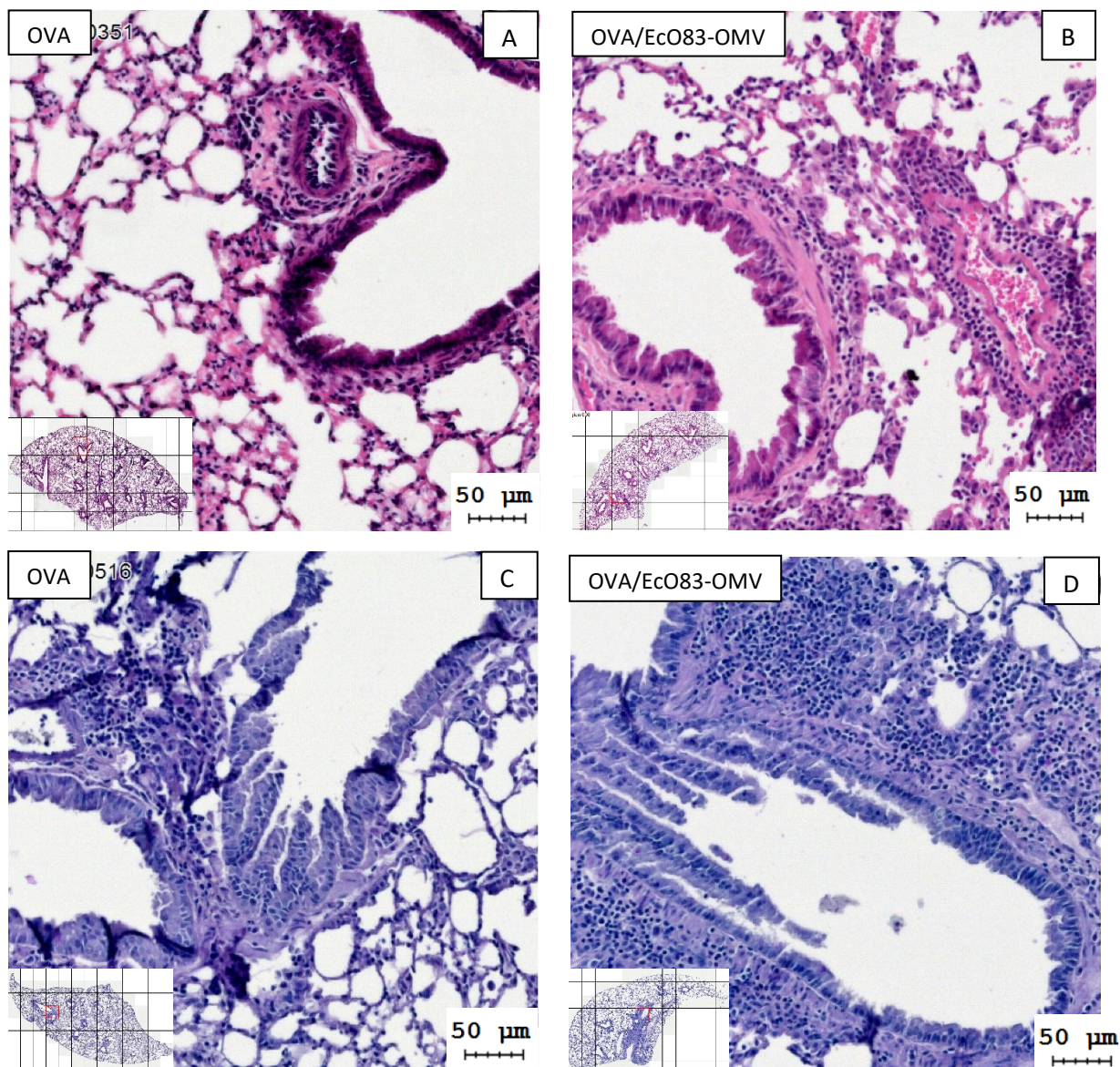


**Figure 22: Lung pathology.** Histological sections were made of lung tissues. H&E staining (A, B) and PAS staining (C, D) of lung lobes from IL-1 $\beta$  KO C57BL/6J mice. Lung lobes of both groups (OVA and OVA/EcO83-OMV) were conserved and embedded in paraffin. Histological section were cut, followed by H&E and PAS staining and the images were recorded with FAXSi PLUS.

### 7.5.2 Production of cytokines in lung and spleen derived from EcO83-OMV-treated/non-treated OVA sensitised and challenged IL-1 $\beta$ KO C57BL/6J mice

The lung cells and splenocytes of IL-1 $\beta$  KO C57BL/6J mice were isolated and stimulated with media only, OVA or ConA. Supernatants were collected and levels of cytokines analysed by ELISA. In the lung, a significant IL-5 and IL-13 reduction was observed (**figure 23**) in OVA-stimulated lung cultures of OVA/EcO83-OMV mice in comparison to controls. No effect on levels of IL-4 and IL-10 was observed but EcO83-OMV increased levels of OVA-specific IFN- $\gamma$ . IL-5, IL-13, and IL-10 cytokines induced *ex vivo* by ConA were significantly reduced in cells from OVA/EcO83-OMV-treated mice in comparison to allergic controls (**figure 23**). ConA-induced IFN- $\gamma$  production was increased in the group treated with EcO83-OMV (**figure 23**). As shown in **figure 24** for OVA stimulated splenocytes, the level of IL-4, IL-10 and IFN- $\gamma$  was significantly increased in the OVA/EcO83-OMV group relative to the OVA group, while the level of IL-5 was

not influenced by EcO83-OMV treatment. After ConA stimulation, spleen cells derived from EcO83-OMV-treated mice exhibited increased production of IL-5 cytokine, reduced production of IFN- $\gamma$  and no effect on levels of IL-4 and IL-10 compared to the OVA group (**figure 24**).

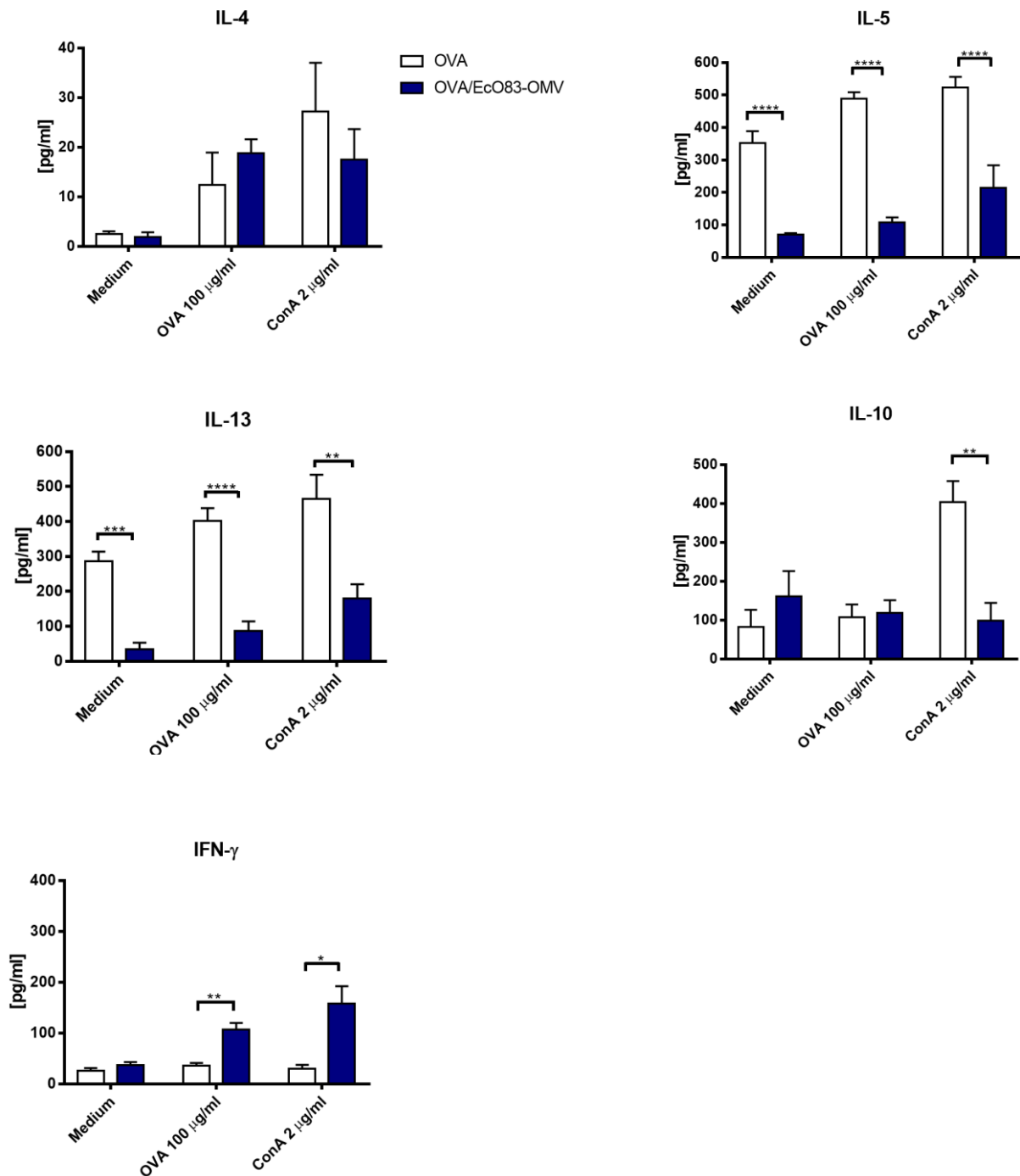


**Figure 23: Cytokine production of lung cells derived from allergic IL-1 $\beta$  KO C57BL/6J mice.** Lung cells were cultured with medium only or stimulated with OVA (100  $\mu$ g/ml) and ConA (2  $\mu$ g/ml) for 72 hours. Supernatants were collected and levels of cytokines were measured by ELISA. The two treatment groups that are presented are: OVA and OVA/EcO83-OMV. The statistical analysis was done by using a multiple t test. \*p < 0.05, \*\*p < 0.01, \*\*\*p < 0.001 \*\*\*\*p < 0.0001. n=4, n=5.

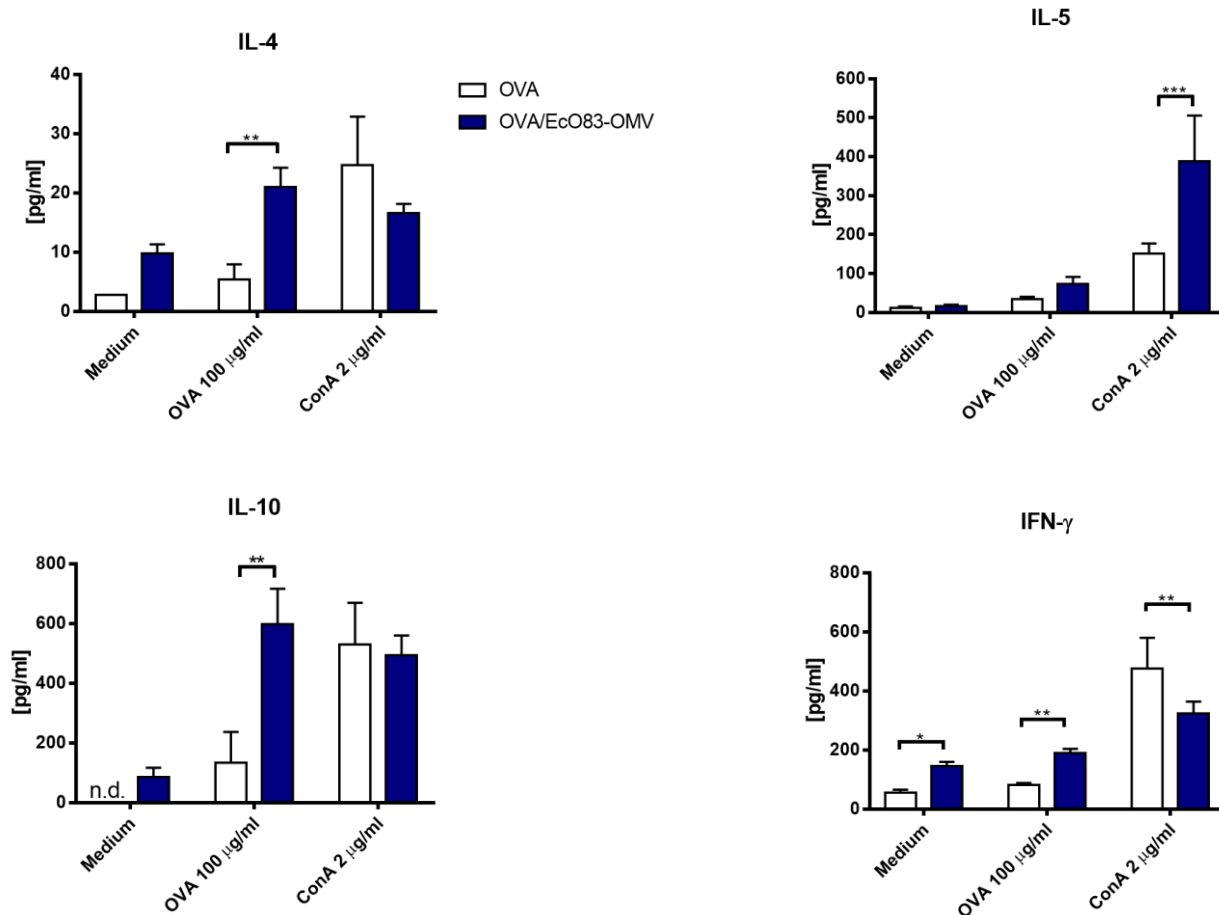


**Figure 24: Cytokine production of splenocytes derived from allergic IL-1 $\beta$  KO C57BL/6J mice.** Splenocytes were cultured with medium only or stimulated with OVA (100  $\mu$ g/ml) and ConA (2  $\mu$ g/ml) for 72 hours. Supernatants were collected and levels of cytokines were measured by ELISA. The two treatment groups that are presented are: OVA and OVA/EcO83-OMV. The statistical analysis was done by using a multiple t test. \*\*p < 0.001, \*\*\*p < 0.001. n.d. = not detected. n=4, n=5.



### 7.5.3 Levels of IgA in BAL fluid of IL-1 $\beta$ KO mice treated with EcO83-OMV and sensitised and challenged with OVA

BAL fluid was used to perform IgA antibody ELISA to see if there is a production of IgA. A higher production of IgA is shown in the EcO83-OMV treated group (**figure 25**).

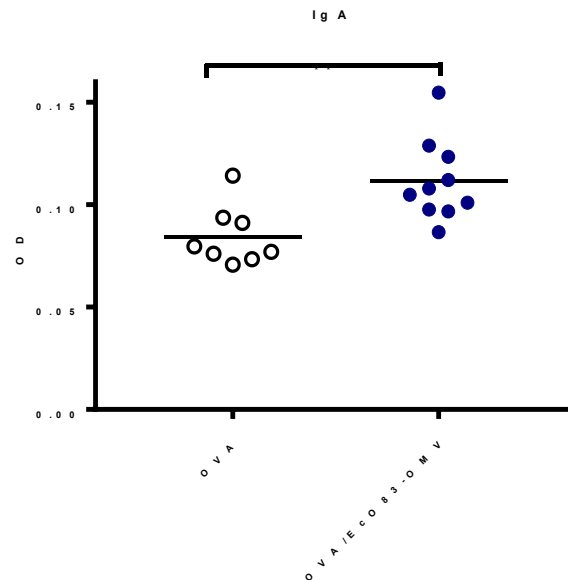


**Figure 25: IgA production in BAL fluid of IL-1 $\beta$  KO C57BL/6J mice.** The level of IgA was measured in the BAL fluid in two presented groups: OVA and OVA/EcO83-OMV. ELISA was performed, and the OD was measured. Statistical analysis was done by using a multiple t test. \*\* 0.001 to 0.01. n=4, n=5.

### 7.5.4 OVA-specific antibody production in sera from IL-1 $\beta$ KO C57BL/6J mice

To measure the level of different OVA-specific antibodies in sera of the IL-1 $\beta$  KO C57BL/6J mice, blood was taken via tail bleeding on day 0, day 20 after sensitisation and on the day of sacrifice (day 24) and the serum was isolated. Reduced IgG1 levels were detected in sera collected on day 20 and 24 in the EcO83-OMV-treated group relative to the OVA-treated controls (**figure 26**). Because of the knowledge that IgG antibodies compete with IgE antibodies by either blocking or inhibiting the binding of IgE to the specific antigens, an additional RBL assay was performed. The RBL assay is a sensitive tool to analyse the IgE levels by analysing the allergenicity to OVA. On day 0 and day 20 there was a low IgE production, whereas, on day 24 there was a highly significant increase of IgE in the OVA/EcO83-OMV group compared to the OVA group (**figure 26**). IgG2c remained the same level on all four days (**figure 26**).

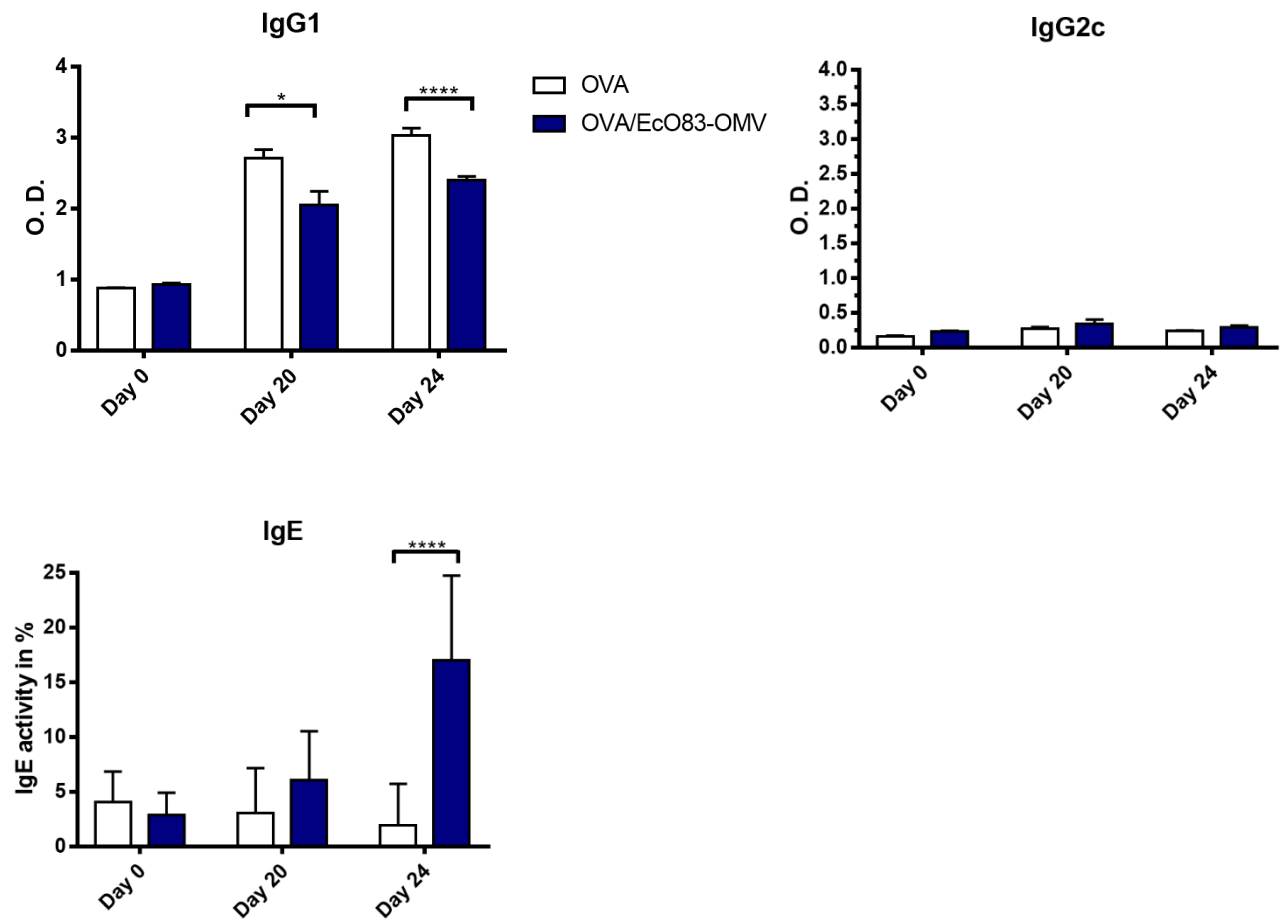


**Figure 26: OVA-specific antibody production in sera from IL-1 $\beta$  KO C57BL/6J mice.** Serum was taken on day 0, 20 and 24. An antibody ELISA for IgG1 and IgG2c were measured by ELISA and the levels of IgE activity by RBL assay. The two treatment groups that are presented are: OVA and OVA/EcO83-OMV. The statistical analysis was done by using a multiple t test. \* $p < 0.05$ , \*\*\*\* $p < 0.0001$ .  $n=4$ ,  $n=5$ .

## 7.6 Stimulation of mouse splenocytes derived from TLR9 KO C57BL/6J mice and WT C57BL/6J mice with EcO83-OMV

Murine splenocytes of TLR9 KO C57BL/6J and WT C57BL/6J mice were isolated and stimulated to observe if the immune response induced by EcO83-OMV is TLR9-dependent. The level of cytokine production induced by LPS and Pam3CSK4 was comparable in KO and WT cells (**figure 27**). Similarly, levels of cytokines induced by *E. coli* O83 was comparable between KO and WT cells, except IL-1 $\beta$  which was reduced in TLR9 KO cells (**figure 27**). Stimulation of cells by increasing concentration of EcO83-OMV led to similar levels of cytokines and these were not different between KO and WT cells. The only difference was observed in the levels of TNF- $\alpha$  stimulated by EcO83-OMV, which was reduced in TLR9 KO in comparison to WT cells (**figure 27**). This experiment was performed twice, n=2.

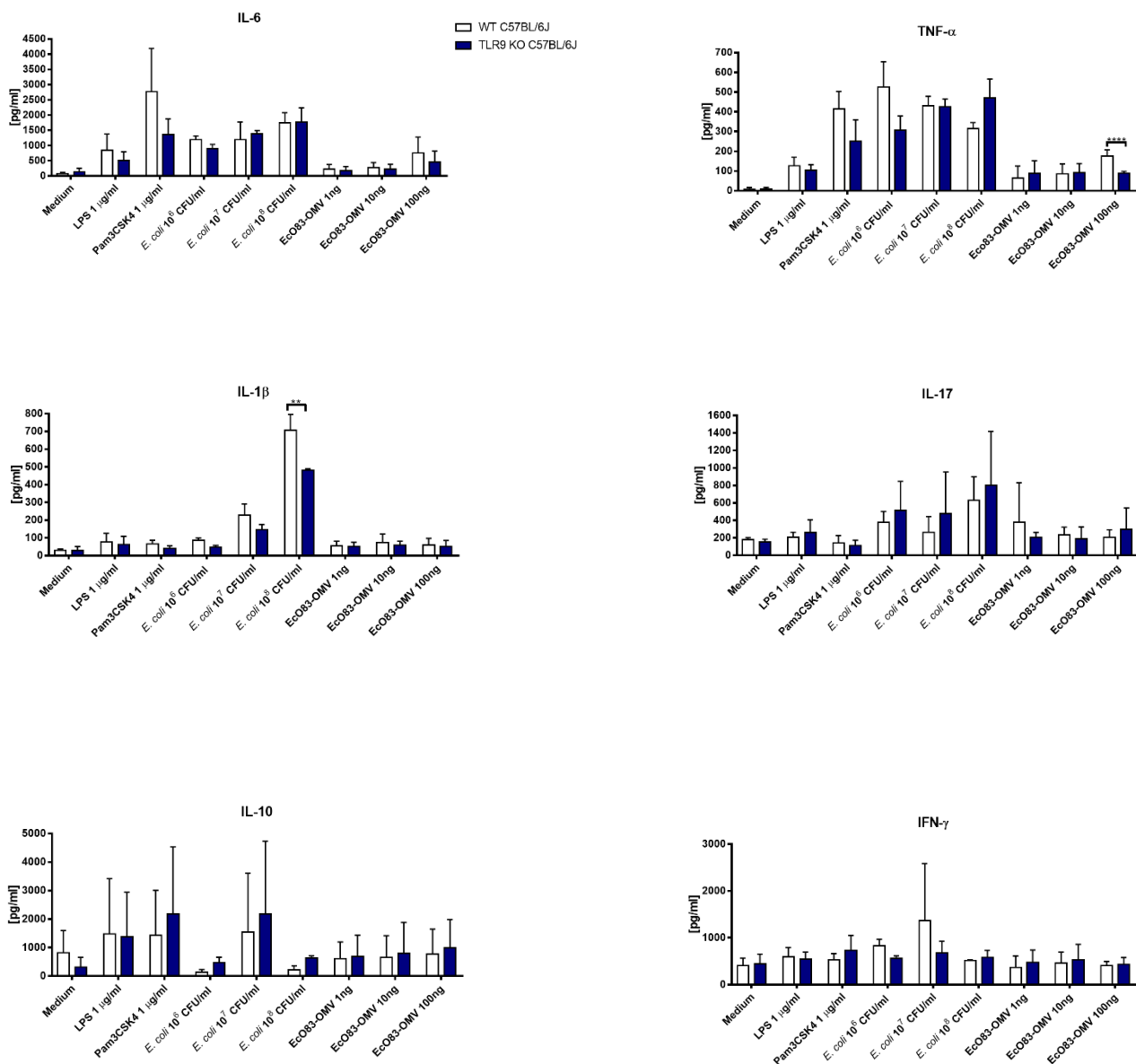


**Figure 27: Production of cytokines in splenocytes derived from TLR9 KO C57BL/6J and WT C57BL/6J mice.** Splenocytes cultured with medium only or LPS (1  $\mu$ g/ml), *E. coli* O83 ( $10^6$ ,  $10^7$ ,  $10^8$  CFU/ml), control *E. coli* OMVs (1 ng/ml, 10 ng/ml or 100 ng/ml) or EcO83-OMV (1 ng/ml, 10 ng/ml and 100 ng/ml) for 72 hours. Supernatants

were collected and levels of cytokines were measured by ELISA. The statistical analysis was done using a multiple t test. \*\*p< 0.01. n=2.

### **7.7 Stimulation of BMDCs derived from TLR9 KO C57BL/6J mice and WT C57BL/6J with EcO83-OMV**

To determine the role of TLR9 in the recognition of EcO83-OMV, cytokine production by BMDCs derived from TLR9 KO and WT mice upon stimulation with EcO83-OMV was evaluated. Production of IL-6, TNF- $\alpha$ , IL-12p70, IL-12/23p40, and IL-23 exhibited comparable levels by all stimuli in both strains (**figure 28**). When stimulated by *E. coli*  $10^7$  and *E. coli*  $10^8$  CFU/ml, levels of IL-10 were reduced in TLR9 KO cells (**figure 28**). This experiment was performed twice, n=2.

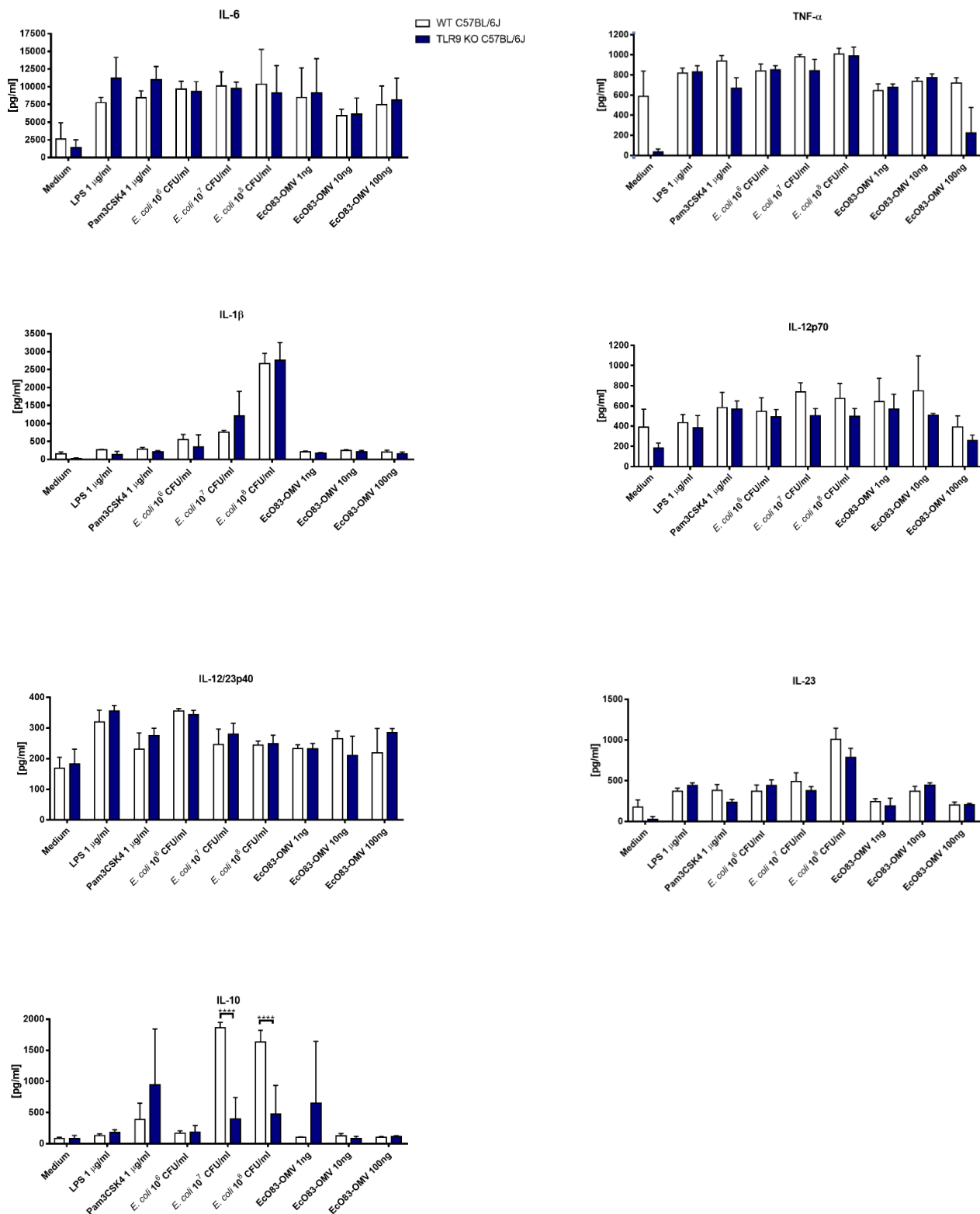


**Figure 28: Production of cytokines in BMDCs derived from TLR9 KO C57BL/6J and WT C57BL/6J mice.** BMDCs were cultured with medium only or stimulated with LPS (1  $\mu$ g/ml), Pam3CSK4 (1  $\mu$ g/ml), *E. coli* O83 ( $10^6$ ,  $10^7$ ,  $10^8$  CFU/ml), control *E. coli* OMV (1 ng/ml, 10 ng/ml or 100 ng/ml) or Eco83-OMV (1 ng/ml, 10 ng/ml and 100 ng/ml) for 24 hours. Supernatants were collected and levels of cytokines were measured by ELISA. The statistical analysis was done with a multiple t test. \*\*\*\*p < 0.0001. n=2

## 7.8 The role of human TLR2, TLR2/CD14, TLR4/CD14/MD2, NOD1, and NOD2 for recognition of EcO83-OMV by using transfected HEK 293 cells

In HEK 293 cells transfected with TLR4 receptor, CD14 and MD2, the level of IL-8 cytokine production induced by Pam3CSK4 and LPS was comparable (**figure 29, A**). 10 ng/ml, 100 ng/ml, 1 µg/ml EcO83-OMV induced increased production of IL-8 in comparison to media, suggesting the recognition of EcO83-OMV by **figure 29 (A)**.

In HEK 293 cells transfected with TLR2 or TLR2/CD14, increased levels of IL-8 after EcO83-OMV stimulation were measured. Similarly, stimulation with all three concentrations of *E. coli* O83 resulted in a high IL-8 production in both cell cultures (**figure 29, B and C**).

For HEK 293 cells transfected with NOD1 there was a significant production of IL-8 induced by the TriDap control, but a very low production induced by endotoxin and LPS (**figure 29, D**). Stimulation by *E. coli* O83 showed a dose dependent production of IL-8 (**figure 29, D**). The cytokine level induced by EcO83-OMV was comparable and was not dose dependent (**figure 29, D**). In **figure 29 (D)** we see a significant cytokine production induced by the highest EcO83-OMV concentration (1 µg/ml) compared to the medium.

In HEK 293 cells transfected with NOD2, the IL-8 cytokine production induced by MDP reveals a high production level compared to the medium (**figure 29, E**). The cytokine levels induced by endotoxin and LPS showed a comparable low level (**figure 29, E**). The cytokine induction by all three concentrations of *E. coli* O83 indicates a dose dependent level of production, the level of cytokine production induced by 10<sup>7</sup> CFU/ml *E. coli* O83 and 10<sup>8</sup> CFU/ml *E. coli* O83 is significantly higher compared to the medium. In the NOD2 graph (**figure 29, E**) the IL-8 level of production induced by the highest concentration of EcO83-OMV (1 µg/ml) was significantly higher than the medium. Between the four concentrations of EcO83-OMV there is a significant dose dependent manner in cytokine production.

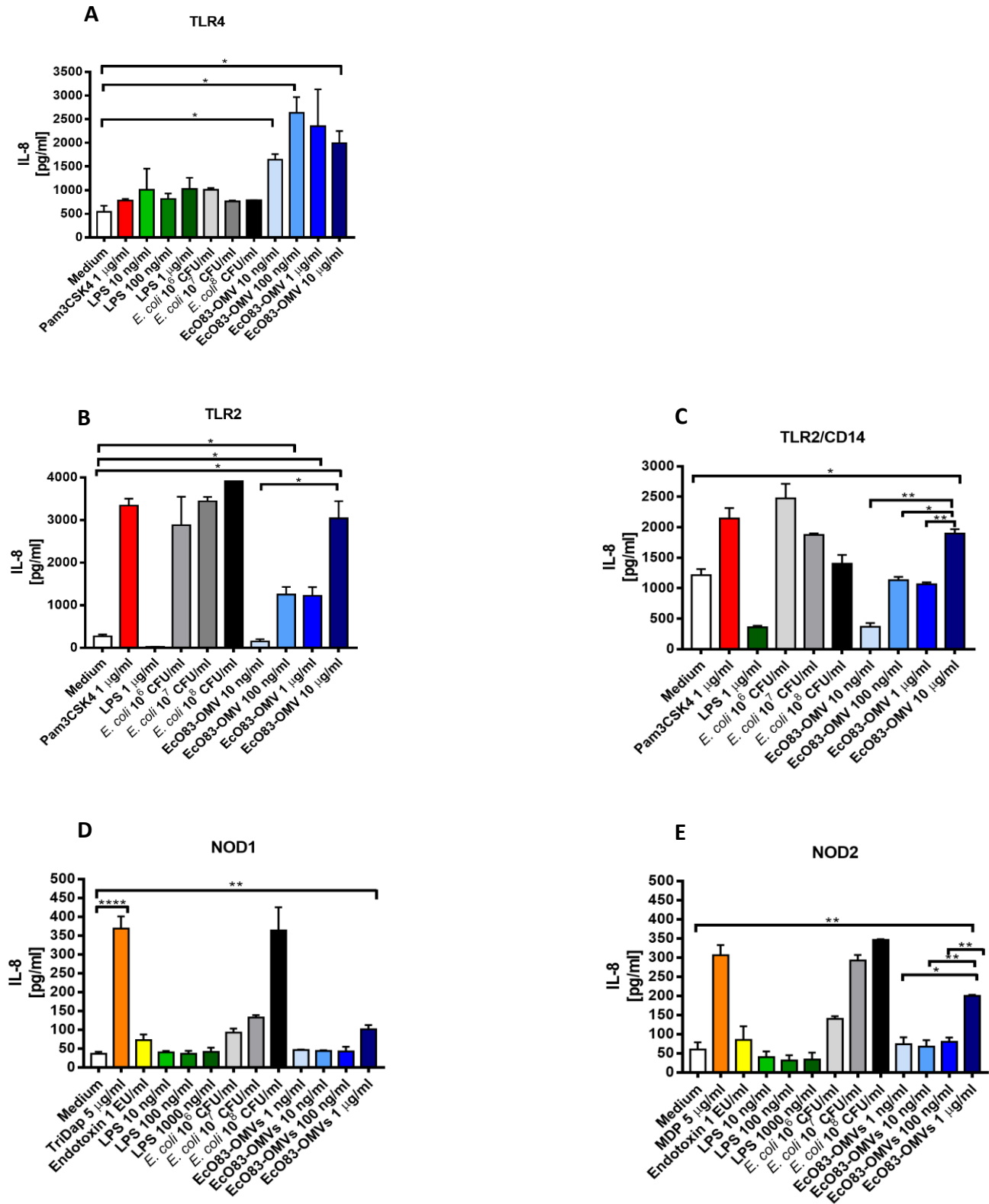


**Figure 29: Cytokine production of human IL-8 in HEK 293 cells transfected with TLR4/CD14/MD2, TLR2, TLR2/CD14, NOD1 and NOD2.** HEK 293 cells were cultured with medium only or stimulated with MDP (5  $\mu$ g/ml), TriDap (5  $\mu$ g/ml), Endotoxin (1 EU/ml), Pam3CSK4 (1 $\mu$ g/ml), LPS (10 ng/ml, 100 ng/ml and 1 $\mu$ g/ml), *E. coli* O83 (10<sup>6</sup>, 10<sup>7</sup>, and 10<sup>8</sup> CFU/ml), and Eco83-OMV (10 ng/ml, 100 ng/ml, 1  $\mu$ g/ml and 10  $\mu$ g/ml). Supernatants were collected and levels of cytokines were measured by ELISA. The statistical analysis was done by using a multiple t test. \* $p$  < 0.05. \*\* $p$  < 0.01. \*\*\*\* $p$  < 0.0001. (A) TLR4  $n$ =1, (B) TLR2  $n$ =2, (C) TLR2/CD14  $n$ =1, (D) NOD1  $n$ =2, (E) NOD2  $n$ =2.





## 8 Discussion

Through previous studies focusing on the probiotic gram-negative bacterial strain *E. coli* O83, it was already demonstrated that this strain exhibits beneficial effects in the prevention of allergic airway inflammation in mice by applying the bacteria intranasally, directly targeting the airways<sup>47</sup>. Because of these prospective results, another study by Schmid *et al.* (2020)<sup>64</sup>, focused on the outer membrane vesicles of *E. coli* O83 strain, EcO83-OMV. Their intranasal application reduced the development of experimental allergic airway inflammation. In this thesis the major goal was to investigate further the immuno-modulatory effects of EcO83-OMV *in vitro* and *in vivo* and to characterise the mechanism involved in the prevention/treatment of allergy by EcO83-OMV.

*E. coli* O83 is a probiotic bacterial strain which has proven to be efficient and safe for human treatment. However, it proliferates in the body after application and it contains a virulence factor  $\alpha$ -haemolysin<sup>65, 66</sup>. OMVS contain several features of the parental bacterial strain, but their important advantage is that they are nonreplicating<sup>48</sup>, thus more safe.

When using probiotic bacteria or compounds derived from these bacteria, the route of administration is of great importance. It was demonstrated that intranasal application of therapeutics in patients suffering from allergic rhinitis showed to be very efficient because it requires a lower dose and the compound is directly delivered to the target organ<sup>67</sup>. Zwicker *et al.* (2018) demonstrated through using intranasal application of *E. coli* O83 in allergic airway inflammation that reduction was observed<sup>47</sup> and furthermore, Schmid *et al.* (2020) showed as well through applying EcO83-OMV directly into the lungs through the airways, a reduction of inflammation in lungs and airways<sup>64</sup>. In this thesis, when applying EcO83-OMV *in vivo*, intranasal administration was used, which showed to have an immunomodulatory effect.

Another important factor is the time of treatment of probiotic bacteria or probiotic bacterial compounds, and the different properties of each strain. wise. Schabussova *et al.* (2010) demonstrated that these two factors differ among the strains<sup>68</sup>. The difference of immune modulatory properties of *Lactobacillus paracasei* NCC 2461 and *Bifidobacterium longum* NCC 3001 in a birch-pollen sensitised mouse models were shown. When both strains were applied at the time of sensitisation and challenge a significant suppression of airway inflammation and a down-regulated immune response were observed, but when probiotic bacteria were applied prior sensitisation and challenge only *B. longum* revealed a protective effect<sup>68</sup>. Zwicker *et al.* (2018) demonstrated that the treatment with *E. coli* O83 was effective in both prophylactic and therapeutic settings<sup>47</sup>. Schmid *et al.* (2020) applied the EcO83-OMV at the time of sensitisation and challenge and observed a beneficial immune modulatory effect when treating allergic airway inflamed mice<sup>64</sup>. In this thesis we applied the EcO83-OMV at the same time using a comparable treatment model (**figure 5-6, table 1-2**).

In this thesis, we used exclusively crude EcO83-OMV, but we also isolated the pure fraction (**chapter 6 Material and methods**) by density gradient purification (**figure 4**), for future studies as it is known that crude vesicles might still contain other bacterial compounds such as flagella, pilli, and free proteins<sup>69</sup>. The isolation of EcO83-OMV was done by using a protocol of Schild *et al.* (2008)<sup>70</sup>, followed by characterising the EcO83-OMV via BCA and LAL-assay to measure the amount of protein and endotoxin content, respectively. Furthermore, TEM (**figure 9 (B)**) and NTA (**figure 10**) were performed confirming the presence and purity of vesicles and their

size distribution ranging from 50 to 400 nm. The pure fraction contained smaller and more homogeneous vesicles which was also observed by *Schmid et al.* (2020)<sup>64</sup>. In general, vesicles on the TEM pictures (**figure 9**) appear to be smaller in size as the actual size via the NTA (**figure 10**) is revealing which is due to the way of treatment to prepare the samples for both methods<sup>71</sup>.

*Zwicker et al.* (2018) showed that the application of *E. coli* O83 in an allergic airway inflammation (AAI) OVA model was TLR4-dependent<sup>47</sup>. Furthermore, *Schmid et al.* (2020) indicated further that certain cytokines in the spleen such as IL-6, IL-17, IL-10 and IFN- $\gamma$  are induced by EcO83-OMV in a TLR4-dependent manner. In our data depicted on **figure 11**, we observed similar results for IL-6 and TNF- $\alpha$  in splenocytes treated with EcO83-OMV. We could see the same effect of TLR4-dependency (**figure 12**) in BMDCs for IL-6, TNF- $\alpha$ , IL-1 $\beta$ , IL-12p70, IL-12/23p40 and IL-23 when treating with EcO83-OMV. In several studies, it was already shown that OMVs activate the production of pro-inflammatory cytokines such as IL-6, IL-1 $\beta$ , but also drive production of anti-inflammatory IL-10<sup>72, 73, 74, 75</sup>.

We performed an *in vivo* experiment in an AAI OVA mouse model (**figure 6, table 2**) in TLR4 KO BALB/c mice. On one hand the BAL fluid depicted in **figure 13** and confirmed by the absolute cell count of cell population (**figure 14**) indicated that the immune modulatory pathway of EcO83-OMV was not TLR4 dependent, showing a high reduction of eosinophils in the EcO83-OMV treated group. On the other hand, the cell population in the lung analysed and measured via FACS in **figure 15** and **figure 16** indicated no difference between the OVA and EcO83-OMV group. The percentage of eosinophils in the lung was comparable between the two treatment groups, which would confirm the TLR4-dependency of EcO83-OMV (**figure 15**). In terms of the isolated TLR4 KO BALB/c lung cells (**figure 17**) from the OVA-induced allergic mouse model (**figure 6, table 2**) treated with EcO83-OMV there was no significant reduction of the Th2 cytokines IL-4 and IL-5 was observed, but both treatment groups (OVA and OVA/EcO83-OMV) showed a comparable cytokine production which was also observed in the TLR4 KO studies with the parental *E. coli* O83 strain by *Zwicker et al.* (2018)<sup>47</sup>.

Looking at a more remote organ from the side of treatment data (**figure 18**) showed that intranasal treatment with EcO83-OMV altered the cytokine release in splenocytes when comparing to cells derived from control mice. For example, levels of IL-4 and IL-5 induced by OVA (**figure 18**) were reduced in TLR4 KO mice, indicating that EcO83-OMV-facilitated reduction of systemic allergic response is TLR4-independent. IgE antibodies are one of the first molecules in immune defence and the IgE-Fc $\epsilon$ RI complex mediates hypersensitivity which is one of the allergic hallmarks<sup>76</sup>. The IgE level (**figure 19**) in sera collected during immunisation were comparable in EcO83-OMV-treated and the OVA group. The IgE levels were reduced by EcO83-OMV in sera collected on day 26. This observation is in contrary to experiments by Anna, where EcO83-OMV did not impact levels of IgE in WT mice<sup>64</sup>.

The TLR4-dependent immune response of EcO83-OMV was additionally investigated by using HEK 293 cells transfected with human TLR4 (**figure 29**). TLR4 is one of the reported PRR that interacts with OMV, as *E. coli* contains LPS which drives the TLR-dependent CXCL8 production, as shown in human epithelial cells<sup>52</sup>. Along these line, also other studies on OMV derived from gram negative bacteria show TLR4-dependent cytokine production<sup>77, 52</sup>. In our data (**figure 29**) pure LPS induction of IL-8 showed a lower level of production compared to EcO83-OMV which was also demonstrated in another study where pure LPS deriving from OMVs was used and compared with the whole vesicle<sup>77</sup>. Another study demonstrated that LPS administered intranasally, suppressed Th2 responses *in vivo* via signalling through TLR4<sup>57</sup>.

*Schmid et al.* (2020) demonstrated that *E. coli* O83 induced high production of IL-1 $\beta$  in splenocytes<sup>64</sup>. In this thesis we investigate whether EcO83-OMV exhibit the same potential to induce this cytokine.

We performed an *in vivo* experiment (**figure 5, table 1**) with IL-1 $\beta$  KO C57BL/6J OVA-induced allergic mice, where one group of mice was treated intranasally with EcO83-OMV. An infiltration of eosinophils in the BAL is one of the trademarks of AAI. We have shown that IL-1 $\beta$  KO mice treated with EcO83-OMV exhibited reduced numbers of eosinophils in BAL compared to the OVA group (**figure 21**), similarly as observed in the WT mice<sup>64</sup>, indicating the immunomodulatory effects of EcO83-OMV are not IL-1 $\beta$  dependent. The histological examination of lungs has shown that OVA-treatment in both sham- and EcO83-OMV-treated mice led to recruitment of inflammatory cells (**figure 22**). Along these lines, we have shown (**figure 21**) that *E. coli* O83 or its OMVs induce recruitment of neutrophils. It has already been shown that *E. coli* OMV stimulate a high infiltration of neutrophils<sup>78</sup>.

The lung cell culture isolated from IL-1 $\beta$  KO mice in **figure 23** showed a reduction of pro-inflammatory IL-5 and IL-13 cytokines in the EcO83-OMV treated group, which confirms the previous data by *Schmid et al.* (2020). Furthermore, the OVA re-stimulated splenocytes isolated from EcO83-OMV-treated mice (**figure 24**) produced less IL-4 and more regulatory/anti-inflammatory IL-10. IL-10 plays a critical part in regulating allergies and is even used in specific immune therapies<sup>79</sup>, this regulatory/anti-inflammatory cytokine is produced by mononuclear phagocytes, NK cells, Th1, Th2 cells, but predominantly by regulatory T cell (Tregs)<sup>79, 80</sup>. This cytokine can down-regulate both Th1 and Th2 pathways<sup>80</sup> and it is also known to have inflammatory properties against allergen-specific Th2 response demonstrated in experimental models and in humans<sup>79, 81</sup>. A study showed that the application of *E. coli* O83 promotes the level of DCs and increases the level of IL-10 cytokine production in DCs and it was suggested that *E. coli* O83 could contribute to the prevention of allergies through increased level of IL-10 production<sup>82</sup>. Several studies with probiotic bacteria and allergy models revealed a shift from Th2 to Th1 immune response<sup>40</sup>.

It has been shown that OMVs derived from bacteria contain various MAMPs, which communicate with the host immune system via PRR<sup>48</sup>, in particular we wanted to investigate whether TLR9 which is known to interact with microbial unmethylated cytosine-phosphate-guanosine (CpG) DNA<sup>83, 84</sup>. However, here we have shown that production of the cytokines IL-6, TNF- $\alpha$ , IL-1 $\beta$ , IL-17, IL-12p70, IL-12/23p40, IL23, IL-10, and IFN- $\gamma$  from splenocytes (**figure 28**) and BDMDs (**figure 28**) is not altered by the absence of TLR9.

Furthermore, peptidoglycan from Gram-negative bacteria can be recognised by another PRR, such as NOD1, resulting in an innate immune response<sup>50</sup>. Also, NOD2 is one of the PRRs and is mainly expressed in immune cells arising from a myeloid origin, whereas NOD1 is expressed in all cell types<sup>85</sup>. Here we have shown that both NOD1 and NOD2 (**figure 29**) play, at least, a partial role for the detection of EcO83-OMV. However, the precise characterisation of respective ligands remains to be investigated.

TLR2 is another receptor that recognises a range of bacterial products such as, lipopeptides, peptidoglycans, and lipoteichoic acid, which are present in the cell membrane of Gram-negative bacteria<sup>86, 87</sup>. It was exhibited that *Porphyromonas. gingivalis* OMVs elicited a signal through C14, C16 and C18 ligands of TLR2 and TLR4<sup>86</sup> and *Acinetobacter baumannii* showed that LPS in OMV is sensed through CD14 and TLR4<sup>73</sup>. Indeed, by using HEK 293 cells transfected with human TLR2 and TLR2/CD14, we have shown that stimulation of cells by

EcO83-OMV activates TLR2. The role of this receptor for EcO83-OMV-induced beneficial effects (**figure 29**), *in vivo* remains to be established.

## 9 Conclusion

In this thesis, we characterised immunomodulatory effects of EcO83-OMV both *in vitro* and *in vivo*. Furthermore, we characterised possible receptors involved in the recognition of EcO83-OMV.

In an experimental model of OVA-induced airway inflammation in TLR4 KO BALB/c mice, we have shown that the beneficial effects of EcO83-OMV are partly TLR4-dependent, which was confirmed by *in vitro* studies.

By using IL-1 $\beta$  KO C57BL/6J mice *in vivo*, we have shown that immunomodulatory effects of EcO83-OMV were not IL-1 $\beta$ -dependent. However, these experiments were performed only once and their repetition is needed.

Finally, EcO83-OMV might be a promising tool for the prevention and treatment of allergic airway inflammation.

## 10 References

1. Papadopoulos, N. G. *et al.* Research needs in allergy: An EAACI position paper, in collaboration with EFA. *Clin. Transl. Allergy* **2**, 1–23 (2012).
2. Abbas, Abul K.; Andrew H. Lichtman, S. P. *Cellular and Molecular Immunology*. (2012).
3. Berger, A. Science commentary: Th1 and Th2 responses: What are they? *Br. Med. J.* **321**, 424 (2000).
4. Maggi, E. The TH1/TH2 paradigm in allergy. *Immunotechnology* **3**, 233–244 (1998).
5. Vignola, A. M., Chanez, P., Godard, P. & Bousquet, J. Relationships between rhinitis and asthma. *Allergy Eur. J. Allergy Clin. Immunol.* **53**, 833–839 (1998).
6. Factors, P. & Options, T. Immunobiology of Asthma and Rhinitis. *Am. J. Respir. Crit. Care Med.* **160**, 1778–1787 (1999).
7. Bousquet, J. *et al.* Review article Allergic Rhinitis and its Impact on Asthma (ARIA) 2008 \* Review Group : *Prim. Care* **63**, 8–160 (2008).
8. Lane, S., Molina, J. & Plusa, T. An international observational prospective study to determine the Cost Of Asthma exacerbations (COAX). *Respir. Med.* **100**, 434–450 (2006).
9. Lambrecht, B. N. & Hammad, H. The immunology of asthma. **16**, (2015).
10. Herrick, C. A. & Bottomly, K. TO RESPOND OR NOT TO RESPOND : T CELLS IN ALLERGIC ASTHMA. **3**, 1–8 (2003).
11. Hirose, K., Iwata, A., Tamachi, T. & Nakajima, H. Allergic airway inflammation: key players beyond the Th2 cell pathway. *Immunol. Rev.* **278**, 145–161 (2017).
12. Nakamura, Y. *et al.* Asthma , rhinitis , other respiratory diseases Gene expression of the GATA-3 transcription factor is increased in atopic asthma. 215–222.
13. Finotto, S. *et al.* Development of Spontaneous Airway Changes Consistent with Human Asthma in Mice Lacking T-bet. **295**, 336–339 (2002).
14. Lambrecht, B. N. & Hammad, H. Allergens and the airway epithelium response: Gateway to allergic sensitization. *J. Allergy Clin. Immunol.* **134**, 499–507 (2014).
15. Kubo, M. Innate and adaptive type 2 immunity in lung allergic inflammation. *Immunol. Rev.* **278**, 162–172 (2017).
16. Stephen J. Galli<sup>1, 2</sup>, Mindy Tsai<sup>1</sup>, and A. M. P. The development of allergic inflammation. *Nature* **454**, 445–454 (2008).
17. Jutel, M. *et al.* International consensus on allergy immunotherapy. *J. Allergy Clin. Immunol.* **136**, 556–568 (2015).
18. Larsen, J. N., Broge, L. & Jacobi, H. Allergy immunotherapy: The future of allergy treatment. *Drug Discov. Today* **21**, 26–37 (2016).
19. Calderón, M. A. *et al.* Allergen immunotherapy: A new semantic framework from the European Academy of Allergy and Clinical Immunology/American Academy of Allergy, Asthma and Immunology/PRACTALL Consensus Report. *Allergy Eur. J. Allergy Clin. Immunol.* **68**, 825–828 (2013).
20. Shamji, M. H. & Durham, S. R. Mechanisms of immunotherapy to aeroallergens. *Clin. Exp. Allergy* **41**, 1235–1246 (2011).
21. Bousquet, J., Van Cauwenberge, P. & Khaltaev, N. Allergic rhinitis and its impact on asthma. *J. Allergy Clin. Immunol.* **108**, (2001).
22. Bousquet, J. *et al.* Allergen immunotherapy: Therapeutic vaccines for allergic diseases - A WHO position paper. *J. Allergy Clin. Immunol.* **102**, 558–562 (1998).
23. Shamji, M. H. *et al.* Functional rather than immunoreactive levels of IgG4 correlate closely with clinical response to grass pollen immunotherapy. *Allergy Eur. J. Allergy*

- Clin. Immunol.* **67**, 217–226 (2012).
24. Brompton, R., National, H., Service, H., Laboratories, M. C. & Uni-, M. Long-term clinical efficacy of grass-pollen immunotherapy. (1999).
  25. Calderon, M. A., Carr, V. A., Jacobson, M., Sheikh, A. & Durham, S. Allergen injection immunotherapy for perennial allergic rhinitis. *Cochrane Database Syst. Rev.* **2019**, (2019).
  26. Okubo, K. & Gotoh, M. Sub-lingual immunotherapy for allergic rhinitis. *Pract. Otorhinolaryngol. (Basel)*. **106**, 769–775 (2013).
  27. Martens, K. *et al.* Probiotics for the airways: Potential to improve epithelial and immune homeostasis. *Allergy Eur. J. Allergy Clin. Immunol.* **73**, 1954–1963 (2018).
  28. Haspeslagh, E., Heyndrickx, I., Hammad, H. & Lambrecht, B. N. The hygiene hypothesis: immunological mechanisms of airway tolerance. *Curr. Opin. Immunol.* **54**, 102–108 (2018).
  29. Burbank, A. J., Sood, A. K., Kesic, M. J., Peden, D. B. & Hernandez, M. L. Environmental determinants of allergy and asthma in early life. *J. Allergy Clin. Immunol.* **140**, 1–12 (2017).
  30. Kalliomäki, M., Salminen, S., Poussa, T., Arvilommi, H. & Isolauri, E. Probiotics and prevention of atopic disease: 4-year follow-up of a randomised placebo-controlled trial. *Lancet* **361**, 1869–1871 (2003).
  31. Kalliomäki, M. *et al.* Probiotics in primary prevention of atopic disease a randomised.pdf. *Lancet* **357**, 1076–1079 (2001).
  32. Noverr, M. C. & Huffnagle, G. B. The ‘microflora hypothesis’ of allergic diseases. *Clin. Exp. Allergy* **35**, 1511–1520 (2005).
  33. Björkstén, B., Sepp, E., Julge, K., Voor, T. & Mikelsaar, M. Allergy development and the intestinal microflora during the first year of life. *J. Allergy Clin. Immunol.* **108**, 516–520 (2001).
  34. Björkstén, B., Naaber, P., Sepp, E. & Mikelsaar, M. The intestinal microflora in allergic Estonian and Swedish 2-year-old children. *Clin. Exp. Allergy* **29**, 342–346 (1999).
  35. Petersen, C. & Round, J. L. Defining dysbiosis and its influence on host immunity and disease. *Cell. Microbiol.* **16**, 1024–1033 (2014).
  36. Spacova, I. *et al.* Intranasal administration of probiotic *Lactobacillus rhamnosus* GG prevents birch pollen-induced allergic asthma in a murine model. *Allergy Eur. J. Allergy Clin. Immunol.* **74**, 100–110 (2019).
  37. Pellaton, C. *et al.* Intra-gastric and intranasal administration of *Lactobacillus paracasei* NCC2461 modulates allergic airway inflammation in mice. *Int. J. Inflam.* **2012**, (2012).
  38. Mårtensson, A. *et al.* Clinical efficacy of a topical lactic acid bacterial microbiome in chronic rhinosinusitis: A randomized controlled trial. *Laryngoscope Investig. Otolaryngol.* **2**, 410–416 (2017).
  39. Shandilya, U. K., Jadhav, S., Panwar, V. & Kansal, V. K. Probiotics: Potent Immunomodulatory Tool Against Allergy. *Probiotics Antimicrob. Proteins* **3**, 151–158 (2011).
  40. Repa, A. *et al.* Mucosal co-application of lactic acid bacteria and allergen induces counter-regulatory immune responses in a murine model of birch pollen allergy. *Vaccine* **22**, 87–95 (2003).
  41. Lodinova-Zadnikova, R., Cukrowska, B. & Tlaskalova-Hogenova, H. Oral administration of probiotic *Escherichia coli* after birth reduces frequency of allergies and repeated infections later in life (after 10 and 20 years). *Int. Arch. Allergy Immunol.* **131**, 209–211 (2003).
  42. Lodinova-Zadnikova R, Bartakova Z, T. H. The effect of oral colonization by non-

- pathogenic *E. coli* on the immune response in neonates and possibilities of its use in the prevention of nosocomial infections in children at risk. *Ceskoslov. Epidemiol.* **42**, 126–132 (1992).
43. Lodinova-Zadnikova R, Sonnenborn U, T. H. Probiotics and *E. coli* infections in man. *Vet.* **3**, 78–81 (1998).
  44. Lodinova R, Jouja V, Vinsova N, Vocel J, M. J. New attempts and possibilities in prevention and treatment of intestinal coli-infections in infants. *Czech Med* **3**, 47–58 (1980).
  45. Lodinova-Zadnikova, R., Prokešová, L., Kocourková, I., Hrdý, J. & Žižka, J. Prevention of allergy in infants of allergic mothers by probiotic *Escherichia coli*. *Int. Arch. Allergy Immunol.* **153**, 201–206 (2010).
  46. West, C. E., Jenmalm, M. C., Kozyrskyj, A. L. & Prescott, S. L. Probiotics for treatment and primary prevention of allergic diseases and asthma: looking back and moving forward. *Expert Rev. Clin. Immunol.* **12**, 625–639 (2016).
  47. Zwicker, C. *et al.* Prophylactic and therapeutic inhibition of allergic airway inflammation by probiotic *Escherichia coli* O83. *J. Allergy Clin. Immunol.* **142**, 1987–1990.e7 (2018).
  48. Kaparakis-Liaskos, M. & Ferrero, R. L. Immune modulation by bacterial outer membrane vesicles. *Nat. Rev. Immunol.* **15**, 375–387 (2015).
  49. Toyofuku, M., Nomura, N. & Eberl, L. Types and origins of bacterial membrane vesicles. *Nat. Rev. Microbiol.* **17**, 13–24 (2019).
  50. Kaparakis, M. *et al.* Bacterial membrane vesicles deliver peptidoglycan to NOD1 in epithelial cells. *Cell. Microbiol.* **12**, 372–385 (2010).
  51. Kuehn, M. J. & Kesty, N. C. Bacterial outer membrane vesicles and the host-pathogen interaction. *Genes Dev.* **19**, 2645–2655 (2005).
  52. Söderblom, T. *et al.* Effects of the *Escherichia coli* toxin cytolysin A on mucosal immunostimulation via epithelial CA2<sup>+</sup> signalling and Toll-like receptor 4. *Cell. Microbiol.* **7**, 779–788 (2005).
  53. Shen, Y. *et al.* Outer Membrane Vesicles of a Human Commensal Mediate Immune Regulation and Disease Protection. *Cell Host Microbe* **12**, 509–520 (2014).
  54. Mazgaeen, L. & Gurung, P. Recent advances in lipopolysaccharide recognition systems. *Int. J. Mol. Sci.* **21**, (2020).
  55. Rizzo, M. C. *et al.* Endotoxin exposure and symptoms in asthmatic children. *Pediatr. Allergy Immunol.* **8**, 121–126 (1997).
  56. Michel, O. *et al.* Severity of asthma is related to endotoxin in house dust. *Am. J. Respir. Crit. Care Med.* **154**, 1641–1646 (1996).
  57. Rodríguez, D. *et al.* Bacterial Lipopolysaccharide Signaling Through Toll-Like Receptor 4 Suppresses Asthma-Like Responses Via Nitric Oxide Synthase 2 Activity. *J. Immunol.* **171**, 1001–1008 (2003).
  58. Kips, J. C. *et al.* Interleukin-12 inhibits antigen-induced airway hyperresponsiveness in mice. *Am. J. Respir. Crit. Care Med.* **153**, 535–539 (1996).
  59. De, B., Report, R. & Medicine, I. Interferon  $\gamma$  regulates antigen-induced eosinophil recruitment into the mouse airways by inhibiting the infiltration of CD4<sup>+</sup> T cells. **177**, 2–5 (1993).
  60. Stuehr, D. J. & Marletta, M. A. Mammalian nitrate biosynthesis: Mouse macrophages produce nitrite and nitrate in response to *Escherichia coli* lipopolysaccharide. *Proc. Natl. Acad. Sci. U. S. A.* **82**, 7738–7742 (1985).
  61. P J Barnes 1, K F Chung, C. P. P. Inflammatory mediators of asthma: an update. *Pharmacol Rev.* 50:515 (1998).



62. O'Donoghue, E. J. *et al.* Lipopolysaccharide structure impacts the entry kinetics of bacterial outer membrane vesicles into host cells. *PLoS Pathog.* **13**, 1–18 (2017).
63. Strauss, J., Burnham, N. A. & Camesano, T. A. Atomic force microscopy study of the role of LPS O-antigen on adhesion of *E. coli*. *J. Mol. Recognit.* **22**, 347–355 (2009).
64. Schmid, A. Characterization of mechanisms underlying beneficial effects of the probiotic bacterial strain *E. coli* O83 in allergy prevention. (Medical University of Vienna, 2020).
65. Sheshko, V. *et al.* HlyA knock out yields a safer *Escherichia coli* A0 34/86 variant with unaffected colonization capacity in piglets. *FEMS Immunol. Med. Microbiol.* **48**, 257–266 (2006).
66. Hejnova, J. *et al.* Characterization of the flexible genome complement of the commensal *Escherichia coli* strain A0 34/86 (O83:K24:H31). *Microbiology* **151**, 385–398 (2005).
67. Salib, R. J. & Howarth, P. H. Safety and tolerability profiles of intranasal antihistamines and intranasal corticosteroids in the treatment of allergic rhinitis. *Drug Saf.* **26**, 863–893 (2003).
68. Schabussova, I. *et al.* Distinctive anti-allergy properties of two probiotic bacterial strains in a mouse model of allergic poly-sensitization. *Vaccine* **29**, 1981–1990 (2011).
69. Klimentová, J. & Stulík, J. Methods of isolation and purification of outer membrane vesicles from gram-negative bacteria. *Microbiol. Res.* **170**, 1–9 (2015).
70. Schild, S., Nelson, E. J. & Camilli, A. Immunization with *Vibrio cholerae* outer membrane vesicles induces protective immunity in mice. *Infect. Immun.* **76**, 4554–4563 (2008).
71. Jarzębski, M., Kościński, M. & Białopiotrowicz, T. Determining the size of nanoparticles in the example of magnetic iron oxide core-shell systems. *J. Phys. Conf. Ser.* **885**, (2017).
72. Ellis, T. N., Leiman, S. A. & Kuehn, M. J. Naturally produced outer membrane vesicles from *Pseudomonas aeruginosa* elicit a potent innate immune response via combined sensing of both lipopolysaccharide and protein components. *Infect. Immun.* **78**, 3822–3831 (2010).
73. Jun, S. H. *et al.* *Acinetobacter baumannii* Outer Membrane Vesicles Elicit a Potent Innate Immune Response via Membrane Proteins. *PLoS One* **8**, (2013).
74. Fábrega, M. J. *et al.* Activation of immune and defense responses in the intestinal mucosa by outer membrane vesicles of commensal and probiotic *Escherichia coli* strains. *Front. Microbiol.* **7**, 1–14 (2016).
75. Cecil, J. D. *et al.* Outer membrane vesicles prime and activate macrophage inflammasomes and cytokine secretion in vitro and in vivo. *Front. Immunol.* **8**, 1–22 (2017).
76. Gould, H. J. & Sutton, B. J. IgE in allergy and asthma today. *Nat. Rev. Immunol.* **8**, 205–217 (2008).
77. Bielaszewska, M. *et al.* Enterohemorrhagic *Escherichia coli* O157 outer membrane vesicles induce interleukin 8 production in human intestinal epithelial cells by signaling via Toll-like receptors TLR4 and TLR5 and activation of the nuclear factor NF- $\kappa$ B. *Int. J. Med. Microbiol.* **308**, 882–889 (2018).
78. Lee, J. *et al.* Outer membrane vesicles derived from *Escherichia coli* regulate neutrophil migration by induction of endothelial IL-8. *Front. Microbiol.* **9**, 1–12 (2018).
79. Akdis, C. A., Blesken, T., Akdis, M., Wüthrich, B. & Blaser, K. Role of interleukin 10 in specific immunotherapy. *J. Clin. Invest.* **102**, 98–106 (1998).
80. P., K. Th1/Th2 balance: The hypothesis, its limitations, and implications for health and

- disease. *Altern. Med. Rev.* **8**, 223–246 (2003).
81. Gad, M. *et al.* Regulation of the IL-10/IL-12 axis in human dendritic cells with probiotic bacteria. *FEMS Immunol. Med. Microbiol.* **63**, 93–107 (2011).
  82. Súkeníková, L. *et al.* Different capacity of in vitro generated myeloid dendritic cells of newborns of healthy and allergic mothers to respond to probiotic strain E. coli O83:K24:H31. *Immunol. Lett.* **189**, 82–89 (2017).
  83. Lai, C. Y., Yu, G. Y., Luo, Y., Xiang, R. & Chuang, T. H. Immunostimulatory activities of CpG-oligodeoxynucleotides in teleosts: Toll-like receptors 9 and 21. *Front. Immunol.* **10**, 1–13 (2019).
  84. Bauer, S. *et al.* Human TLR9 confers responsiveness to bacterial DNA via species-specific CpG motif recognition. *Proc. Natl. Acad. Sci. U. S. A.* **98**, 9237–9242 (2001).
  85. Cañas, M. A., Fábrega, M. J., Giménez, R., Badia, J. & Baldomà, L. Outer membrane vesicles from probiotic and commensal escherichia coli activate NOD1-mediated immune responses in intestinal epithelial cells. *Front. Microbiol.* **9**, 1–13 (2018).
  86. Cecil, J. D. *et al.* Differential responses of pattern recognition receptors to outer membrane vesicles of three periodontal pathogens. *PLoS One* **11**, 1–20 (2016).
  87. Takeda, K. & Akira, S. Microbial recognition by Toll-like receptors. *J. Dermatol. Sci.* **34**, 73–82 (2004).

## 11 List of tables

Table 1 Specific treatment of IL-1 $\beta$ KO mice.....	24
Table 2 Specific treatment of TLR4 KO mice .....	24
Table 3 Fluorophores and antibody surface markers for live/dead and Fc-Block staining.....	27
Table 4 Myeloid panel with fluorophores and antibody surface markers .....	27
Table 5 Lymphocyte panel with fluorophores and antibody surface markers .....	27
Table Stimulation settings of HEK 293 cells transfected with NOD1, NOD2, TLR2, TL2/CD14, and TLR4/CD14/MD2. .....	31
Table 7 Reaction step for reverse transcriptase .....	32
Table 8 Master mix for cDNA real time qPCR .....	32
Table 9 Reaction steps for real time qPCR.....	33
Table 10 List of all media and solution that were used for the experiments .....	33-37

## 12 List of figures:

Figure 1 Schematic depiction of allergic asthma .....	14
Figure 2 Forming of outer membrane vesicles by blebbing of the outer membrane .....	17
Figure 3 Isolation of crude EcO83-OMV .....	20
Figure 4 Gradient ultracentrifugation of crude EcO83-OMV .....	21
Figure 5 Experimental set up of OVA-induced allergic IL-1 $\beta$ KO mice and the treatment of EcO83-OMV .....	23
Figure 6 Experimental set up of OVA-induced allergic TLR4 KO mice and the treatment of EcO83-OMV .....	23
Figure 7 Gating strategy for the lymphoid panel and the corresponding cell populations .....	28
Figure 8 Gating strategy for the myeloid panel and the corresponding cell populations .....	29
Figure 9 Characterisation of EcO83-OMV using TEM. Image s of crude (A) and pure (B) EcO83-OMV .....	38
Figure 10 NTA analysis of EcO83-OMV .....	39
Figure 11 Production of cytokines in mouse splenocytes derived from WT and TLR4 KO BALB/c mice .....	40
Figure 12 Production of cytokines in mouse BMDC derived from WT and TLR4 KO BALB/c mice ....	42
Figure 13 Microscope images of stained BAL fluid cells .....	43
Figure 14 Absolute numbers of cell populations in BAL fluid of TLR4 KO mice .....	44
Figure 15 FACS analysis of myeloid cells in lung cells derived from TLR4 KO BALB/c mice .....	45-46
Figure 16 FACS analysis of lymphoid cells in lung cells derived from TLR4 KO BALB/c mice .....	47-48
Figure 17 Cytokine production of lung cells derived from allergic TLR4 KO BALB/c mice .....	50
Figure 18 Cytokine production of splenocytes derived from allergic TLR4 KO BALB/c mice .....	51
Figure 19 Level of OVA-specific antibody production in TLR4 KO BALB/c mice .....	52
Figure 20 Microscope images of stained BAL fluid cells .....	53
Figure 21 Absolute numbers of cell populations in BAL fluid of IL-1 $\beta$ KO C57BL/6J mice .....	53
Figure 22 Lung pathology .....	54
Figure 23 Cytokines production of lung cells derived from allergic IL-1 $\beta$ KO C57BL/6J mice .....	55
Figure 24 Cytokine production of splenocytes derived from allergic IL-1 $\beta$ KO C57BL/6J mice .....	56
Figure 25 IgA production in BAL fluid of IL-1 $\beta$ KO C57BL/6J mice .....	57
Figure 26 OVA-specific antibody production in sera from IL-1 $\beta$ KO C57BL/6J mice .....	58
Figure 27 Production of cytokines in splenocytes derived from TLR9 KO C57BL/6J and WT C57BL/6J mice .....	59
Figure 28 Production of cytokines in BMDCs derived from TLR9 KO C57BL/6J and WT C57BL/6J mice .....	61

<b>Figure 29 Cytokine production of human IL-8 in HEK 293 cells transfected with TLR4/CD14/MD2, TLR2, TLR2/CD14, NOD1 and NOD2 .....</b>	<b>63</b>
--	-----------